ATOMIC ENERGY OF CANADA LIMITED

AECL--6440

DE82 902004

AN ASSESSMENT OF MATERIALS FOR NUCLEAR FUEL IMMOBILIZATION CONTAINERS

by

K. Nuttall and V.F. Urbanic*

* System Materials Branch,
Chalk River Nuclear Laboratories

Whiteshell Nuclear Research Establishment
Pinawa, Manitoba ROE 1LO
1981 September

AECL-6440

AN ASSESSMENT OF MATERIALS FOR NUCLEAR FUEL IMMOBILIZATION CONTAINERS

by

K. Nuttall and V.F. Urbanic

ABSTRACT

A wide range of engineering metals and alloys has been assessed for their suitability as container materials for irradiated nuclear fuel intended for permanent disposal in a deep, underground hard-rock vault. The expected range of service conditions in the disposal vault are discussed, as well as the material properties required for this application. An important requirement is that the container last at least 500 years without being breached. The assessment is treated in two parts. Part I concentrates on the physical and mechanical metallurgy, with special reference to strength, weldability, potential embrittlement mechanisms and some economic aspects. Part II discusses possible mechanisms of metallic corrosion for the various engineering alloys and the expected range of environmental conditions in the vault. Localized corrosion and delayed fracture processes are identified as being most likely to limit container lifetime. Hence an essential requirement is that such processes either be absent or proceed at an insignificant rate.

Three groups of alloys are recommended for further consideration as possible container materials: AISI 300 series austenitic stainless steels, high nickel-base alloys and very dilute titanium-base alloys. Specific alloys from each group are indicated as having the optimum combination of required properties, including cost. For container designs where the outer container shell does not independently support the service loads, copper should also be considered. The final material selection will depend primarily on the environmental conditions in the vault. Some recommendations are given for future research on the candidate materials.

Atomic Energy of Canada Limited
Whiteshell Nuclear Research Establishment
Pinawa, Manitoba R0E 1L0
1981 September

AECL-6440

UNE EVALUATION DES MATERIAUX POUR CONTENEURS DESTINES A L'IMMOBILISATION DU COMBUSTIBLE NUCLEAIRE

par

K. Nuttall et V.F. Urbanic

RESUME

On a évalué une grande variété de métaux et d'alliages industriels du point de vue de leurs possibilités d'utilisation comme matériaux pour conteneurs de combustible nucléaire irradié destinés à l'évacuation permanente dans une enceinte située à grande profondeur dans la roche dure. On examine les diverses conditions de service prévues dans l'enceinte d'évacuation de même que les propriétés des matériaux nécessaires pour cette application. Une condition importante est que le conteneur doit durer 500 ans sans se rompre. On traite l'évaluation en deux parties. La première partie porte surtout sur la métallurgie physique et mécanique et traite particulièrement de la résistance, de la possibilité de soudage, des mécanismes de fragilisation possibles et de certains aspects économiques. La deuxième partie traite des mécanismes possibles de corrosion métallique de divers alliages industriels et des diverses conditions prévues dans le milieu de l'enceinte. On considère les processus de corrosion localisés et de fissuration retardés comme étant les plus susceptibles de limiter la durée de vie des conteneurs. La condition essentielle est donc que ces processus ne se produisent pas du tout ou qu'ils se produisent à une vitesse négligeable.

On recommande l'étude poussée de trois groupes d'alliages comme matériaux possibles de conteneurs: la série AISI 300 d'aciers inoxydables austénitiques, les alliages à teneur élevée en nickel et les alliages au titanium très dilué. On indique que les alliages particuliers de chaque groupe possèdent la combinaison optimale de propriétes nécessaires ainsi que le coût. On pourrait considérer aussi le cuivre pour les types de conteneurs dont l'enveloppe extérieure n'a pas à supporter elle-même des charges en service. Le choix final du matériel dépendra surtout des conditions existant dans le milieu de l'enceinte. On donne quelgues conseils pour les recherches futures sur les matériaux possibles.

6. SUPERALLOYS AND HIGH-ALLOY AUSTENITICS 27

6.1 [illegible] 29
6.2 [illegible] 30
[illegible] 30
[illegible] 32

L'Energie Atomique du Canada Limitée
Etablissement de Recherches Nucléaires de Whiteshell
Pinawa, Manitoba ROE 1LO
1981 septembre

AECL-6440

CONTENTS

		Page
1.	INTRODUCTION	1
2.	GUIDELINES FOR MATERIAL SELECTION	4
	PART I - PHYSICAL AND MECHANICAL METALLURGY	7
3.	LOW-MELTING-POINT ALLOYS	7
	3.1 ALUMINUM-BASE ALLOYS	7
	3.2 MAGNESIUM-BASE ALLOYS	10
4.	PLAIN CARBON AND LOW-ALLOY STEELS	11
5.	STAINLESS STEELS	13
	5.1 FERRITIC STAINLESS STEELS	13
	5.1.1 Welding	14
	5.1.2 Embrittlement Effects	14
	5.1.3 Corrosion	18
	5.1.4 Recent Developments	18
	5.2 AUSTENITIC (γ) STAINLESS STEELS (WROUGHT)	19
	5.2.1 Constitution	19
	5.2.2 Welding and Weld Decay	20
	5.2.3 Embrittlement Effects	23
	5.3 MARTENSITIC STAINLESS STEELS	25
	5.4 PRECIPITATION HARDENING (PH) STAINLESS STEELS	26
6.	SUPERALLOYS AND HIGH-ALLOY AUSTENITICS	27
	6.1 WELDABILITY	29
	6.2 EMBRITTLEMENT EFFECTS	30
	6.2.1 Sigma Phase	30
	6.2.2 Transgranular Stress Corrosion Cracking	30
	6.2.3 Intergranular Stress Corrosion Cracking	31

.../cont.

CONTENTS, continued

		Page
7.	TITANIUM AND TITANIUM ALLOYS	33
	7.1 WELDABILITY	35
	7.2 CORROSION	37
	7.3 EMBRITTLEMENT EFFECTS	37
	7.3.1 Stress Corrosion Cracking	37
	7.3.2 Hydrogen Embrittlement and Delayed Fracture	40
8.	COPPER AND COPPER ALLOYS	48
	8.1 PURE COPPER AND HIGH COPPER ALLOYS	49
	8.2 BRASSES	51
	8.3 BRONZES	51
	8.3.1 Tin Bronzes	51
	8.3.2 Aluminum Bronzes	52
	8.3.3 Silicon Bronzes	53
	8.4 COPPER-NICKEL ALLOYS	53
	8.5 WELDABILITY	54
	8.6 CORROSION	56
	8.7 EMBRITTLEMENT EFFECTS	57
	8.7.1 Stress Corrosion Cracking	57
9.	COST AND DESIGN ASPECTS	57
	9.1 MATERIALS PROPERTY SPECIFICATIONS	57
	9.2 MATERIAL COSTS	58
	9.3 FABRICATED MATERIAL	60
	9.4 AVAILABILITY	61
	9.5 CLADDING	62
10.	SUMMARY OF PART I	63

.../cont.

CONTENTS, continued

		Page
	PART II - CORROSION	70
11.	INTRODUCTION	70
12.	CORROSION OF METALS	71
	12.1 GENERAL INTRODUCTION	71
	12.2 GENERAL PRINCIPLES	72
	12.3 ENVIRONMENTAL EFFECTS	75
	12.4 TYPES OF CORROSION	77
	12.4.1 Uniform Corrosion (or General Attack)	78
	12.4.2 Crevice Corrosion	78
	12.4.3 Pitting	79
	12.4.4 Intergranular Corrosion	82
	12.4.5 Stress Corrosion Cracking	84
	12.4.6 Galvanic Corrosion	85
	12.4.7 Erosion Corrosion	85
	12.4.8 Selective Leaching	85
13.	GROUNDWATER CHEMISTRY	86
14.	SELECTION OF CANDIDATE MATERIALS	88
	14.1 ALUMINUM- AND MAGNESIUM-BASE ALLOYS	89
	14.1.1 Aluminum and Aluminum-Base Alloys	89
	14.1.2 Magnesium and Magnesium-Base Alloys	91
	14.2 PLAIN CARBON AND LOW-ALLOY FERRITIC STEELS	92
	14.3 STAINLESS STEELS	94
	14.4 SUPERALLOYS AND HIGH-ALLOY AUSTENITICS	99
	14.5 TITANIUM AND TITANIUM ALLOYS	102
	14.6 COPPER AND COPPER ALLOYS	107
15.	SUMMARY OF PART II	111

.../cont.

CONTENTS, concluded

		Page
16.	CONCLUSIONS	116
	ACKNOWLEDGEMENTS	118
	REFERENCES	119
	TABLES	135
	FIGURES	166

- Encapsulate irradiated fuel in copper containers having a wall thickness of 200 mm and inner bore around the fuel.

- Encapsulate vitrified high-level waste in a titanium outer container, of wall thickness 6 mm, which is lined with high-purity lead 30[illegible] thick.

---

* CANDU = Canada Deuterium Uranium

** MAD = Megawatt-day, where a megawatt is a million watts

1. INTRODUCTION

As part of the Canadian program for the safe management and disposal of radioactive fuel wastes from CANDU* nuclear reactors, a study is being made of the immobilization and disposal of irradiated fuel bundles in a stable, deep, hard-rock vault[1,2]. If, after a comprehensive assessment phase, the disposal concept is considered to be valid, the overall program calls for the construction of a demonstration vault in which active experiments will be monitored as part of the evaluation of the complete facility. Ultimately, an industrial-scale vault for the permanent disposal of irradiated fuel is planned. One of the active experiments in the demonstration vault will involve emplacing a quantity of radioactive fuel isolated from the host environment by specially engineered containers[2].

The approach being used in the Canadian Nuclear Fuel Waste Management Program is closely similar to that adopted by several other countries[2]. For example, the Swedish nuclear power utilities, in response to government legislation, organized a joint project (the KBS** project) to develop and assess concepts to safely immobilize and dispose of irradiated fuel and vitrified high-level waste. They recommended that final disposal should be in igneous rock at a depth of about 500 m. Their proposals for immobilization are as follows[3]:

- Encapsulate irradiated fuel in copper containers having a wall thickness of 200 mm and invest lead around the fuel.
- Encapsulate vitrified high-level waste in a titanium outer container, of wall thickness 6 mm, which is lined with high-purity lead 100 mm thick.

---

* CANDU ≡ CANada Deuterium Uranium

** KBS ≡ Kärnbränslesäkerhet = Nuclear Fuel Safety

Due to time constraints, however, these proposals were not optimized in terms of container design and fabrication.

The objective of the present assessment is to select a short list of candidace container materials for a relatively simple containment system to be emplaced during the demonstration phase of the program, but with the future option of permanent disposal. Thus, the containers should be capable of retrieval for at least the duration of the demonstration. A container design life of at least 500 years before perforation has been selected during which time the fission product activity of the fuel will decay substantially[2]. The following assumptions concerning the conditions in the hard-rock vault will also be taken into account in the material selection and container design:

1. The container temperature will be 150°C or less.
2. Groundwater will contact the container (a brief discussion of groundwater composition is given in Part II of this report).
3. The vault may be expected to flood to its depth below the surface (500 - 1000 m), creating a hydrostatic pressure which the container must withstand without being breached.

As an initial approach, a simple, cylindrical metal container is being considered. Since the container must by definition be leak-tight, end closures will be joined to the cylindrical body by welding. The materials selected in this assessment may be used to fabricate and test a number of prototype containers.

Two basic concepts for the design of a simple container are being examined, both of which use a cylindrical shell of large diameter (300 - 900 mm). In the stressed-shell concept, the container itself is designed to independently support the stresses imposed by fabrication,

handling and subsequent service in the disposal vault. This will necessitate a fairly large wall thickness, in the range 10 - 50 mm, depending on the material, container diameter and vault depth. In the supported-shell concept, the design is such that the externally imposed hydrostatic stresses on the container will be supported by an internal medium. A number of options for the supporting medium are being studied, such as:

1. investment with a fairly low-melting-point metal, e.g., lead, zinc, aluminum, or their alloys;

2. packing with a particulate material, e.g., sand, glass beads;

3. fabrication of internal periodic, rigid bracing.

Thus the wall thickness of a supported-shell container can be appreciably smaller than that of a stressed-shell container and, in the absence of other criteria, would be determined primarily by the handling stresses and required corrosion allowance. The final design of a fuel immobilization container for the demonstration and commercial vaults will be based, at least in part, on the present materials assessment, future laboratory studies, and the container fabrication and testing program.

In the following section, simple guidelines for material selection are proposed. They attempt to take into account the specialized application of the material (containment of radioactive fuel), the specific type of disposal environment (hardrock vault at a depth of 500 - 1000 m)[2], and the remote-handling procedures likely to be involved in the container fabrication.

2. GUIDELINES FOR MATERIAL SELECTION

Ideally, the material chosen should conform to the following guidelines:

1. The simplest matrix microstructure consistent with other requirements, i.e., a single-phase pure metal or solid-solution alloy, so that complicating effects due to precipitation hardening, tempering treatments, etc. are not deliberately introduced into the fabrication process.

2. A stable microstructure, to avoid adverse metallurgical changes during long periods at low temperature.

3. Adequate short-term strength and impact resistance, to support the fuel and to withstand handling and accidental impact loading. The container must resist buckling, collapse and/or excessive creep under the hydrostatic pressure attained if the vault floods (9.8 MPa at a depth of 1000 m). There is likely to be some flexibility here for selecting different materials with different strengths to give a range of container thicknesses with the same specific strength.

4. Good weldability with, preferably, no requirement for pre- or post-weld heat treatment.

5. Acceptable toughness and cracking resistance in the parent and weld metal, to resist fracture generally, and also that due to delayed fracture mechanisms, such as stress corrosion cracking and hydrogen embrittlement.

6. Acceptably low rates of uniform corrosion and immunity to localized corrosion, e.g., pitting and crevice corrosion, in the vault environment.

7. Preferably an established background of knowledge and experience.

8. Reasonable assurance of an adequate supply at acceptable cost.

The range of commercially available metals and alloys used for structural and containment applications can be categorized as:

1. Low-melting-point alloys, e.g., aluminum-base, magnesium-base.

2. Plain carbon and low-alloy ferritic steels.

3. Stainless steels:
   - ferritic
   - austenitic
   - martensitic
   - precipitation hardening
   - austenitic/ferritic

4. Superalloys and high-alloy austenitics:
   - nickel-copper - Monels
   - nickel-chromium - Inconels, Hastelloys Nimonics
   - iron-nickel-chromium - Incoloys

5. Commercially pure titanium and its alloys.

6. Commercially pure copper and its alloys.

The above list is not exhaustive and does not include the refractory metals, for example, or zirconium and its alloys.

This study considers the important properties of the alloy groups above, either in general or with special reference to the more likely specific alloys within a group. Part I discusses some of the

physical metallurgy aspects of the alloy groups, particularly as they affect mechanical properties, weldability, delayed fracture processes and, to some extent, metallurgical compatibility. Since corrosion behaviour is clearly of prime importance for this application, it is discussed separately in some detail in Part II.

Since this review attempts to cover the broad spectrum of available engineering metals and alloys, it was necessary to adopt a selective approach in order to limit its size. This was achieved by placing greater emphasis on those aspects of the properties and behaviour of a material that are both controversial and perceived to be a potential limiting factor in the fabrication and performance of containers for fuel immobilization. Conversely, those aspects of properties and behaviour that are non-controversial and understood and will not, in themselves, limit the container integrity, are considered in less depth.

Some overlap exists in Parts I and II in some specific areas, e.g., stress corrosion cracking, which has both a mechanical and environmental component. In these cases, Part I emphasizes the physical metallurgy and fracture toughness aspects whilst Part II concentrates more on electrochemical factors.

PART I - PHYSICAL AND MECHANICAL METALLURGY

3. LOW-MELTING-POINT ALLOYS

3.1 ALUMINUM-BASE ALLOYS

Wrought aluminum-base alloys are basically divided into two groups namely, heat-treatable (H.T.) and non-heat-treatable. Most alloys are designated according to the Aluminum Association series[4] shown in Table 1, which indicates the major alloying additions and the amenability of the alloy series to heat treatment[4-6]. The 4000 series alloys have a rather specialized use and are not regarded as structural materials.

The strength properties of the pure aluminum and non-heat-treatable alloys are developed by strain hardening (cold working), and by alloying additions which promote either solid solution or second-phase dispersion strengthening. In the 3000 series alloys, manganese additions produce dispersed precipitates, whereas in the 5000 series magnesium in solution is the main strengthening agent.

In the heat-treatable aluminum alloys, the alloying additions are retained in solid solution by quenching from an elevated temperature (solution heat treating). Strengthening is then effected by precipitating a portion of the soluble elements in a finely divided form during an age-hardening heat treatment.

The range of strength and ductility which can be developed in some commonly used alloys is shown in Table 2. For the non-heat-treatable alloys, the thickness requirements place a practical limit on the strengthening that can be achieved by cold working. Thus, for thicknesses in the range 15-50 mm, the highest minimum yield strengths

are generally < 210 MPa. Moreover, the ductility in these high-strength conditions can be fairly low (∿ 5%). Appreciably higher minimum yield strengths can be developed in the heat-treatable alloys, without thickness limitations, although the ductility in the high-strength conditions is again low. In the annealed condition, the yield strength of all the aluminum alloys is quite low, typically 28-140 MPa. Moreover, being low-melting-point alloys, the strength in any condition decreases markedly with increase in temperature, and, at 150°C, the yield stress of the non-heat-treatable alloys (even in the fully cold-worked temper) and of most of the heat-treatable alloys, is less than 210 MPa[5].

With extended service at ∿ 150°C, the yield stress of all alloys would be expected to decrease progressively due to overageing in the heat-treatable alloys and recovery processes in the cold-worked alloys[6]. Typical age-hardening temperatures for aluminum-base alloys are 100 - 175°C, which embraces the possible service temperature of the container. Thus, unless very heavy section thickness are used, container buckling due to creep is likely to occur under the hydrostatic pressure developed in the event of flooding of the vault.

With the exception of the heat-treatable 2000 and 7000 series, most aluminum-base alloys can be welded by conventional techniques, gas metal-arc and gas tungsten-arc being the most commonly used[7,8]. Welds in the heat-treated alloys, particularly the 2000 and 7000 series, are characterized by low joint efficiency and a lack of ductility. After post-weld ageing, the strengths are similar to, and the ductilities are lower than, those obtained in some non-heat-treatable alloys, which do not require post-weld thermal treatment. Solution heat treatment and ageing after welding restore much of the strength, but the ductility remains low (∿ 1-3% elongation). The low ductility in heat-treatable alloy welds is due to remelting of low-melting eutectic constituents, mainly at grain boundaries[7]. These intermetallic phases cause the observed brittleness after welding. In thick sections, the weld stresses alone may be sufficient to cause fissuring in the eutectic regions of

the heat-affected zone. This problem has not been adequately solved in most heat-treatable alloys and they are, therefore, not generally recommended for welded pressure vessels or containers[8]. The non-heat-treatable alloys, however, do not suffer from embrittlement problems although, due to recrystallization in the heat affected zone, there is a considerable loss of strength after welding which cannot be recovered. Typically, the yield strength in gas metal-arc welds is < 150 MPa, although the ductility is reasonably high[7].

Stress corrosion cracking (SCC) has not been reported in any of the non-heat-treatable alloys, with the exception of series 5000 Al Mg alloys containing > 3% Mg[9]. However, problems due to general corrosion and SCC do arise in the heat-treatable alloys, e.g., Al-Cu, Al-Zn-Mg, and Al-Zn-Mg-Cu, when exposed to some environments, particularly those containing chlorides with or without oxygen[9]. Failure due to SCC is invariably intergranular and appears to be associated with grain boundary precipitation effects, either during fabrication or natural ageing during service. In the Al-Mg alloys, which do not depend on precipitation strengthening, appreciable magnesium is retained in solution after annealing or stabilization heat treatments. Subsequent precipitation of a Mg-Al intermetallic phase can render the material susceptible to SCC. At low service temperatures, such a sensitized microstructure may take many years to develop[10]. Moreover, although 3% Mg is generally considered to be the lower limit for observation of SCC, alloys containing 2.77% Mg (which is approaching the lower limit for most commercial Al-Mg alloys) have failed in laboratory tests after extended periods of time ($\sim$ 8 years at $\sim$ 90°C) during alternate immersion in 3.5% NaCl solution[11]. In an Al-5% Mg alloy, SCC has been observed in extremely dilute NaCl solutions ($\sim$ 50 µg/g) when stressed at about 75% of the yield stress[12].

The most effective method of preventing SCC, and improving the general corrosion of some alloys, is to clad the susceptible material with a more anodic nonsusceptible aluminum-based material. This technique is widely used on Al-Cu and Al-Zn-Mg alloys.

3.2 MAGNESIUM-BASE ALLOYS

The technological base for magnesium alloys is considerably less extensive than for aluminum alloys and only a relatively small fraction of the magnesium produced today is used in the manufacture of structural alloys. Most alloys can be divided into two groups: those used at low temperature (< 100°C) and those used at elevated temperature (> 150°C)[13-15]. The former group is based essentially on the Mg-Al-Zn and Mg-Zn-Zr systems, while the second group contains thorium and rare earth elements as major alloying additions. Depending on the alloy, strengthening is developed either by strain hardening during fabrication or by age hardening, although the response to heat treatment is limited compared to the high-strength aluminum-base alloys. Yield strengths are generally less than 210 MPa for heat-treatable alloys, and less than 140 MPa for cold-worked alloys, although on a strength/weight basis, magnesium alloys are at least comparable to other common structural materials[13].

Magnesium alloys suffer from a similar loss of strength as aluminum alloys after extended periods at low temperatures (∿ 150°C), resulting in low yield strengths (70-140 MPa) and relatively poor creep properties. A further problem with magnesium alloys used in compression is that the yield stress in compression is ∿ 15% lower than in tension[13] due to the preferred orientation developed during fabrication. In addition, the modulus of elasticity is less than a quarter that of steel, i.e., magnesium alloys thus require relatively thicker sections for a given deflection. Finally, in relation to design, many alloys are relatively notch sensitive, exhibiting low ductility and fracture toughness.

Most wrought magnesium alloys can generally be welded satisfactorily, gas tungsten-arc and gas metal-arc again being the most commonly used techniques[7,8,13]. The heat required is lower than that for most other structural metals due to a combination of low melting

point, low latent heat of fusion and low specific heat. However, their high thermal conductivity and coefficient of thermal expansion may result in more distortion and higher welding stresses than with other materials. Post-weld stress-relieving heat treatments (150 - 260°C) are specified for many alloys to reduce their susceptibility to SCC. Such cracking tends to occur in the heat-affected zone (HAZ) of the weld and is usually transcrystalline. In cold-worked or precipitation-hardened alloys some loss of strength may occur in the HAZ, compared to the base metal and weld deposit, due to local recrystallization and grain growth or partial resolution and overageing, or both[7,8].

The general corrosion properties of magnesium alloys in atmospheric or aqueous environments are inferior to those of aluminum alloys, and in many situations are only comparable to low carbon steels[14]. On exposure to water, a hydroxide film forms which undergoes spontaneous exfoliation. This is due, apparently, to the presence of compressive stresses in the film, so that, in general, film formation offers only slight protection[13]. Wrought magnesium alloys, in particular, are also susceptible to SCC in chloride-containing environments. Alloying additions of aluminum and zinc, especially aluminum up to $\sim$ 6%, increase the susceptibility to SCC.

4. PLAIN CARBON AND LOW-ALLOY STEELS

This group of materials is the most widely used for general structural and containment applications because the materials are relatively inexpensive and have properties that are adequate for most purposes[7,8,16].

Alloys in this group are readily available in large diameter (up to 1.2 m O.D.) and heavy wall-thickness pipe, either seamless or welded. Specifications for pressure pipe and pressure tube material

call for yield strengths in the range 210-300 MPa, depending on the alloy composition, grade and method of fabrication.

Welding of low-carbon and low-alloy steels is readily achieved using most of the commercial techniques. Preheating and, less frequently, post-weld stress relieving may be necessary, particularly for large section sizes (> ∿ 25 mm thickness), depending on the carbon content and amount of alloying additions[7,8,16]. The amount of martensite formed during cooling from the weld temperature increases with cooling rate and carbon content (in alloy steels the carbon content is effectively increased in accordance with the "carbon equivalence" of the particular alloying elements). Moreover the hardness of the martensite increases with carbon content. If significant quantities of martensite are formed during welding, post-weld tempering of the HAZ is usually required. Carbon steels containing > 0.5% C are difficult to weld because of their susceptibility to cracking. Medium carbon steels (0.25 - 0.5% C) can be satisfactorily welded, but preheating and/or post-heating are often necessary, particularly in large sections. Low-carbon steels (< 0.25% C) can generally be welded with no special precautions. Hydrogen embrittlement during and after welding can be a problem in steels but is usually controlled by proper attention to the welding parameters, e.g., cooling rate and electrode composition.

The most serious and obvious disadvantage of carbon and low-alloy steels, however, is their relatively poor corrosion properties (see Part II). Uniform corrosion rates in the atmosphere, water or soil generally fall within the range of 0.025 - 0.15 mm/a depending on the specific conditions[16,17]. Moreover the rates of pitting corrosion may be appreciably greater (∿ 0.3 mm/a). Improvements in the corrosion properties by small alloying additions of copper, chromium or manganese only reduce corrosion rates by a factor of about two.

5. STAINLESS STEELS

There are several excellent reviews which discuss the physical metallurgy and properties of stainless steels[18-23]. These alloys are used primarily in corrosion-resistant and heat-resistant applications. In the following, some of the more important aspects of the commercially available stainless steels will be reviewed with regard to their potential use as container materials.

5.1 FERRITIC STAINLESS STEELS

The ferritic (α) stainless steels are based on the Fe-Cr system with chromium contents in the range 11-30% (more generally 17-29%). High-purity Fe-Cr alloys with $> \sim 12\%$ Cr are ferritic at all temperatures due to the closed austenite (γ) loop in the Fe-Cr phase diagram. However small amounts of carbon and nitrogen and other γ stabilizers expand the loop and broaden the ($\alpha+\gamma$) phase region. For example, the ($\alpha+\gamma$)/α phase boundary is shifted to $\sim$ 29% Cr with the addition of 0.05% C and 0.25% N[24] (see Figure 1[18] for the individual effect of carbon). Consequently many commercial AISI 400 ferritic stainless steels undergo partial transformation to the γ-phase during heat treatment, depending on the exact quantities of γ- and α-forming elements present. The γ-phase transforms to either (a) ferrite and carbides at slow cooling rates, or (b) martensite or retained γ-phase at high cooling rates.

The typical compositions and mechanical properties of some AISI series 400 ferritic stainless steels and various proprietary modifications are shown in Table 3.

5.1.1 Welding

Welding of ferritic stainless steels is generally considered to be a problem because:

1. the absence of a phase transformation in many alloys allows coarse grains to develop in the weld and HAZ, which causes embrittlement at room temperature (because of greater atomic mobility in the ferritic structure, grain growth is considerably more rapid than in austenitic stainless steels), and

2. if the steel passes through the ($\alpha+\gamma$) phase field during welding, ferrite grain growth occurs, with subsequent γ-phase precipitation as a grain boundary network and as a coarse Widmanstatten lath structure. On cooling to room temperature the γ-phase transforms to martensite, resulting, for example, in marked embrittlement and poor stress corrosion resistance in a 17% Cr (type AISI 430) steel unless it is heat treated after welding (Figure 2[25]). In type 442 (21% Cr) however, solute partitioning depresses the temperature at which martensite formation begins (M_s), such that any γ-phase formed is retained at room temperature, resulting in a less brittle weld.

Although post-weld tempering can alleviate the martensite embrittlement problem, the coarse ferrite grain structure after welding remains. Moreover, post-weld annealing may precipitate carbides which can further harden and embrittle[25].

5.1.2 Embrittlement Effects

5.1.2.1 Grain Size

Chromium-rich ferrite is naturally brittle and ferritic stainless steels show a ductile-brittle cleavage transition at a temperature

considerably higher than that for mild steel[26]. Grain growth is known to occur quite rapidly above ∿ 600°C in these materials and, since the impact transition temperature increases with grain size (Figure 3), this constitutes a major problem, particularly with regard to welding[25]. Grain growth can be restricted by the addition of stabilizing elements such as titanium or niobium which produce undissolved carbonitrides. However post-weld annealing of these stabilized steels may precipitate further NbC or TiC in a finer form, again causing hardening and embrittlement.

5.1.2.2 475°C Embrittlement

Ageing Fe-Cr alloys for extended periods at temperatures near 475°C causes marked low-temperature embrittlement[18]. However, for most practical purposes, some degree of embrittlement can occur within the temperature range 320-550°C, particularly for 16-26% Cr content. The origin of the embrittlement is believed to be the existence of a solid state miscibility gap in the Fe-Cr system below ∿ 540°C (Figure 4)[18,27]. Below this temperature, decomposition occurs producing a fine, coherent chromium-rich precipitate (α'), which has the effect of greatly raising the impact transition temperature. The rate of embrittlement, i.e., the rate of precipitation, increases with chromium content (12% Cr alloys being least affected) and, at least for 18% Cr alloys, is accelerated by molybdenum additions. No additions have been found which prevent or significantly reduce the rate of α'-phase formation. The kinetics of the reaction appear to follow a nucleation and growth pattern[18], although spinodal decomposition has been suggested for alloys with higher chromium contents[28]. This is consistent with enhanced precipitation observed in Fe-30% Cr alloys[28]. Thus one of the principal unanswered questions is the minimum temperature at which the reaction can be detected after very long times. This problem is important in the selection of a ferritic stainless steel for use in nuclear reactors at service temperatures of ∿ 315°C over the 40-year projected lifetime[29]. It is also of concern when considering these

materials as containers for fuel immobilization at somewhat lower service temperatures, but for even longer times.

5.1.2.3 Sigma (σ) Phase

Sigma phase is a slightly chromium-rich Fe-Cr intermetallic compound which is extremely hard and brittle. It often forms as a continuous grain boundary film and can result in a degradation in ductility and toughness in stainless steels. In Fe-Cr alloys, σ-phase generally forms very slowly at temperatures > 520°C and chromium contents > ∿ 20%[18,30], though experimental data from long-term ageing studies (76 000 h) show that σ-phase can form in cold-worked alloys (12-16% Cr) at 480°C[31]. This apparently occurs by overageing of the α'-phase and gradual replacement of the α'-phase by σ-phase. The overlapping of these two precipitation reactions is shown schematically in Figure 5[32]. The addition of manganese, molybdenum, silicon and phosphorus greatly enhances the σ-phase formation kinetics, as does cold working. With increasing chromium content, the nose of the time-temperature-transformation (TTT) curve for σ-phase formation moves to higher temperatures and shorter times[18].

5.1.2.4 Ductile - Brittle Transition Temperature (DBTT)

The temperature of the ductile to brittle transition is clearly of paramount importance in the application of ferritic stainless steels. Unfortunately, as indicated earlier, most factors involved in fabrication increase the transition temperature. The practical situation is well illustrated in Figure 6 which shows that the DBTT increases with section thickness[30]. At thicknesses > ∿ 6.5 mm, the DBTT is above room temperature for most alloys. The effect of thickness on ductility stems from:

1. the smaller grain size that can be achieved with increase in rolling reduction. Since thinner material receives more cold reduction, it generally has smaller grains and is tougher.

2. the effect of thickness on the cooling rate from the annealing temperature. In alloys with higher chromium contents, fast cooling improves the toughness due to the shorter exposure time in the α'-phase precipitation range (320-550°C).

Both of the above effects are likely to be important during welding operations since grain growth will occur and, in thick sections, the cooling rate from the welding temperature will be slow. Both factors produce an increase in DBTT in the weld HAZ and possibly in the weld metal.

5.1.2.5 Intergranular Corrosion

Ferritic stainless steels are susceptible to intergranular corrosion in the HAZ of welds. This is due to precipitation of chromium carbides and nitrides at ferrite grain boundaries, with a consequent local depletion of chromium in solution and, hence, preferential corrosion[18]. This sensitization occurs only at temperatures > ∿ 900°C (e.g., welding) due to the low solubility of carbon and nitrogen in ferrite. It may be overcome to some extent by post-weld annealing at 650-850°C, to even out the chromium gradient, or by using steels stabilized with titanium or niobium[19]. However, the sensitization in ferritic stainless steels is extremely rapid compared with the austenitic stainless steels because of the greater diffusion rates of chromium, carbon and nitrogen[18]. Thus sensitization can occur even with extremely rapid cooling rates, and at low carbon contents (∿ 0.03%).

5.1.2.6 Stress Corrosion Cracking

In contrast to austenitic stainless steels (see Section 5.2), one of the major advantages of ferritic stainless steels is their relative immunity to transgranular stress corrosion cracking, particularly in chloride environments[19,21,30]. However the resistance to SCC can be greatly impaired after welding because of the presence of grain

boundary networks of martensite or retained austenite. Also, the presence of chromium carbides at the α-grain boundaries can lead to a form of stress-accelerated intergranular corrosion, leading to severe cracking[25,33]. It is, therefore, essential to post-weld heat treat these materials to overcome these embrittlement effects.

5.1.3 Corrosion

Although general corrosion behaviour is covered in detail in Part II of this assessment, it should be pointed out here that the excellent corrosion resistance of ferritic stainless steels is due to the formation of a stable, passive chromium oxide film. The addition of molybdenum (AISI 434, 436) improves the stability of the protective film and confers added resistance to pitting corrosion in chloride environments.

5.1.4 Recent Developments

Over the past ten years, some of the problems of ferritic stainless steels have been partially overcome, due to developments in melting technology and alloy design[21,22,30,34]. The application of electron beam hearth refining, argon-oxygen decarburisation (AOD) and other processes has enabled extremely low (C + N) contents (< 0.02%) to be attained, with some improvements in toughness and a marked increase in the resistance to intergranular corrosion. Alloy development has proceeded mainly at the higher chromium levels with the introduction of 26% Cr - 1% Mo and 29% Cr - 4% Mo alloys (Table 3). The molybdenum improves the resistance to pitting corrosion. The resistance to stress-corrosion cracking of these fully-ferrite materials in a chloride environment is superior to that of the 300 series stainless steels. However, as indicated in Figure 6, they still exhibit a DBTT, due to grain size and α' precipitation effects, which exceeds room temperature, and which, in any case, has not been firmly established in material thicknesses greater than $\sim$ 0.6 cm[35,36]. In addition, very stringent shielding

precautions are required during welding (similar to those for titanium) to avoid contamination by elements which dissolve interstitally, e.g., oxygen, nitrogen and carbon. For thicker sections, pre- and post-weld heat treatments are also recommended.

5.2 AUSTENITIC (γ) STAINLESS STEELS (WROUGHT)

5.2.1 Constitution

The addition of nickel to 18% Cr steels enlarges the γ loop considerably (Figure 7). Increasing nickel has two principle effects on the constitution and microstructure[18,19]:

(i) It increases the amount of γ present at the solution treatment temperature (∿ 1050°C), but at low nickel contents the γ may transform partially to martensite.

(ii) It decreases the M_s temperature; at about 8% Ni the M_s is just below room temperature, so that the metastable γ is retained after cooling from the solution-treatment temperature.

An 18Cr-8Ni low-carbon steel (∿ 0.01% C) is borderline with respect to a fully γ structure, and may contain some δ ferrite. Since carbon is a powerful γ stabilizer, however, an 18Cr-8Ni-0.1C steel is fully γ above ∿ 900°C, although the M_s is only just below room temperature.

The standard austenitic stainless steels are those contained in the AISI "300" series shown in Table 4, in which the stability of the γ-phase increases from 301 (16 - 18 Cr, 6 - 8 Ni) to 310 (24 - 26 Cr, 19 - 22 Ni). Grades 304 (0.08% C) and 304 L (0.03% C) contain less carbon than 301 and 302 steels; similarly, grades 316 and 316 L are low carbon, but contain 2% Mo for improved resistance to general and pitting

corrosion in chloride solutions and H_2SO_4. However, the nickel content is increased in these steels (10 - 14%) to compensate for the ferrite-forming tendency of molybdenum[19].

The standard γ stainless steels cannot be strengthened by heat treatment but, depending on composition and γ-phase stability, they work-harden rapidly when cold-worked, due to martensite formation. Typical yield strengths in the annealed condition are 210 - 280 MPa accompanied by high ductility. Due to the lower carbon content, the strength of the "L" grades is somewhat less than the standard grades.

5.2.2 Welding and Weld Decay

Austenitic steels can be readily welded by most of the conventional techniques with no brittle structures occurring in the HAZ. Some detrimental effects can, however, arise[7,18,19,25,37.38]:

(i) A fully γ weld metal can produce hot cracking (crater cracking) because of contraction stresses accompanying solidification of the weld. This can be overcome by ensuring that the weld metal contains a small quantity (∿ 5%) of δ-ferrite.

(ii) Various forms of liquation cracking can occur in the weld metal and HAZ if low-melting-point phases such as borides are present.

(iii) During welding, parts of the HAZ are heated in the range in which $Cr_{23}C_6$ precipitates at the γ grain boundaries. This locally lowers the chromium content, so that preferential corrosive attack can occur in the chromium-depleted zone adjacent to the grain boundaries. This is the well known process of "weld decay"; it occurs due to a "sensitization" heat treatment, which may consist of

slow cooling through the sensitization range (450-850°C), as in welding, or isothermal annealing within this range[37]. Intergranular corrosion of sensitized material can occur at ambient temperatures in very dilute aqueous solutions containing chlorides, oxygen or both. Although stress is not a prerequisite, the rate of attack increases quite markedly with both stress and temperature[37]. During welding, the degree of sensitization depends on alloy composition (particularly carbon content), heat input and the rate of cooling; high heat inputs and slower cooling rates favour increased sensitization. A number of post-weld remedial heat treatments can be carried out, such as solution treatment at ∿ 1050°C to dissolve grain boundary carbides or annealing at ∿ 900°C to even out the chromium gradient. These have the disadvantage, however, of introducing potential distortion during heating and problems associated with achieving a rapid cooling rate from the heat treatment temperature to prevent further carbide precipitation.

The problem of sensitization during welding can usually be overcome by:

1. the use of low-C (< 0.03%) steels specially developed for this purpose, e.g., AISI 304 L or 316 L.
2. the use of stabilized steels, e.g., AISI 321 or 347, containing small additions of titanium and niobium, respectively, which preferentially form carbides and reduce the carbon in solid solution to levels below which $Cr_{23}C_6$ will form.

Although low-C austenitic steels (0.03% max.) are generally immune to sensitization during welding, the carbon content still exceeds the solubility limit, so that sensitization would still occur during

extended holding[18,37]. The kinetics of precipitation of chromium carbide are diffusion-controlled and are expected to follow the usual time-temperature-transformation relationship. The question arises as to the lowest service temperature at which carbide formation would occur over long times. When considering the immobilization of fuel, it is important to assure a reasonable margin between the service temperature and temperatures at which sensitization may occur after long times. An Argonne National Laboratory study, for example, quotes a maximum temperature for AISI 304L of 343°C for 100-year retrievable storage in air[39]. Atlantic Richfield Hanford has recommended a maximum temperature of ∿ 275°C for normal conditions and 427°C for abnormal conditions for long-term (∿ 100 years) retrievable sealed-cask storage[40].

The stabilized grades of stainless steel (AISI 321, 347, 348) are usually more difficult to weld successfully, particularly in thicker sections[7,25]. They can be susceptible to cracking in the HAZ immediately adjacent to the fusion line in the as-welded condition or after stress relieving. AISI 347 is especially prone to this type of cracking, which can be associated with either hot shortness or strain-induced precipitation of NbC, usually during post-weld heat treatment or during service. In exceptional circumstances, all three steels can become sensitized in a narrow zone adjacent to the weld in which the NbC or TiC is dissolved during welding. Subsequent exposure at ∿ 650°C results in preferential grain-boundary precipitation of chromium carbides in this zone, which consequently becomes sensitized and susceptible to intergranular attack[25]. This so-called "knife line attack" is overcome by post-weld annealing at ∿ 900°C, to reprecipitate the Nb or Ti carbide in the affected zone. This form of sensitization can occur, for example, during multi-pass welding on thick plate in which a potentially susceptible zone created by one pass is sensitized by a subsequent pass[37].

5.2.3 Embrittlement Effects

5.2.3.1 General

Unlike ferritic stainless steels, the austenitics do not suffer from 475°C embrittlement. On heating to 500 - 900°C, however, the brittle intermetallic σ-phase can occur[18]. The tendency for σ-phase formation increases with chromium content, and molybdenum, titanium, silicon and niobium also promote its formation. Precipitation of σ-phase from γ-phase is relatively sluggish but, if δ-ferrite is present, this rapidly transforms to σ-phase and γ-phase due to the δ-ferrite being richer in chromium than is the γ-phase. In general though, σ-phase does not present a problem in the austenitic alloys unless they are exposed for prolonged periods between 500 and 950°C.

5.2.3.2 Stress Corrosion Cracking

The principle problem with the use of austenitic stainless steels is their susceptibility to SCC due to a combination of residual and/or applied stress with a suitable corrosive environment; the most potent are those containing halides, especially chlorides. There is a considerable volume of literature on this topic[41-44], the details of which are beyond the scope of this review, but in general SCC is enhanced by increases in the chloride and/or oxygen content, temperature and stress level. Sensitization (Section 5.2.2) due to welding or stress relieving increases the susceptibility to SCC, although the crack path is usually intergranular, as opposed to the transgranular cracking typically observed in the absence of sensitization[44]. The role of solution pH is less clearly defined, mainly because of the difficulty in relating pH at a crack (often unknown or not measured) to that of the bulk solution. In general though, the higher pH solutions (but not actually caustic) appear less likely to cause cracking[44].

Although the factors of importance to SCC are well known qualitatively, there are no models available which allow a reliable quantitative prediction of the possibility of SCC or time of failure. Moreover, it has been stated that even the considerable amount of empirical data available is generally inadequate in attempting to estimate the probability of failure[45]. On the other hand, there are many successful practical applications of γ stainless steels where both chlorides and stresses near the yield stress are present. It is difficult therefore to define upper limits of the various parameters below which safe operation can be assumed.

Truman has pointed out in a survey of service failures that most failures occurred at temperatures > 70°C, although the same author has clearly demonstrated SCC in 304 stainless steel at 60°C in an aqueous solution of 10 000 µg/g NaCl at a pH of 2[45]. Other results indicate that SCC can occur with very low chloride levels (< 2 µg/g) in aerated water, although deaerated water is considerably less aggressive[41]. However, even in relatively pure environments, concentrating effects due to reflux mechanisms, or at crevices, can further promote and accelerate SCC. Stress levels often approach the yield stress in many as-fabricated components, but it is also known that SCC can occur at lower stress levels, with the possibility of a threshold value, for given conditions, below which SCC will not occur. Experimentally measured values of this stress for specific conditions are difficult to apply generally, and moreover, the levels of stress involved in a practical situation cannot be determined simply.

Finally, it is interesting to note that Sandia workers have eliminated the 300 series type stainless steels from their list of candidate alloys for waste and fuel immobilization containers for the Waste Isolation Pilot Plant because of the likelihood of SCC in the salt environment[46].

5.3 MARTENSITIC STAINLESS STEELS

These steels generally contain 12% - 18% Cr with sufficient C (0.1 - 0.6%) and other austenite formers, such as nickel, to ensure that the structure is fully γ at a solution treatment temperature of $\sim$ 1050°C; this produces a martensitic structure on air cooling to room temperature[18,19]. The compositions of some of the standard AISI grades of martensitic stainless steels are shown in Table 5. To develop optimum strength, toughness and resistance to SCC, tempering of the martensitic structure is required. Secondary hardening can be developed during heat treatment of these steels, but unfortunately the temperature at which maximum secondary hardening occurs (450 - 550°C) produces temper embrittlement and a minimum in fracture toughness (Figure 8). Consequently, these steels can be tempered either at low temperatures ($\sim$ 300°C) to give the highest strength but lower toughness and resistance to SCC, or at higher temperatures ($\sim$ 600 - 650°C) to provide good toughness at lower strength and the optimum resistance to SCC.

Somewhat higher strength 12% Cr stainless steels have been developed by alloy additions (Mo, V, Nb), which intensify the secondary hardening effect or produce precipitation hardening reactions based on NiTi, NiAl or Cu-rich intermetallics during tempering. Even greater strength increments can be achieved in the higher chromium (low carbon) precipitation hardening alloys; in order to produce a fully austenitic structure at the solution annealing temperature, and hence martensite on air cooling, these alloys have a higher nickel content (4 - 9%). Some typical compositions and mechanical properties of this group of alloys are shown in Table 6 (see Section 5.4).

In general, the martensitic stainless steels air-harden during welding (requiring post-weld heat treatment), are susceptible to temper embrittlement, possess the lowest corrosion resistance of all the stainless steels, and are susceptible to hydrogen embrittlement and SCC in a number of environments containing chlorides and sulphides[18,19].

5.4 PRECIPITATION HARDENING (PH) STAINLESS STEELS

There are three main categories of PH stainless steels, all of which are termed non-standard grades in the AISI classification:

1. PH martensitic steels
2. PH semi-austenitic stainless steels
3. PH austenitic stainless steels.

Some examples of alloys in each of the three categories are shown in Table 6, together with typical mechanical properties in the heat-treated condition[18,19,46].

PH martensitic steels were discussed briefly in the previous section. The PH semi-austenitic stainless steels are all essentially controlled transformation steels having compositions (Table 6) such that (a) austenite is retained at room temperature to facilitate cold work and fabrication, (b) the M_s temperature is sufficiently below room temperature to avoid transformation during fabrication, but high enough that transformation to martensite can be achieved by a simple technique, e.g. refrigeration after fabrication, (c) tempering and precipitation hardening to increase the proof stress can be carried out at low temperatures, < 500°C. These steels are relatively complex metallurgically and require close control of composition and thermal treatments to ensure the correct transformation characteristics. They are therefore expensive and their general use has been limited[19].

Precipitation hardening in the austenitic steels has been achieved by additions of carbon and nitrogen to Cr-Ni, Cr-Mn or Cr-Ni-Mn base steels, e.g., 21Cr-4Ni-9Mn and ageing in the temperature range 650 -800°C. Another hardening system is based on additions of carbon and phosphorus, e.g., Armco 17/10P (17Cr-10Ni) and Crucible HMN (18Cr-9Ni). The optimum ageing temperature is generally ∿ 700°C. Perhaps the most widely known PH austenitic steels are those containing

aluminum and titanium added to form the γ'-$Ni_3(Al,Ti)$ phases which provide age hardening. These steels contain at least 20% Ni in order to form γ'-phase, e.g., A 286 (26Ni-15Cr), Unitemp 212 (26Ni-14Cr). Ageing is generally carried out in the temperature range 750 - 800°C.

The main disadvantage of all PH stainless steels is the general requirement for post weld heat treatment to restore the strength and ductility in the region of welds. In addition, they tend to be metallurgically more complex and hence more expensive than the non-hardenable AISI 300 and 400 series steels. In particular, the PH austenitic steels are used for high strength, elevated temperature applications and hence overlap somewhat with the development of the precipitation-hardening Ni base superalloys (see Section 6).

6. SUPERALLOYS AND HIGH-ALLOY AUSTENITICS

There are well in excess of 100 alloys of standard and proprietary designation whose compositions fall between the true nickel-base superalloys and the AISI 300 series stainless steels[47-52]. Most of these materials are austenitic and were developed primarily for elevated temperature applications where combinations of high strength, creep and oxidation resistance are required. Other alloys combine moderate strength levels with high corrosion resistance for use at lower temperatures. It is not necessary to consider individually all the commercially available alloys since many of them refer to similar basic alloy compositions with only minor differences in specifications. This is especially true of the iron-base austenitic alloys containing $< \sim 35\%$ nickel and $< \sim 25\%$ chromium. On the other hand, the selection of more highly alloyed materials available, including nickel-base alloys, is more limited. This section will concentrate on those materials which have been developed primarily for corrosion resistance or

which have been successfully used in corrosive environments, particularly aqueous chloride. Of this group, those alloys which rely on a complex heat treatment to develop strength and corrosion resistance will not generally be considered.

Most of the alloys which have been used in corrosion resistant applications are shown in Table 7, grouped into iron- and nickel-base[47-52]. Representative room temperature mechanical properties are listed in Table 8[47-52]. Due to their high nickel and chromium contents, most of these alloys have a stable austenite structure, falling well within the γ-phase field of the Fe-Cr-Ni phase diagram, as shown in Figure 9[18,53,54].

Of the nickel-base alloys, Hastelloy C-276, which replaced Hastelloy-C, is very similar in composition to Hastelloy C-4, except that C-276 contains 4% tungsten. The C-276 alloy is, however, more popular and easier to procure. It contains ∿ 5% less chromium and nickel than Inconel 625, but has more iron and molybdenum, and additions of tungsten and cobalt. Inconel 600 has the largest nickel content (∿ 76%), and constitutional γ is the simplest alloy, containing only ∿ 15% chromium and ∿ 8% iron. The nickel content of Inconel 601 is similar to Inconel 625 (∿ 60%), although its composition (high chromium and aluminum additions) is essentially optimized for resistance to high temperature oxidizing, carburizing and sulphur-containing atmospheres[49].

Of the iron-base alloys, the nickel content ranges from ∿ 20% (AISI 310) to ∿ 42% (Incoloy 825), while the chromium varies between 20 and 25%. Some alloys contain between 2 and 6% molybdenum for increased resistance to localized corrosion (see Part II).

The strength of all these alloys depends, essentially, on solid solution hardening of the austenite matrix. Since, for most alloys, the most potent strengthening elements, interstitial carbon and nitrogen, are present in similar, small quantities, the strengths are

also similar. This is particularly evident in the iron-base alloys, with the possible exceptions of Carpenter 20 Cb-3 alloy and Incoloy 801, which can be precipitation-hardened. More important, the strengths in the annealed condition (lower values in Table 8) are generally only comparable to the annealed austenitic 300-series stainless steels. The outstanding exceptions to this are the high nickel-base alloys Inconel 625, Hastelloy C-276 and C-4, whose yield strengths in the annealed condition are appreciably higher. This is mainly due to their high molybdenum content[18]. Alloy C-4 has a somewhat lower strength due to its lower carbon content and the absence of tungsten. In some alloys, e.g., Incoloy 800, Inconel 625, age hardening can occur during high temperature service (> 500°C) due to precipitation of carbides, nitrides or γ' particles[49]. Note that the strength of the copper-nickel alloy, Monel 400, is significantly less than that of the iron-nickel-chromium alloys. Being face-centered-cubic solid solution alloys, the yield strengths are only weakly temperature-dependent with no significant changes in relative values. In the absence of localized embrittling effects (Section 6.2), all the alloys exhibit high ductility and fracture toughness. On the basis of strength, therefore, the principal alloys of interest are the molybdenum-containing nickel-base alloys.

6.1 WELDABILITY

The alloys being considered in this section can be welded by most processes, the most commonly-used being gas-tungsten-arc, submerged-arc and various gas-metal-arc techniques[8,55]. The mechanical properties of the weld metal itself and transverse to the weld are typically comparable to those of the annealed parent plate.

Nickel and its alloys are susceptible to high temperature embrittlement by sulphur, phosphorus, lead and some other low-melting-point substances. Therefore, cleanliness is an important requirement for successful welding[7,8,55].

A general characteristic of nickel alloys is the sluggish nature of the weld pool which limits penetration, compared with other metals. This usually necessitates the use of smaller lands in the root of the weld joint and, hence, a somewhat different joint design. For the best results, gas-tungsten-arc welding should be used for the root pass. Shielding of the weld root is usually required to avoid excessive oxidation or porosity on the underside of the weld bead.

Pre- and post-weld annealing are generally not required for high-nickel and nickel-base alloys, although care should be exercised to minimize sensitization of susceptible alloys (see Section 6.2.3).

6.2 EMBRITTLEMENT EFFECTS

6.2.1 Sigma Phase

Due to slow kinetics, the precipitation of σ-phase is generally not a problem in austenitic alloys, unless prolonged exposures in the range 500 - 900°C are incurred[18,54].

6.2.2 Transgranular Stress Corrosion Cracking

It is generally agreed that, as the nickel content of iron-chromium-nickel alloys is increased, the resistance to classical transgranular SCC in chloride or chloride plus oxygen environments also increases and, that above ∿ 45% nickel, SCC is not observed in the standard boiling 42% magnesium chloride test solution[37,41,42,56]. In fact, maximum susceptibility to SCC occurs at a nickel content ∿ 9%, which corresponds to the composition of most AISI 300 austenitic steels. Thus, the nickel-base alloys, e.g., Inconel 600 and 625, Hastelloy C-276 and C-4, have virtual immunity to transgranular SCC in many environments. Alloys with intermediate nickel content, e.g., Incoloy 800 and 825, Carpenter 20 Cb-3, are more susceptible than nickel-base alloys, but are superior to the 300 series steels. Moreover, in general,

stresses at least as high as the yield stress are required for transgranular SCC in the intermediate nickel alloys[41,42]. As with the 300 series stainless steels, susceptibility increases with chloride and/or oxygen level and with temperature, although very few instances of SCC at temperatures < 200°C appear to have been reported. This observation is supported by both accelerated laboratory tests and service experience with commercial alloys[49].

6.2.3 Intergranular Stress Corrosion Cracking

Despite their virtual immunity to transgranular SCC in chloride solutions, the nickel-base austenitic alloys, and the iron-base alloys with high nickel content, can be quite susceptible to both intergranular corrosion and intergranular SCC in some environments[37,57-60]. Perhaps the most important environment which has caused cracking is high purity, high temperature water. This is especially well documented for Inconel 600 because of its use in primary circuits and steam generators for nuclear reactors, but is also well established in other high nickel alloys[37,57,58,59,61].

The degree of susceptibility to SCC depends on metallurgical conditions and may, therefore, be influenced by mill processing or welding fabrication[62-65]. Most alloys become more susceptible when thermal treatments cause grain boundary precipitation of carbides or intermetallic compounds. The material is then in a sensitized condition, and the overall effect on intergranular corrosion is similar to that in sensitized AISI 300 stainless steels, although the mechanism may differ in detail[37,57].

In the laboratory, susceptibility in high-nickel alloys is usually detected by a standard corrosion test[60,64]. The results of such tests indicate that, in the sensitized condition, none of the alloys considered in this section are consistently immune to intergranular corrosion. Material shown to be susceptible in a standard

evaluation test may or may not be attacked intergranularly in another environment; this must be established independently by tests in the specific environment.

As mentioned earlier, susceptibility to intergranular SCC increases when the alloy is in the sensitized condition. An important factor that contributes to sensitization in the high nickel austenitic alloys is the decreasing solubility of carbon in austenite with increasing nickel content[57]. Therefore, even with the low maximum carbon levels specified for some alloys (0.02% for Hastelloy C-276, 0.015% for Hastelloy C-4), large primary carbides, which are not deleterious with respect to corrosion, still exist in the microstructure after solution annealing at 1200°C[64]. The carbon solubility decreases with temperature and, during subsequent exposure in the range 600 -1050°C, secondary carbides precipitate at the grain boundaries. In most alloys, such carbides are chromium-rich, resulting in a chromium-depleted zone adjacent to the boundaries. However, in molybdenum-containing alloys, e.g., Hastelloys C-276 and C-4, molybdenum rich carbides precipitate, producing a molybdenum depleted zone[63,64]. It is these local variations in composition which can give rise to intergranular corrosion. In Hastelloy C-276, a carbon content < 0.004% is required to effectively eliminate secondary carbide precipitation[64].

Elements such as titanium and niobium are added to some alloys to form stable carbides and hence reduce the degree of chromium depletion during a sensitization heat treatment, e.g., Incoloy 800 and 825, Inconel 625. This certainly reduces susceptibility but does not eliminate it completely. Moreover, in Incoloy 825 at least, maximum stabilization is not obtained by relying on titanium carbide as the only stabilizing agent[62]. The principal mechanism used commercially is that of precipitating a mixed chromium-titanium carbide at a temperature (~ 950°C), where chromium diffusion is sufficiently rapid to prevent local chromium depletion. This minimizes further carbide precipitation (hence, sensitization) at lower temperatures. Incoloy 800 contains

< 0.06% titanium, which affords only limited protection against sensitization[66]. A development of this alloy, Incoloy 801, contains 0.75 - 1.5% titanium and this, together with a stabilization anneal similar to that used for Incoloy 825, provides greater resistance to sensitization[49]. Hastelloy C-276 does not contain any stabilizing elements but relies on achieving low carbon content to minimize carbide precipitation. Hastelloy C-4, a modification of C-276, is AOD melted and contains even lower carbon; moreover, titanium is added to C-4, making it more resistant to carbide precipitation than the C-276 alloy[64,65]. A complicating factor with both the Hastelloys is that carbide precipitation is not the only source of sensitization. Precipitation of a molybdenum-rich intermetallic phase occurs in the range 700 - 1100°C. Hastelloy C-276, for example, shows precipitation in about 6 min at 850°C. The compositional modifications in Hastelloy C-4 delay this sensitizing reaction for about two hours at the same temperature. Inconel 600 exhibits the greatest susceptibility to intergranular SCC of the high-nickel-content austenitic alloys[59]. This alloy does not contain stabilizing elements and, furthermore, has a relatively high maximum carbon content (0.15%).

There is some question as to whether intergranular SCC in these alloys is the result of carbide formation. One observation which suggests that it is not is that significant intergranular corrosion can occur even in the non-sensitized (solution annealed and water quenched) condition[58,59].

7. TITANIUM AND TITANIUM ALLOYS

Most of the advances in refining technology and alloy development associated with the manufacture of titanium and its alloys have occurred during the last 30 years as a result of the introduction of the Kroll process[67-69]. The use of titanium alloys has progressively

increased, the major applications being in the aerospace industry, where the high strength-to-weight ratio is of prime importance, and in the chemical processing, paper and petrochemical industries, where the main consideration is corrosion resistance.

The suitability of commercial pure (C.P.) titanium for the outer container for vitrified nuclear waste in Sweden has already been assessed in some detail[3,70], and a dilute titanium alloy, ASTM grade 12, is the current container reference material for the Waste Isolation Pilot Plant project[46].

Titanium has a close-packed hexagonal structure (α) at low temperatures, but undergoes a phase transformation to a body-centred cubic structure (β) at 885°C. A range of alloys has been developed to produce either α, β or (α+β) microstructures. Some elements (Al, Sn, C, O, N) stabilize the α-phase, whereas most substitutional elements (Fe, Mn, Cr, Mo, V) stabilize the β-phase. Much of the physical metallurgy of titanium is similar to that of zirconium.

The (α+β) titanium alloys constitute the largest group, since they can be heat treated to develop the high strengths demanded in the aerospace industry. However, the highest resistance to corrosion and hydrogen embrittlement effects is found in the C.P. and dilute alloy grades of α-titanium. The composition and mechanical properties of some commercially available titanium alloys are shown in Tables 9 and 10 respectively[71-73]. In addition to ASTM grades 1-3, which are essentially different purities of commercial titanium, two very dilute alloy grades are produced: Ti-0.2% Pd (ASTM grades 7 and 11), and Ti-0.3% Mo-0.8% Ni, of which the Titanium Corporation of America (Timet) product Ticode-12 is an example[72,74]. An important feature of Table 10 is the significant increase in yield strength, with some loss in ductility, as the impurity content, particularly of oxygen and iron, increases. Similarly, alloying additions produce significant strength increases. For example, the minimum yield strength of grades 3 and 12 titanium is

more than double that of grade 1. This is due to a combination of interstitial solute strengthening and the formation of small quantities of β-phase. Higher strengths are obtained in the more highly alloyed grades 5 (α-alloy) and 6 (α+β-alloy), but these materials have inferior corrosion properties and are more susceptible to SCC and hydrogen embrittlement effects compared to the C.P. or low alloy grades[74].

The Ti-0.2% Pd alloy has better corrosion properties than grades 1-3 but, at best, is only comparable in strength with grade 2, the most commonly used C.P. grade. Moreover, the Ti-0.2% Pd alloy is currently about 75% more expensive than grade 2[75]. The Ti-0.3% Mo-0.8% Ni (Ticode-12) alloy has greater strength than either the C.P. grades or Ti-0.2% Pd alloys, with corrosion properties approaching those of the Ti-0.2% Pd alloy for many applications; it is only ∿ 20% more expensive than the grade 2 alloy[76]. For a given design stress, this slight cost premium may be offset by the reduced thickness requirements in the stronger Ticode-12 alloy. However, although it has been accepted by ASTM as grade 12, it is a new alloy introduced in 1974 by Timet, so that there is only limited practical experience in its use.

One disadvantage of titanium and its alloys is that their strength decreases rather rapidly with temperature as shown in Figure 10[8]. This is essentially due to the strong temperature dependence of interstitial solute strengthening mechanisms. Thus at 150°C the yield strength of C.P. titanium is only ∿ 60% of the room temperature value, whereas for nickel- and iron-base austenitic alloys, the corresponding figure is ∿ 80%. As indicated in Figure 10, C.P. titanium is generally quite ductile and, moreover, is insensitive to notches. Its modulus of elasticity is about half that of austenitic alloys.

7.1 WELDABILITY

The only commonly used fusion welding processes which can be successfully applied to titanium alloys are inert-gas shielded arc

methods[8,77-79]. The tungsten-inert gas method is much more widely used than the metal-inert gas method. The use of these inert-gas techniques is essential due to the high affinity of titanium for certain elements, particularly oxygen, nitrogen, carbon and hydrogen. These dissolve interstitially and can result in severe embrittlement when present in relatively small quantities, as shown in Figure 11[8]. The rate of impurity absorption decreases with decreasing temperature, but remains significant even at 500°C. Therefore additional inert gas shielding must be provided during welding to protect those parts remote from the molten pool. This usually requires a trailing shield and a backing shield of argon gas to protect the as-welded surface and the weld root respectively. In general, good quality preparation and a high degree of cleanliness must be maintained during all phases of titanium welding if acceptable results are to be obtained. The same careful shielding precautions are also necessary for tack welding during setting up a joint.

For many corrosion applications, grade 2 titanium is selected as a compromise between the superior weldability of the low interstitial grades and the greater strength of the higher interstital grades.

Due to the α-β phase transformation in titanium, microstructural modifications occur during welding both in the fusion zone and HAZ. These consist of grain growth in the β-phase and the subsequent formation of a coarse acicular or serrated grain boundary α-phase morphology during cooling from the β-phase. This structure may exhibit somewhat lower strength and ductility than the equiaxed grain morphology typical of α-annealed material[8]. High heat inputs during welding should therefore be avoided to minimize both the extent of acicular α-phase and also the risk of impurity contamination. Due to the relatively low thermal conductivity of titanium, close control of heat input is required to avoid high metal temperatures[77].

Pre- and post-weld heat treatments are not usually required for C.P. titanium even on large section sizes, since its low expansion coefficient results in lower residual stresses than with most other materials. In addition, embrittlement problems associated with residual stresses in titanium are relatively rare. On the other hand, distortion during welding can be a greater problem in titanium due to the relatively rapid decrease in strength with temperature[77].

7.2 CORROSION

About one-third of all titanium produced is used in applications where corrosion resistance is of primary importance[74]. Consequently there is a considerable amount of data which demonstrates that titanium alloys in general, but particularly the commercial and dilute α-grades, are highly corrosion resistant[72,76,80].

7.3 EMBRITTLEMENT EFFECTS

7.3.1 Stress Corrosion Cracking

In the Swedish assessment of the suitability of titanium for a container for vitrified reprocessing waste, it was concluded that neither C.P. nor Pd-alloyed titanium is susceptible to SCC in the chloride concentrations found in sea water[70,81]. This conclusion is only partially correct. It is certainly true that few, if any, service failures of Ti or Ti-Pd alloys due to SCC in marine applications have been reported[82,83]. Essentially, this has been attributed to the extremely stable oxide film, which, under passivating conditions, does not readily break down and rapidly heals. Thus it is very difficult to initiate SCC on a smooth surface of C.P. titanium in aqueous chloride solutions. However, it has been demonstrated in laboratory experiments, particularly by Scully and co-workers[84,85], that SCC does occur in C.P. titanium under conditions where the protective film is broken down mechanically, e.g., by local plastic deformation at the root of a notch

under stress or deformation at low strain rates (creep). These processes effectively produce ideal crevices, and in aqueous solutions containing ∿ 3.5% NaCl, SCC can proceed rapidly at room temperature.

In both mechanical and chemical film breakdown, hydrogen formation is suggested to occur, followed by diffusion and hydride formation. In aqueous chloride solutions, this occurs at the crack or crevice tip resulting in transgranular cleavage fracture through the hydride. There is, however, some controversy about the suggested role of hydride in the mechanism of SCC, primarily because of the difference between the maximum crack velocities observed (∿ 0.1 mm/s) and the relatively low value of H diffusivity (∿ 10^{-8} mm^2/s)[83,85].

The susceptibility of α-titanium to SCC in aqueous chloride solutions increases with alloy content, particularly with oxygen and aluminum additions[83,86,87]. For example, Ti-50A* (ASTM grade 2 C.P. titanium) containing ∿ 0.12% oxygen was found to be immune to SCC in a 3.5% NaCl solution using pre-fatigued bend specimens, i.e., the threshold stress intensity for SCC, K_{ISCC}, was identical to the plane strain fracture toughness, K_{IC} ∿ 66 MPa $\sqrt{m}$ (see Table 11)[86]. However, for the C.P. titanium designated Ti-70** (∿ 0.38% oxygen) and the alloys containing aluminum, K_{ISCC} was appreciably less than K_{IC}. Lower values of K_{ISCC} were observed if the samples were loaded in the salt solution rather than loaded in air prior to immersion in the salt solution. The values in Table 11 were determined using the former method. At least one other study has shown a decrease in the fracture strength of notched bend specimens of C.P. titanium in sea water at room temperature[87].

In C.P. titanium and nominally α-titanium alloys (Table 9), small quantities (< 5%) of metastable β-phase can form, particularly if the iron content is sufficiently large. For example, in the Ti-70

---

* Titanium Corporation of America trade name.

** Reactive Materials Inc. trade name.

material in Table 11, about 3 vol.% β-phase was detected for an iron content of 0.38%[86]. Transformation products formed in the β-phase during subsequent heat treatments tend to increase the susceptibility to SCC, but complete transformation to β-phase followed by rapid cooling to form α' martensite apparently reduces the susceptibility[83,86]. This latter observation may be of relevance to weld regions. However, the potential influence of β-phase on the SCC properties of the relatively new alloy Ticode-12 will likely require study.

Some results indicate that the level of susceptibility to SCC increases with thickness, an effect which has been attributed to a changeover from plane stress to plane strain conditions with increasing specimen thickness[83]. Similarly, preferred orientation and loading rate during testing can affect the level of susceptibility[83]. An increase in grain size also contributes to an enhanced susceptibility to SCC[83]. There appears to be little quantitative information available on the effect of temperature on the SCC of C.P. titanium in salt solutions, although the crack velocity would be expected to increase with temperature.

In summary, several laboratory studies suggest that SCC can occur in C.P. titanium in aqueous chloride solutions, although there are few, if any, reports of service failures in C.P. titanium in this particular environment. Initiation of SCC on smooth surfaces of C.P. titanium is evidently a difficult process unless the applied stress is high enough to produce significant rates of deformation. For example, the strain rates necessary to cause enbrittlement of unnotched samples were ≈ 0.01/h in the constant cross-head speed experiments carried out by Scully and Adepoju[85]. In the presence of a notch, local plastic deformation can rupture the protective oxide film and result in SCC at much lower applied stresses. However, most observations of SCC reported for C.P. titanium pertain to the less pure grades. There are few definitive demonstrations in ASTM grades 1 and 2. Even so, for a new

application, a comprehensive testing program in the anticipated environment would usually be recommended. Examination of the literature suggests an added reason for caution: many laboratory tests for SCC are typically terminated after < ∿ 1000 hours, with the implication that if SCC has not initiated within this period, then K_{ISCC} is high, approaching K_{IC}. If the incubation period for SCC is extensive, however, these relatively short term tests could lead to erroneous conclusions.

7.3.2 Hydrogen Embrittlement and Delayed Fracture

Titanium, like zirconium, is an exothermic occluder of hydrogen and hence forms a solid hydride phase at low temperatures[67,88]. The titanium-hydrogen phase diagram has been thoroughly studied in recent years and is now reasonably well established as shown in Figure 12[89]. The equilibrium hydride is an ordered compound which is stable over the approximate composition range TiH to TiH_2. From a metallurgical viewpoint, the solid solubility limit of hydrogen in α-titanium and its temperature dependence are the most important aspects of Fig. 12. The equilibrium solubility has proved difficult to determine due to effects of stress, deformation, and heating and cooling rates, all of which can produce differences in apparent solubility in addition to hysteresis effects, i.e., differences between the solubility measured during heating and during cooling[89,90]. Perhaps the most reliable solubility data at temperatures below 250°C are those of Paton et al[90], given by:

$$C_s = 34\ 250 \exp - \frac{4450}{RT}$$

where C_s is the hydrogen solubility in μg/g, R is the gas constant and T the absolute temperature. This expression is valid for cooling (hydride precipitation); the solubility during heating (hydride dissolution) was somewhat higher, although the heat of solution was the same. The terminal

solubility increases with temperature to a value of ∿ 0.18%* at the eutectoid temperature of 325°C, above which the β-Ti phase is stable in the presence of hydrogen.

Various specifications for C.P. titanium limit the hydrogen content to 150 μg/g maximum[71]. Using the data of Paton et al.[90] solid hydride would be present in the microstructure at temperatures less than ∿ 135°C for this hydrogen content.

The detrimental effect of hydrogen on titanium and its alloys is well known from the early days of titanium production when hydrogen-induced failures were relatively frequent[89]. With the introduction of improved production techniques, the hydrogen content of mill products can be controlled at low levels so that hydrogen-related failures are now rare. However, all commercial titanium products do contain some hydrogen, which can, under certain conditions, influence their mechanical properties.

7.3.2.1 Tensile Embrittlement

The types of embrittlement observed in titanium alloys are similar to those found in zirconium alloys, which also form a hydride at low temperatures. Two main types of embrittlement have been identified: impact, or high-strain-rate hydrogen embrittlement and slow-strain-rate hydrogen embrittlement[67,68,83,89,91,92].

Hydrogen only influences the tensile properties of α-titanium alloys when the solubility limit is exceeded, and even then a marked effect is not observed at hydrogen contents less than ∿ 200 μg/g[92]. On the other hand, the presence of hydride markedly increases the notch sensitivity of titanium.

---

* For hydrogen solubility in α-titanium, 0.1 wt.% = 1000 μg/g ≈ 5 at.%

Embrittlement at high strain rates, i.e., during impact testing, is most often observed in α-phase alloys and appears to be associated with the brittle fracture of hydrides leading to a decrease in load-bearing area. Thus the degree of embrittlement increases with hydride size and volume fraction, as shown for C.P. titanium (Figure 13), in which the slow-cooled condition produces a coarse dispersion of large hydrides[92]. It should be noted that the impact strength decreases significantly with hydrogen content in the range 25 - 200 μg/g, and that time-dependent decreases occur in rapidly-cooled samples. The degree of embrittlement is increased indirectly by increases in grain size and oxygen content, or by decreasing temperature, all of which reduce the tolerance of the matrix to microcracks formed within hydrides[93]. Paton and Williams suggest that the probable origin of this form of embrittlement is related to the high strain rate sensitivity of the flow and fracture stress of titanium hydride[89].

Slow-strain-rate embrittlement is more typically observed in (α+β)-phase alloys, but has also been reported in α-phase alloys. The effects of hydrogen content, strain rate and temperature on the tensile ductility of a typical (α+β) alloy are shown schematically in Figure 14[91]. Of significance is the fact that embrittlement is absent at high strain rates, which is the basis for distinguishing between impact and slow-strain-rate embrittlement. A further important difference is that the presence of hydrides appears not to be a prerequisite for the slow-strain-rate effect[89]. It is known, however, that large hydrogen supersaturation effects can occur in some titanium alloys, so that, at low temperatures, hydride nucleation from a supersaturated solid solution may be enhanced by the application of either a critical stress or strain[91,94]. Embrittlement then occurs only at low train rates because of the slow kinetics of growth of hydrides to a size which reduces ductility[91]. It should be emphasized that most of the reports and discussion on slow-strain-rate tensile embrittlement refer to (α+β)-phase alloys. There is a scarcity of data on α-phase alloys generally, and C.P. titanium in particular.

7.3.2.2 Sustained Load Cracking (SLC)

This term generally refers to the growth of sub-critical cracks under a static load at stress intensities less than K_{IC}. Terms such as stable or slow crack growth, and delayed cracking are usually synonymous. In the present context, we are referring to sustained load cracking (SLC) as affected by hydrogen present internally in titanium and its alloys. Other effects due to an external source of hydrogen will be discussed later.

Paton and Williams report a number of examples of SLC, primarily in (α+β)-phase alloys, which were attributed to the presence of hydrogen[89]. They also point out the similarities between SLC and slow-strain-rate embrittlement. However, there are very few observations of SLC in α-phase alloys, the most frequently cited example being unpublished work by Paton, who demonstrated hydride precipitation during SLC in an α-phase Ti-4% Al alloy containing as little as 100 μg/g hydrogen[94]. Since this is below the normally accepted limit of solubility for this alloy, it was proposed that the nucleation of hydrides at the growing crack tip was strain-induced.

Work on (α+β)-phase alloys, however, has shown SLC at even lower hydrogen contents. For example, Williams tested a Ti-4%Al-3%Mo-1%V alloy containing 10 μg/g hydrogen in both vacuum and moist air environments and found SLC at stress intensities $\sim 0.4\ K_{IC}$, which was also less than K_{ISCC} in 3.5% salt water[95]. He concluded that the mechanism of SLC in this case did not involve hydrogen. However, in a later study of a number of (α+β)-phase alloys, the same author concluded that increasing hydrogen reduced both K_{IC} and the time to failure during SLC[96]. Moreover, the threshold stress intensity for SLC varied with hydrogen content from a value $\sim$ 27 MPa $\sqrt{m}$ at 7 μg/g hydrogen to $\sim$ 50 MPa $\sqrt{m}$ at 71 μg/g in a Ti-6%Al-4%V alloy. This apparently anomalous behaviour was attributed to separate effects of hydrogen on creep resistance and susceptibility to brittle fracture.

Meyn observed SLC in (α+β)-phase alloys with hydrogen contents between 5 and 215 μg/g[97]. An increase in hydrogen content up to 50 μg/g increased the rate of SLC and decreased K_{IC}. No specific conclusions were reached about the role of hydrogen, except to rule out hydride cracking on the basis that the cleavage fracture plane (near the basal plane) did not correspond with the habit plane of hydrides in titanium. Moreover, hydrides had not been observed in the Ti-Al alloys studied at such low hydrogen contents (< 50 μg/g). However, Paton and Spurling showed that aluminum additions to titanium cause a change in the hydride habit plane from predominantly $\{10\bar{1}0\}$ in pure titanium to {0001} in titanium with 3 - 6.6% aluminum[98]. This appears to remove at least one of Meyn's objections to a hydride cracking mechanism for SLC in his study. A more recent study of SLC in Ti-6%Al-4%V alloys containing 50-255 μg/g hydrogen concluded that hydride formation at the crack tip was an essential feature of the process[99].

It is evident from the foregoing that the mechanism of SLC in titanium alloys is not well understood. There seems little doubt that, in most cases, hydrogen plays a role, but there is considerable uncertainty as to whether the embrittlement is caused by hydrogen in solution or hydride precipitate, or both. Hydrides are difficult to detect, particularly if their volume fraction is small, and, in (α+β)-phase alloys, the hydrides precipitate preferentially at the α/β phase boundaries. On the other hand, observations of SLC at very low hydrogen contents (∿ 10 μg/g) are difficult to rationalize in terms of hydride cracking since hydrides would not be expected to be present. It should be reemphasised, however, that solubility limits are not precisely known, particularly in (α+β) alloys, and in addition, marked supersaturation effects can occur.

It is instructive to examine some aspects of SLC in zirconium alloys, which have received detailed study due to the occurrence of SLC at the end fitting region of several cold-worked Zr-2.5% Nb pressure tubes in a CANDU nuclear reactor[100]. The (α+β) Zr-2.5% Nb alloy is

the most susceptible to SLC, although some α-Zr alloys (e.g., Zircaloy-2) are also susceptible. The important experimental observations from recent studies are[101-103]:

1. SLC occurs only if hydride precipitates are present, i.e., embrittlement is not observed when all the hydrogen is in solid solution.

2. clusters of hydride plates reoriented into the crack plane accumulate at the tip of a growing crack.

3. crack propagation proceeds in a discontinuous manner.

4. the crack velocity (V) is essentially independent of stress intensity (K_I) over a wide range of K_I, but decreases rapidly at low K_I values with an indication of a threshold value $\sim 5 - 10$ MPa $\sqrt{m}$.

Most of these observations can be accounted for using a model in which the crack velocity depends on the rate of growth of hydrides at a stressed crack tip by the diffusive ingress of hydrogen into this region[101]. The driving force for diffusion arises from the local stress gradient which, in the presence of hydrides, sets up a hydrogen concentration gradient which directs hydrogen to the crack tip. When the crack tip hydride has grown to a critical size, it fractures instantaneously, and the cycle of hydride growth is repeated[103]. Therefore, compared to the situation for titanium, all the experimental results and the theoretical model for SLC in zirconium alloys are relatively self-consistent.

In view of the many similarities between titanium and zirconium it might be expected that similar behaviour would occur in titanium and its alloys. However, few, if any, of the characteristic features of hydride cracking in zirconium alloys have been convincingly demonstrated in titanium alloys. Even so, it would be premature to

suggest that a similar mechanism cannot operate in titanium, since a number of the individual physical phenomena involved in hydride cracking in zirconium can occur in titanium, e.g., diffusion of hydrogen in a stress or temperature gradient, and stress reorientation of hydrides during thermal cycling[104-106]. Clearly a more comprehensive experimental study is required, especially for C.P. titanium and the dilute α-titanium alloys such as Ticode-12, to determine their susceptibility to SLC and how this relates to hydrogen.

Assuming that the mechanism of hydride cracking postulated for zirconium alloys[101] could occur in C.P. titanium, the Swedish KBS study attempted to calculate the crack velocity for their disposal conditions, to determine if this would significantly limit the container life[81]. They assumed residual stresses in the container = yield stress, and a mean temperature of 100°C for the first 100 years and 45°C for the next 900 years. They concluded that if any hydride were present, the crack velocity would always be sufficiently high to breach the container within 1000 years. In the model used, the crack velocity is essentially independent of the stress intensity factor (hence the stress), and therefore heat treatments to reduce residual stresses would likely only have a small effect on crack propagation unless the yield stress was also reduced appreciably. The final recommendation from the Swedish assessment was to limit the hydrogen content to a maximum of 20 μg/g, which, on the basis of the data of Paton et al, is less than the terminal solubility at 45°C[90]. There are a number of objections to this recommendation, some of which have been discussed by the authors and the reviewers of the KBS study[70,81]:

1. The data base of hydrogen solubility measurements is probably not adequate to give any confidence that hydrides would be absent at 45°C with 20 μg/g hydrogen.

2. Even with 20 μg/g hydrogen, the actual container temperature would decrease below the assumed mean of 45°C and at this time hydrides would precipitate.

3. Data on (α+β)-phase alloys indicates that SLC can occur at a hydrogen concentration of 7 μg/g[96].

The Swedish study has questioned the relevance of the last result to C.P. titanium. However the poor understanding of SLC in titanium alloys generally, together with the fact that α-zirconium alloys can be susceptible to SLC, suggests there is little basis for assuming that similar behaviour will not occur in C.P. titanium. A further complicating factor is that the crack velocities reported for the (α+β) alloys can be up to 1000 times faster than those calculated in the Swedish assessment, so that if SLC does occur in C.P. titanium, the model used in the assessment may not be appropriate. However, it should also be noted that equally large discrepancies in the apparent diffusion coefficient of hydrogen in (α+β) alloys have been reported[104].

In a supplementary review of SLC in titanium, the KBS study group examined a fracture mechanics approach to eliminating the risk of SLC. It was argued that, if a very low K_I value ($\sim$ 2 MPa $\sqrt{m}$) were specified for design purposes, this would either be less than the threshold stress intensity for SLC or result in an acceptably low crack velocity. Using a residual stress value of 120 MPa this gives a value for the maximum permissible defect of $\sim$ 0.2 mm. Since the internal stresses in the welded regions may approach the yield stress (275 MPa minimum in grade 2 titanium) the maximum defect size to retain K_I $\sim$ 2 MPa $\sqrt{m}$ would be appreciably smaller. Although this is a more realistic approach to the problem, the value of K_I selected is clearly somewhat arbitrary in the absence of a reasonable data base.

7.3.2.3 Environmental Hydrogen Embrittlement

This section briefly considers the embrittlement of titanium alloys due to external hydrogen[83,89]. The possible deleterious role of hydrogen formed during SCC has already been mentioned and will not be discussed further.

A number of studies have shown that (α+β) titanium alloys are susceptible to SLC at ambient temperatures in a gaseous hydrogen atmosphere[89,107,108]. The degree of susceptibility depends on microstructure, temperature, strain rate and hydrogen pressure. For example, at a hydrogen pressure of ∿ 1 atmosphere, the degree of embrittlement is much more severe in alloys with a continuous β-phase (acicular α) than in those with a continuous, equiaxed α-phase microstructure. In the acicular α-phase microstructure the degree of embrittlement decreases with pressure and temperature, whereas pressure has little effect on the equiaxed α-phase alloys. The process is characterized by a two-stage relationship between crack velocity (V) and stress intensity (K_I), V increasing rapidly with K_I at low values of K_I and less rapidly at intermediate values of K_I.

The mechanism of gaseous hydrogen embrittlement has not been established, although there is a greater measure of consistency in experimental results than for SLC in the absence of a hydrogen environment. Models based on either hydride formation or internal hydrogen bubble formation have been proposed[108,109].

8. COPPER AND COPPER ALLOYS

The standard designation for copper and copper alloys used by most producers in North America is that published by the Copper Development Association Inc.[110]. Within this designation system, compositions are grouped into the following families of alloys:

(1) Coppers.

(2) High copper alloys (96-99.3% copper).

(3) Brasses - copper-zinc
copper-lead-zinc
copper-zinc-tin.

(4) Bronzes - copper-tin-phosphorus (phosphor bronzes)
copper-aluminum (aluminum bronzes)
copper-silicon (silicon bronzes).

(5) Copper-nickels.

(6) Copper-nickel-zinc.

There are over 200 wrought alloy compositions covered by the Copper Development Association designations. The compositions and mechanical properties in the annealed condition of some of the most commonly used alloys in each group are given in Tables 12 and 13, respectively[110,111].

8.1 PURE COPPER AND HIGH COPPER ALLOYS

Pure copper is available in three basic grades as defined by the method of casting or processing: tough pitch copper, electrolytic oxygen-free copper and phosphorus deoxidised copper. The high conductivity coppers used for electrical applications are produced mainly from the tough pitch and oxygen-free grades, tough pitch copper being the cheaper and more readily available. Phosphorus-deoxidised copper is the standard grade for the construction of chemical and food processing plant and pressure vessels, particularly if welding is involved[112,113]. In the Swedish KBS study, the reference container material for fuel immobilization was an oxygen-free high conductivity copper, although there appeared to be little rationale for their choice[114].

The principal disadvantage of copper, evident in Table 13, is its low tensile yield strength in the annealed condition (~ 70 MPa), which, for a given level of design stress, necessitates the use of much thicker sections compared with most materials. Significant increases in yield strength, at the expense of ductility, can be achieved by cold working, although this benefit cannot be realized if welding is involved in the fabrication. Moreover, there are practical limitations to the amount of cold work that can be introduced in thick sections. As might be expected, the creep properties of copper are also poor, even at low temperatures (< 300°C). Of the three basic grades, the phosphorus deoxidized copper has the best creep properties at 150°C, as shown in Table 14[112].

Appreciably higher strengths, with adequate ductility, are obtained in the heat treatable high copper alloys, such as those containing small quantities (< 3%) of beryllium, chromium, zirconium or cobalt. High yield strengths (450-1200 MPa) can be developed by precipitation harcening heat treatments, although the residual ductility is low (~ 5%). Moreover, if welding is involved during fabrication, post-weld heat treatments at high temperatures would be required to develop such properties.

Copper is alloyed with many elements, the most common being zinc, aluminum, tin and nickel. The yield strengths of the α solid solutions formed by adding any one of the elements increase with alloy addition and the alloys are tough and ductile. A more rapid increase in strength generally occurs when the solid solubility is exceeded and a second phase is formed (copper-nickel alloys, which form a continuous solid solution, are an exception to this). In the following sections some of the properties of these alloys are described.

8.2 BRASSES

The annealed yield strength of copper-zinc alloys (series 200 in Tables 12 and 13) increases from ∿ 70 MPa to 147 MPa with zinc additions, the latter figure corresponding to the 60% Cu - 40% Zn (α+β) brass. A similar range of strengths is observed, with somewhat lower ductility and impact properties, in the series 300 brasses, which contain up to 3% lead for machinability. The so-called high tensile brasses (yield stress ∿ 210 MPa) are obtained by replacing some of the zinc in (α+β) brasses with iron, manganese and aluminum to give the manganese bronze series of alloys, which combine high strength with adequate ductility and corrosion resistance. The mangarese brass and aluminum brass alloys are based on additions of manganese (∿ 4%) and aluminum (< 4%), respectively, to single phase brasses which produce only a limited strength benefit over the basic brass compositions. Nickel-silver alloys are formed by adding nickel to either α or (α+β) copper-zinc alloys. Commercial alloys contain 5-30% nickel with small additions of iron, manganese or zinc. The annealed yield stress increases from ∿ 120 to 190 MPa with nickel content, and the alloys possess excellent ductility, fracture toughness and corrosion resistance.

Moderate increases in the strength of brasses, with some improvement in corrosion resistance, is obtained with the addition of up to 1% tin; above this level, an intermetallic compound forms which causes some embrittlement.

8.3 BRONZES

8.3.1 Tin Bronzes

The wrought tin bronzes, often called phosphor bronzes because they normally contain up to 0.1% phosphorus, are essentially α-type alloys with a tin content in the range 3-9%. They are stronger than

pure copper or single phase brasses (yield stress 100-200 MPa) and are more corrosion resistant than the brasses, with comparable ductility and toughness.

8.3.2 Aluminum Bronzes

The aluminum bronzes are a group of copper alloys containing aluminum (5-12%) as the principal alloying element. They are characterized by their high strength, good working properties and excellent resistance to corrosion and wear. They are equally suitable for castings and mechanical working although, as with many copper alloys, they are used more in the cast form.

Commercial alloys containing < 8% aluminum are single phase (α) and have yield stresses in the annealed temper up to 210 MPa. Above 7% aluminum, a second phase (β) forms at temperatures > 565°C, which confers good hot workability on the alloys. In binary alloys, at < 565°C, the β-phase decomposes eutectoidally to ($\alpha+\gamma_2$) under equilibrium, or slow cooling, conditions. The γ_2-phase is less ductile than the α, and the presence of this eutectoid structure results in poor strength, ductility and corrosion resistance[115]. The volume fraction of γ_2-phase is therefore minimized in binary alloys by limiting the total aluminum content to < 11% and also by avoiding slow cooling during fabrication.

In the more complex commercial alloys, iron or iron plus nickel (up to 5% of each), are added to ($\alpha+\beta$) aluminum bronzes. This, together with close production control, effectively eliminates any eutectoid transformation in wrought products. Although heat treatments can be used to modify the structure and hence the mechanical properties, they are seldom required in commercial practice. In the hot-worked condition, commercial ($\alpha+\beta$) alloys have yield stresses of ~ 350 MPa, with adequate ductility and excellent corrosion resistance.

Both the α and (α+β) alloys retain a significant fraction (80 - 90%) of their room temperature yield stress and impact resistance up to at least 200°C, and are therefore among the most creep-resistant of copper alloys[115]. In common with some other copper alloys, e.g., brasses, the aluminum bronzes exhibit a ductility minimum at ∿ 300°C, and although a useful degree of ductility is still retained, the reduced ductility often makes it difficult to obtain successful welds in conventional alloys[113]. A more weldable version of the α-aluminum bronze has been developed which contains 6% aluminum and 2% silicon, with a yield stress in the extruded condition of ∿ 240 MPa.

A more recent addition to the aluminum bronze group of alloys is the copper-manganese-aluminum alloys, containing about 12% manganese, which are essentially casting alloys. Generally, these have greater ductility and impact strength than the iron-nickel-aluminum bronzes of comparable yield strength. Moreover, the ductility minimum which occurs in conventional alloys is absent in the manganese-containing alloy. They exhibit creep properties up to 175°C which are at least as good as any copper-base casting alloy.

8.3.3 Silicon Bronzes

These alloys contain 3-4% silicon as the principal alloying element with small additions of manganese, iron, zinc or tin. Yield strengths are ∿ 140-210 MPa in the annealed condition, with excellent ductility, toughness and corrosion resistance.

8.4 COPPER-NICKEL ALLOYS

Copper and nickel form a continuous solid solution over the complete composition range. Commercial alloys contain 5-30% nickel, with small additions of iron, manganese or zinc. Yield strengths increase from ∿ 90 to 210 MPa with increase in nickel content, all compositions exhibiting excellent ductility, toughness and corrosion resistance.

To summarize Sections 8.1 to 8.4: the group of wrought alloys exhibiting the best combination of strength, ductility and toughness is the complex ($\alpha+\beta$) aluminum bronzes. Alloys with somewhat lower strength, but greater ductility and toughness, are the α-phase aluminum bronzes, the high tensile ($\alpha+\beta$) brasses such as manganese bronze, and the silicon bronzes.

8.5 WELDABILITY

The principal fusion welding techniques used on copper and its alloys are the tungsten-inert gas (TIG) and the metal-inert gas (MIG) techniques. In general, TIG is used for thickness up to $\sim$ 3 mm, above which MIG techniques are preferred[8,113].

The outstanding physical property affecting the welding of copper, particularly in thick section, is the very high thermal conductivity which, depending on purity, is 5-10 times as great as that of mild steel. For thicknesses > $\sim$ 3 mm, substantial preheat is required otherwise it is not possible to establish the fully molten pool necessary for complete fusion and deoxidation. For example, the preheat requirements for MIG welding a butt joint in copper plate $\sim$ 12 mm thick may be as high as 700°C[112,113].

Of the basic grades of copper, only the phosphorus deoxidized grade is normally specified for welding applications. The tough pitch oxygen-containing grades present special difficulties due to the formation of copper oxide at the grain boundaries in the fusion zone, which results in inferior mechanical properties. Moreover, porosity in the weld metal, due to the reduction of oxide by hydrogen to form steam (gassing), can occur, although this is a much greater problem in oxy-acetylene welding. The phosphorus deoxidized grades can be readily welded by the inert gas techniques although, to eliminate porosity completely, additional deoxidants are added to the filler wires and electrodes. In welding copper, allowance should be made for the high

coefficient of thermal expansion in terms of both selecting root gaps and minimizing distortion due to the low strength at elevated temperatures.

Copper alloys, in contrast to copper, seldom require pre-weld heating except in large section sizes. Again, the MIG process is preferred commercially for thick sections (> 12 mm), and is selected for some alloys, e.g., aluminum and silicon bronzes, for thicknesses $> \sim 3$ mm[113].

Of the copper alloys, the brasses are the least weldable, the difficulties increasing with zinc content. Generally, the evolution of zinc fumes results in porous welds which have poor mechanical properties, particularly if autogenous welding is attempted. This is partially overcome by using non-matching filler metals, e.g., aluminum or silicon bronze. The risk, however, is that solidification of the weld metal will occur before the parent metal (brasses have a lower solidification temperature than the filler metals), resulting in HAZ cracking and the potential for differential corrosion during service.

In the limited applications where phosphor bronzes require welding, reasonable freedom from porosity can only be attained by using non-matching filler metals containing powerful deoxidants. The use of these also minimizes the oxidation of tin, which occurs preferentially to copper and which embrittles the weld. The wide freezing ranges of the phosphor bronzes can also give rise to cracks at elevated temperatures (hot shortness) and shrinkage cavities on solidification.

High quality welds in aluminum bronze can be produced only by the inert gas arc welding processes, which facilitate the removal of the refractory aluminum oxide film from the weld pool[113,115]. Traditionally, these alloys have been difficult to fabricate and weld due to their susceptibility to hot shortness. For example, nominally α-alloys containing 6-8% aluminum and 2% iron may suffer from root embrittlement

in multi-run welds when autogenous welding is used. This problem has been largely overcome by using non-matching ($\alpha+\beta$) phase filler metal which confers more ductility on the weld. However, the β-phase in the weld metal can, under some conditions, undergo a form of corrosion known as de-aluminification, and it is sometimes necessary to apply a final capping weld of parent metal composition to avoid this electrochemical corrosion effect[116].

In addition, aluminum bronzes exhibit a ductility minimum in a temperature range particularly critical during welding, which sometimes makes successful welding difficult. Thus, whereas the weld metal may be free from cracks, parent metal cracking can be a problem, although this has largely been overcome by careful control of rolling and reheating procedures[113].

The ($\alpha+\beta$) alloys containing iron and nickel, and the high manganese-containing alloys, generally have excellent weldability. Weld strengths equal to the parent metal are typically achieved, but with some reduction in ductility[115].

Copper-silicon alloys are probably the most weldable group of the copper alloys using TIG or MIG if the welding conditions are carefully controlled. The main problem arises due to hot shortness in the temperature range 800-950°C, which can be avoided by relatively rapid cooling after welding. Interpass cleaning of the oxide from the weld bead may be required with these alloys. Copper-nickel alloys also have excellent weldability although, to prevent oxidation and porosity, a filler wire containing a suitable deoxidant should be used for all thicknesses.

8.6 CORROSION

The main assessment of the corrosion behaviour of copper and its alloys is presented in Part II. Suffice it to say here that copper

and several copper alloys are renowned for their excellent corrosion resistance. An evaluation of the corrosion of copper has been carried out by the Swedes in their study of the suitability of thick-walled copper containers for fuel immobilization[114].

8.7 EMBRITTLEMENT EFFECTS

8.7.1 Stress Corrosion Cracking

Copper and its alloys were probably the first metals in which the phenomenon of SCC was observed, this being referred to as "season cracking". The corrosive environments which cause SCC are those containing ammonia (NH_3) or an unstable ammonium salt together with moist air or oxygen[117,118]. Pure copper and copper-nickel alloys appear to be least susceptible and the copper-zinc alloys most susceptible to this form of cracking. The problem can be overcome by a suitable stress relieving treatment. Unlike austenitic stainless steels, copper and its alloys are not susceptible to SCC in chloride-containing environments.

9. COST AND DESIGN ASPECTS

9.1 MATERIALS PROPERTY SPECIFICATIONS

The values of mechanical properties in Sections 3 to 8 are those considered to be typical. However, in selecting values of properties for design calculations, it is common and often mandatory to use those recommended by a materials specification or engineering code, such as the American Society for Testing and Materials (ASTM) or the American Society for Mechanical Engineers (ASME). The room temperature values of mechanical properties specified by these two organisations are usually very similar. Such recommended values generally represent a lower bound of data and will therefore be conservative in most cases.

The room temperature tensile properties specified by ASTM for some of the engineering alloys considered in this report are shown in Table 15. Also shown are the normalized values of yield stress assuming 1.0 for 316L stainless steel; these values indicate the relative thickness of material required if the design criteria were based on yield stress. It is evident that the ferritic stainless steels, the higher grades of C.P. titanium and the high nickel-base alloys, particularly Inconel 625 and Hastelloy C-276, have greater strength than the austenitic stainless steels and aluminum-base and copper-base alloys, and have adequate ductility.

Since the temperature in the disposal vault may be as high as 150°C, the value of the yield stress at the service temperature will also be important for design calculations. For most materials, the temperature dependence of the recommended minimum yield stress can be determined from the ASME Code. The relationships for a number of alloys in the higher strength groups are shown in Figure 15. The significant feature is the high temperature dependence of the yield stress for grade 2 titanium compared to, say, Inconel 625 and 316L stainless steel. This reduces somewhat the strength benefit margin at 150°C of grade 2 titanium over 316L; on the other hand, the strength advantage of, say, Inconel 625 over grade 2 titanium and 316L increases with temperature. Assuming that the yield stress of grade 12 titanium (Ticode-12) has a similar temperature dependence to grade 2, it would still retain an appreciable strength benefit over 316L at 150°C.

9.2 MATERIAL COSTS

In considering the design of containers for fuel immobilization, the overall cost will clearly be an important factor. Depending on the final design, the material cost may be a significant fraction of the total cost. The cost of various engineering metals and alloys is shown in Table 16. The second column contains data from the work of Braithwaite and Molecke[46] and also quotations for plate material

obtained by WNRE. The origin of the former data is not stated, so that the basis for comparison may be different from that for the WNRE data. However, the relative ranking of material costs is probably correct, though differences in costs may be marginally affected by the reference base used in different metal industries, e.g., ingot or fabricated plate price.

An alternative comparison is shown in column 3, which is based on the cost of seam-welded pipe. Where comparisons between columns 2 and 3 can be made, the same relative cost ranking is evident. The higher costs in column 3 will predominantly reflect the costs of fabrication of the pipe. A real indication of these fabrication costs can be obtained where a cost for plate material is given in column 2. Clearly the fabrication costs are significant and can be comparable to the costs of the plate material.

Considering the data in columns 2 and 3 of Table 16, the more highly alloyed nickel-base alloys and titanium are the most expensive materials. Alloys with intermediate corrosion resistance such as Monel and the higher nickel austenitic steels are cheaper, but are still about twice the cost of the 300 series austenitic steels. Copper, aluminum and their alloys are somewhat more expensive than stainless steel.

Probably a more realistic comparison of costs is one based on the cost related to strength. This is shown in Table 16 (column 4) in which the data are normalized to a value of 1.0 for 316L stainless steel. The data were calculated using the relative cross sectional areas required to support a given load (proportional to yield stress), the density and the cost of pipe per unit weight (Table 16, column 3). On this basis, the 300 series stainless steels are among the cheapest materials, with the exception of the more highly alloyed AISI 310, whose cost approaches that of the high nickel-base alloys. In this latter group, Inconel 625 is the cheapest and Hastelloy C-276 the most expensive. The cost of the titanium alloys, particularly Ticode-12, is very

competitive with that of the high nickel-base alloys. Significantly, the high alloy austenitic stainless steels, e.g., Incoloy 825, Incoloy 800, and the high nickel alloys Inconel 600 and Monel 400, are all more expensive than the more corrosion-resistant Inconel 625 and Ticode-12. Copper and copper-nickel are also fairly expensive compared to these latter materials, although aluminum bronze is relatively cheap. Commercial pure aluminum is very expensive, while commonly used structural aluminum alloys appear to be very cheap.

9.3 FABRICATED MATERIAL

It is likely that a design of fairly simple cylindrical geometry will be considered initially for the shell of fuel immobilization containers. If the shell is required to support the potential hydrostatic head at the disposal depth (500 - 1000 m), the shell thickness would necessarily be large. Thus, a fabricated pipe of reasonable diameter would probably be used for the main container shell.

The two most commonly used techniques for producing wrought pipe are seam-welding of fabricated plate and extrusion. The specifications (e.g. ASTM) covering these products are usually very similar, and for some materials are identical, so that nominally there is little difference between pipes manufactured by either route. The presence of the seam weld, however, does represent a discontinuity in the material, which, for some applications, is recognized by engineering codes and an additional safety factor is introduced. If other welding is also required on the container, there appears to be little benefit in using extruded pipe. Some differences in preferred orientation may exist between seam-welded pipe (made from rolled plate) and extruded pipe which could influence the relative susceptibility to delayed failure mechanisms, but such effects have not been studied in any detail. Close dimensional tolerances may be easier to achieve and more reproducible in extruded pipe, but it seems unlikely that tolerances better than those normally specified for seam welded pipe would be required.

On the basis of recent quotations, there would appear to be a significant cost benefit in using seam-welded pipe. The costs for the same pipe geometry in a number of materials are compared in Table 17.

Another fairly common technique for producing pipe, centrifugal casting, is not considered in this assessment since the properties of cast materials are a subject in their own right.

9.4 AVAILABILITY

There are a number of factors which have an important influence on the availability of a particular engineering component and the material used for that component. One factor affecting availability is related to the current market supply and demand situation, which can result in short term problems of supply of a particular material or component.

A more important factor which places a greater limitation on availability is whether a component is traditionally made in the material specified. Clearly if the technology and experience to manufacture a particular component has not been developed, a considerable lead time may be involved before it reaches the production stage. There are two related aspects to this problem. One is involved with the development of the fabrication procedure, and the second concerns the solution of any materials problems which limit the integrity of the fabricated product. For example, the high-chromium ferritic stainless steels are attractive in terms of their corrosion resistance, strength and cost. However, they tend to be brittle when fabricated into thick sections, which has limited their more widespread use and availability. Even if there were sufficient demand for these materials, it could take several years to develop techniques to overcome the problem. Some copper- and aluminum-base alloys are not traditionally made in thick sections or into pipe. Selection of these materials would also result in a problem of availability. Most of the austenitic stainless steels, high nickel-

base alloys and titanium alloys, are commonly fabricated into thick plate and heavy-wall pipe, so that, apart from short-term problems of stock depletion, these materials would generally be readily available.

Another factor in considering containers for fuel immobilization is the impact of the materials selection and total material requirements on availability and natural resource reserves. This aspect is not considered in this report.

9.5 CLADDING

For some applications, where strength and corrosion resistance are the important requirements, it is possible to use a strong but inexpensive material, clad with a much thinner layer of a corrosion-resistant alloy. The cladding is applied by one of a number of techniques depending on the materials involved, e.g., loose sheathing, explosive bonding, roll cladding and fusion weld overlaying.

Cladding thicknesses depend on the corrosion allowance required and are generally in the range 3 - 6 mm, whereas the thickness of the backing material (usually a low alloy steel) is determined by the strength requirements. The most commonly used technique for titanium is explosive bonding; grade 1 titanium is used because its higher ductility aids the bonding process[77]. For austenitic stainless steel and high nickel-base alloys (e.g., Inconel 625), either submerged-arc or metal inert gas welding overlay techniques are generally used[119,120].

The costs of producing clad material on steel are, however, significant. Explosive cladding of titanium, for example, costs $\sim$ \$100/m^2, which, based on the current price of titanium, means that construction from solid titanium would be competitive up to thicknesses of at least 25 mm[77]. Similarly, for weld overlaying with Inconel 625 on steel, the break-even point for clad versus solid construction occurs at a thickness $\sim$ 25 mm[119].

The use of clad material in a construction which requires welding introduces additional difficulties since separate welding operations are required for the steel backing and the cladding. Pre-service inspection is also more complex, which increases the difficulty of defect detection and analysis.

On the basis of industrial experience with titanium and Inconel 625, there appears to be little economic incentive at present to consider clad construction for fuel immobilization containers unless the design thicknesses are appreciably greater than ~ 25 mm, and even then, the additional technical complications introduced would require careful consideration. However, this situation could change if the costs of corrosion-resistant materials such as titanium increased significantly, and if, as is likely, improvements occur in welding and inspection techniques. Thus it would be premature to dismiss the possible use of clad materials for containers, and future developments in this technology should be followed closely.

10. SUMMARY OF PART I

Part I of this report reviews the mechanical properties, physical metallurgy, weldability and embrittlement effects of a wide range of engineering alloys in relation to their potential use for containers for the disposal of irradiated fuel in an underground vault.

In order to optimize the stability of the microstructure and mechanical properties of the container material, it is likely that a fully annealed, single-phase material would be selected. This would minimize the extent of both local changes in structure and properties which might develop during container fabrication (e.g., welding) and of the more general or uniform changes which would occur during extended service at temperatures $\leq$ 150°C. Some materials could, in principle, be

strengthened by heat treatment after the final closure weld on the container, but the significant practical difficulties inherent in such a procedure would probably make it undesirable. In any case, such a strengthened microstructure may overage during service, with consequent reduction in strength. As indicated previously, strengthening by cold working would be of no benefit if a loss of strength occurred locally due to welding.

It is evident from the above that one of the more important properties affecting the container design is the yield strength, since this will probably determine the minimum wall thickness. For example, a container in which the shell alone is designed to support the potential service loads would require wall thicknesses in the range 10 - 100 mm, depending on the material and the design criteria selected. The wall thickness is an important factor in terms of material costs, integrity of container fabrication (e.g., weldability) and container transportation and handling (i.e., weight). Thus, on the basis of yield strength and hence thickness requirements, neither C.P. copper nor aluminum would be suitable. For example, the thickness of a C.P. copper container designed to withstand a hydrostatic pressure of $\sim$ 10 MPa with a safety factor of 2 on yield strength is $\sim$ 90 mm; the required thickness of a C.P. aluminum container is even greater. Welding of these high thermal conductivity materials in such thicknesses by conventional techniques would be very difficult, but could probably be done by processes with a high local heat input such as electron-beam welding. The cost of C.P. copper and aluminum to support a given design stress is also greater than for most other commercial alloys.

Of the copper and aluminum-base alloys, only the aluminum bronzes have sufficiently high strengths to compete with, say, 316 L stainless steel and be in the same cost bracket. However, this material may not be easily obtainable in suitable form. For example, few, if any, of the Canadian copper mills produce any wrought copper-base alloy in thicknesses of 25 mm or greater. For a given imposed stress, some

aluminum-base alloys would be among the cheapest container materials, but thicknesses approximately twice that of 316 L would be necessary. Moreover, the range of service temperatures in the vault is high relative to the melting point of aluminum alloys (0.4 - 0.5 T_m, where T_m is the melting point), so that creep could be a problem with these materials. Finally, aluminum-base alloys do not have the best weldability and are susceptible to SCC in chloride environments. Magnesium-base alloys have even lower strength, less creep resistance, and poorer weldability than aluminum-base alloys.

Plain carbon and low alloy steels have yield strengths as high as 316 L stainless steel, have excellent weldability and are by far the cheapest materials available. However, their application for containers is likely to be precluded by their poor corrosion resistance (see Part II) and by their tendency to suffer from delayed hydrogen embrittlement effects, particularly in welded regions.

Of the stainless steels, the ferritic alloys (particularly the high chromium alloys) exhibit both excellent strength properties and resistance to SCC. However, they suffer from a ductile to brittle transition in a potentially low and somewhat poorly defined temperature range, particularly in thick sections and in welded regions. Therefore, in their present state of development, these alloys are not suitable for fuel immobilization containers.

The martensitic stainless steels have a high yield strength but are air-hardenable during welding and hence require post-weld heat treatment. They are also the most susceptible of the stainless steels to SCC and hydrogen embrittlement. Very high strengths can be developed in the PH stainless steels, but they also require complex post-weld heat treatments to restore their properties. In the fully annealed condition these materials offer little strength benefit over austenitic stainless steels.

The most widely used stainless steels are the austenitic AISI 300 series, which are essentially solid solution-strengthened alloys with moderate strength and excellent ductility. They are readily weldable without post-weld heat treatment, and there is considerable experience in their fabrication and service. Their principal drawback is a susceptibility to transgranular and intergranular SCC in chloride environments. However, the use of low carbon or stabilized alloys practically eliminates sensitization during welding and hence intergranular SCC. It is considered unlikely that sensitization due to chromium carbide precipitation would occur in a low carbon alloy at service temperatures of 150°C or less. The low carbon austenitic alloys are generally easier to weld than the stabilized varieties and the latter can also suffer from knifeline corrosion after welding. The 316 L alloy would be preferable to the lower alloy austenitics because of its greater stability and resistance to SCC. It is also one of the cheapest and more widely used austenitic alloys.

Of the significant number of iron-base austenitic alloys with chromium and nickel contents higher than 316 L, few, if any, provide a significant advantage in terms of strength or weldability in the annealed condition. They are, however, more resistant to transgranular SCC than the AISI 300 alloys, but are still susceptible to intergranular SCC if a sensitized microstructure is developed during welding. Moreover, their greater resistance to transgranular SCC is difficult to quantify. Since these alloys are also appreciably more expensive than the 300 series, there is little reason to select them for the present application.

Considering the corrosion resistant nickel-base alloys, Inconel 600 is probably the most widely used because it is virtually immune to classical transgranular SCC in chloride environments. However, it is very susceptible to intergranular SCC even in pure water and in the absence of sensitization. It is also relatively expensive and only marginally stronger than 316 L stainless steel. The only solution-strengthened nickel-base alloys which offer significant strength benefits

over the 300 series steels are those containing molybdenum, i.e., Inconel 625, Hastelloy C-276 and Hastelloy C-4. Of these, Inconel 625 has the highest usable strength and is the cheapest. All these materials are readily weldable and do not generally require post-weld heat-treatment. The molybdenum-containing alloys are among the most resistant materials to SCC in chloride media.

Of the titanium-base alloys, the greatest resistance to uniform corrosion, SCC and hydrogen embrittlement is found in the very dilute α-titanium alloys, i.e., C.P. titanium, Ti-0.2% Pd and the recently developed Ticode-12. The dilute alloys also have greater ductility and are less notch sensitive than the more highly alloyed materials, but they have lower strength and creep resistance. Titanium is one of the most expensive materials on a unit weight basis, but when the strength and density are also taken into account the effective costs of, say, ASTM grades 2 and 12 are at least comparable to the intermediate and high nickel austenitic alloys. Titanium can be readily welded using inert gas techniques, but its high affinity for interstitial impurities which can cause embrittlement means the welding procedure is more complex and more critical than for most materials.

Some of the more concentrated titanium alloys can be susceptible to delayed fracture due to SCC, hydrogen embrittlement or both, although the mechanisms involved are not well characterized. Thus, predictions of behaviour tend to be based more on a combination of experience and empiricism rather than on an established quantitative model. On the other hand, no failures due to SCC or hydrogen embrittlement have been reported in the very dilute alloys, e.g., C.P. titanium, Ti-0.2% Pd, Ticode-12, although there are very few published experimental data on these materials, which introduces some uncertainty in defining possible limits to their non-susceptible behaviour. This is particularly true for the recently developed Ticode-12.

The cost of the Ti-0.2% Pd alloy is about twice that of C.P. titanium for comparable mechanical properties, while Ticode-12 offers a significant strength advantage at a cost only moderately greater than C.P. titanium.

Considering the copper-base alloys, only the aluminum bronzes have strength and ductility comparable to the 300 series stainless steels and a similar cost. The aluminum bronzes generally are readily weldable, but can be susceptible to cracking in the weld and parent metal. The fairly low strength of most of the remaining copper-base alloys would necessitate section thicknesses 50 - 100% greater than for aluminum bronze, resulting in higher costs and increased fabrication difficulties.

In summary, on the basis of the properties considered in Part I, three alloy groups can be identified as meriting further consideration for use as containers for fuel immobilization:

1. AISI 300 series austenitic stainless steels.
2. High nickel-base alloys containing molybdenum.
3. C.P. titanium and very dilute titanium alloys.

Within group 1, 316 L stainless steel is suggested as being the optimum choice, whilst of the group 2 materials, Inconel 625 would be favoured, since it is the cheapest and strongest and has no serious disadvantages compared with other materials in this group. From group 3, ASTM grades 2 and 12 titanium are recommended on the basis of cost, strength and weldability, with the rider that the apparent absence of susceptibility to embrittlement due to hydrogen effects and SCC must be more completely established and understood.

Of these specific alloys, 316 L stainless steel is the cheapest material for a container design based on yield stress, but would result in the greatest wall thickness and weight. This alloy is also by far

the most susceptible to SCC in a chloride-containing environment. On the same basis, the costs of the other three alloys are similar and about 50% more than the 316 L. Inconel 625 would result in the least wall thickness although, on the basis of our current knowledge, the titanium alloys appear to have somewhat greater resistance to SCC.

PART II - CORROSION

11. INTRODUCTION

Since the integrity of fuel immobilization containers must be maintained for at least 500 years, corrosion resistance is of prime importance when selecting container materials. Thus it is mandatory that candidate metals and alloys have acceptably low rates of uniform corrosion and immunity to localized corrosion in the vault environment.

The main objectives in Part II of this report are to present a brief review of the theory and principles of uniform and localized corrosion, to describe the conditions under which different metals and alloy systems are susceptible to localized corrosion and, finally, to compare the probable corrosion performance of the various materials in the disposal vault.

The information on corrosion theory and principles in Section 12 has, for the most part, been abstracted from text books widely used and accepted by corrosion scientists[121-126]. The corrosion conditions in the vault environment are discussed in Section 13 on the basis of probable groundwater chemistry. The corrosion behaviour of the engineering metals and alloys referred to in Part I is discussed in Section 14 in terms of the probable vault environment. The discussion emphasizes localized forms of corrosion, particularly pitting and crevice corrosion. A detailed literature review on the relative susceptibility of various materials to localized corrosion is also presented.

Section 15 summarizes the available data specifically on crevice corrosion of metals and alloys in aqueous chloride solutions up to 200°C. From this comparison a short list of candidate container materials is recommended for further evaluation in laboratory and field tests.

12. CORROSION OF METALS

12.1 GENERAL INTRODUCTION

Corrosion reactions can be broadly classified as "wet" or "dry". The term "wet" includes all reactions in which an aqueous solution is involved in the reaction mechanism; implicit in the term "dry" is the absence of water or an aqueous solution. "Dry" corrosion generally means metal/gas or metal/vapour reactions involving non-metals such as oxygen, halogens, hydrogen sulphide, sulphur vapour, etc., oxidation, scaling and tarnishing being the more important forms. In "wet" corrosion the oxidation of the metal and reduction of a species in solution (electron acceptor or oxidizing agent) occur at different areas on the metal surface with consequent electron transfer through the metal from the anode (metal oxidized) to the cathode (electron acceptor reduced). The thermodynamically stable phases formed at the metal-solution interface may be solid compounds or hydrated ions (cations or anions) which may be transported away from the interface by processes such as diffusion and convection (natural or forced). Under these circumstances the reactants will not be separated by a barrier and the corrosion rate will tend to be linear. Subsequent reaction with the solution may result in the formation of a stable solid phase but, as this will form away from the interface, it will not be protective; the thermodynamically stable oxide can affect the kinetics of the reaction only if it forms a film or precipitates on the metal surface.

It is expected that, after emplacement in the vault, the containers will be surrounded by a buffer material, the composition of which can be selected to give some control over the chemical interactions, and hence corrosion conditions, near each container. For example, the Swedes have recommended bentonite or sand/bentonite mixtures for this purpose[3]. Corrosion in soil is aqueous and the mechanism is electro-chemical, but the conditions in the soil can range from

"atmospheric" to completely immersed. Which conditions exist depends on the compactness of the soil and the water content. Moisture retained within a soil is largely held within the capillaries and pores of the soil. Soil moisture is extremely significant and qualitatively, the degree of corrosion occurring in soil will be related to its moisture-holding capacity. Since the moisture-holding capacity of a clay is much greater than that of a sandy-type soil, a dry sandy soil will, in general, be less corrosive than a wet clay.

In soil, water is needed for:

1. ionization of the metal to the oxidized state at the metal surface.

2. ionization of the soil electrolyte, which completes the circuit and allows a current flow that maintains corrosive activity. The water acts as a solvent for salts in the soil, the result being the soil solution.

Water in soils can be classified into three groups: capillary water, gravitational water and free groundwater. Capillary water is held in the capillary spaces of the silt and clay particles. Gravitational water enters the soil from rainfall or other sources and percolates downward to the level of the free groundwater. Free groundwater is continuously present at some depth below the surface. Only a small amount of the metal used in underground service is present in the groundwater zone (e.g., well casings and under-river pipelines). Containers for fuel immobilization will see service under these conditions, which are essentially those of an aqueous environment.

12.2 GENERAL PRINCIPLES

In Section 12.1 it was pointed out that aqueous corrosion is electrochemical in nature and is controlled by oxidation (anodic) and

reduction (cathodic) processes occurring on the metal surfaces. When viewed from the standpoint of these processes, all corrosion can be classified into a few generalized reactions.

The anodic reaction in every corrosion reaction is the oxidation of a metal to its ion,

$$M \rightarrow M^{+n} + ne \qquad (1)$$

where n is the number of electrons produced and is equal to the valence of the ion. There are several different cathodic reactions frequently encountered in metallic corrosion, the most common being:

Hydrogen evolution:	$2H^{+} + 2e \rightarrow H_2$	(2)
Oxygen reduction: (acid solutions)	$O_2 + 4H^{+} + 4e \rightarrow 2H_2O$	(3)
Oxygen reduction: (neutral or basic solutions)	$O_2 + 2H_2O + 4e \rightarrow 4OH^{-}$	(4)
Metal ion reduction:	$M^{+3} + e \rightarrow M^{+2}$	(5)
Metal deposition:	$M^{+} + e \rightarrow M$	(6)

All the above reactions are similar in that they consume electrons at cathodic sites.

Oxygen reduction is very common, since any aqueous solution in contact with air is capable of producing this reaction. During corrosion more than one oxidation and one reduction reaction may occur. For example, aerated acid solutions are more corrosive than air-free acids because oxygen reduction (reaction (3)) provides an additional source of electron acceptors. The same effect is observed if an oxidizer is present in the solution. Reduction of metal ions (reaction (5)), such as ferric or cupric ions, provides an additional cathodic reaction.

Since anodic and cathodic reactions are mutually dependent, corrosion rates can be reduced by reducing the rate of either reaction. Generally speaking, decreasing the acidity, and lowering the concentration of oxygen and oxidizing species all tend to lower the rate of cathodic reduction, resulting in less severe corrosion. The rate of an electrochemical reaction is limited by various physical and chemical factors. An electrochemical reaction is said to be polarized or retarded by these environmental factors. Activation polarization refers to an electrochemical process which is controlled by the reaction sequence at the metal-solution interface and is predominant in media containing a high concentration of active species (e.g., concentrated acid solutions). Concentration polarization refers to electrochemical reactions which are controlled by diffusion in the solution and is predominant in media where the concentrations of reducing species are small (e.g., dilute acids, aerated salt solutions). Depending on the kind of polarization controlling the reduction reaction, environmental variables such as oxygen and oxides, concentration of the corrosive species, temperature and velocity, produce different effects.

In broad terms, the above general principles are valid for what are considered to be "active" metals or alloys. Another group can be defined which exhibits the phenomenon called "passivity". Essentially, passivity refers to the loss of chemical reactivity under certain environmental conditions. In effect, certain metals or alloys may become essentially inert and act as if they were noble metals. Common engineering and structural materials, including iron, nickel, silicon, chromium, titanium and alloys containing these metals, exhibit passivity effects.

The typical behaviour of such active-passive metals is illustrated schematically in Figure 16, which relates the current density (a measure of the corrosion rate) to the electrode potential (a measure of the solution oxidizing power). The behaviour can be divided into three regions: active, passive and transpassive. In the active region, the

behaviour is identical to that of a normal metal. Slight increases in the oxidizing power of the solution cause a corresponding rapid increase in the corrosion rate. Maximum corrosion occurs at a potential defined as the passivation potential (E_p). If the solution is made more oxidizing, the corrosion rate shows a sudden decrease which corresponds to the beginning of the passive region. Minimum corrosion occurs at a potential defined as the activation potential (E_A). Further increases in oxidizing power produce little or no change in the corrosion rate of the material until, finally, in the presence of very powerful oxidizers, the corrosion rate again increases with increasing oxidizing power. The point at which this occurs is defined as the transpassive potential (E_{trans}) and the region above this point is called the transpassive region. The active-passive-transpassive transition is considered to be a special case of activation polarization, due to the formation of a surface film or protective barrier which is stable over a considerable range of oxidizing power and is eventually destroyed in strong oxidizing solutions. If certain specific agressive species are present in the solution (e.g., chloride ions), the protective film can locally break down at potentials less positive than the transpassive potential, and pits are initiated when this pitting potential (E_{pit}) is exceeded. Thus the pitting potential can be used as a measure of the resistance of metals and alloys to pitting.

12.3 ENVIRONMENTAL EFFECTS

The most common environmental variables influencing corrosion are oxygen and oxidizers, temperature, pH and velocity. The effect of oxygen or oxidizer additions on the corrosion rate depends on both the medium and the metals involved. Their influence on the behaviour of active and active-passive metals has already been mentioned in Section 12.2. Their solubility in various media can also influence corrosion behaviour, especially when their solubility is limited. Although iron can be made to passivate in water, for example, the solubility of oxygen is limited and in most cases is insufficient to produce a passive state.

Temperature increases the rate of almost all chemical reactions and hence the corrosion of most active materials will increase with temperature. Materials exposed in the passive state may show a negligible temperature effect at low or moderate temperatures but a significant one at higher temperatures, since increasing temperature generally increases the oxidizing power of the solution. pH has a large effect on the thermodynamic stability of corrosion products and therefore influences the corrosion rate. Pourbaix et al.[127,128] have calculated the phases at equilibrium for many metal/water systems at 25°C from the chemical potentials of the species involved in the equilibrium diagrams of pH versus the equilibrium potential (E). A typical diagram for the iron/water system is shown in Figure 17. These diagrams provide a thermodynamic basis for the study of corrosion reactions, although their limitations in relation to practical problems must be appreciated since they represent equilibrium conditions only and provide no kinetic information. The diagrams can be divided into zones of corrosion, immunity and passivity depending on the conditions for thermodynamic stability of the metal, metal ions, solid oxides and hydroxides. In practice, however, aqueous environments are more complex than pure water and contain additional anions, with the consequent possibility of forming species other than those predicted in the metal/water system. In general, anions that form soluble complexes tend to extend the zones of corrosion, while anions that form insoluble compounds tend to extend the zone of passivity. Implicit in the concept of passivity is the assumption that the solid compound forms a kinetic barrier between the reactants so that further interaction becomes very slow. Whether this occurs in practice will depend on where the oxide is formed, oxide adhesion to the metal, the solubility of the oxide, etc. It should be emphasized that potential-pH diagrams can also be constructed from experimental E_p-I curves, where E_p is the passivation potential and I is the current[129]. Figure 18 illustrates this concept for the iron/water system containing chloride ions. These diagrams, which are of more direct practical significance than the equilibrium potential-pH diagrams constructed from thermodynamic data, show how a metal or alloy in a

natural environment (e.g., iron in water of given chloride ion concentration) may give rise to general corrosion, pitting, perfect or imperfect passivity or immunity, depending on the pH and potential. Unfortunately, only a limited amount of work has been done in this area, usually with binary alloys in specific chloride environments.

The main uses of potential-pH diagrams are in predicting spontaneous direction of reactions, estimating the composition of the corrosion products and predicting the influence of environmental changes (e.g., pH and oxidizers) on corrosion attack.

The velocity of the aqueous environment can also affect corrosion rates although the effects in a vault environment are probably minimal because of the low flow rates anticiptated. In anv event, the effects depend on the characteristics of the metal and the environment to which it is exposed. For corrosion processes controlled by activation polarization, velocity has no effect on the corrosion rate. If the corrosion process is controlled by concentration polarization, velocity increases the corrosion rate.

12.4 TYPES OF CORROSION

Fontana[121] has classified corrosion into eight forms, based on the appearance of the corroded metal. The eight forms are:

1. uniform corrosion (or general attack),
2. crevice corrosion,
3. pitting corrosion,
4. intergranular corrosion,
5. stress corrosion,
6. galvanic corrosion,
7. erosion corrosion, and
8. selective leaching.

Of these eight forms, uniform, crevice, pitting, intergranular and stress corrosion are the most significant with respect to container corrosion.

12.4.1 Uniform Corrosion (or General Attack)

This is the most common form of corrosion and is characterized by a chemical or electrochemical reaction which proceeds uniformly over the entire exposed surface. The mechanisms for uniform attack were discussed in some detail in Section 12.2. Clearly candidate materials must possess low uniform corrosion rates to be acceptable for fuel immobilization containers with a design lifetime of 500 years.

12.4.2 Crevice Corrosion

This is an intense form of localized attack which may occur within crevices and other shielded areas on metal surfaces exposed to aqueous environments. Deposits such as sand, dirt, corrosion products and other solids, as well as metal-to-metal crevices, can create small volumes of stagnant solution in a crevice only wide enough to permit liquid entry. The soil backfill surrounding the irradiated fuel container will provide an abundance of potential crevice corrosion sites where the backfill material contacts the outside surface of the container. The basic mechanisms of crevice corrosion can be illustrated by considering a metallic crevice immersed in aerated sea water. The overall reaction involves the dissolution of metal M and the reduction of oxygen to hydroxide ions according to reactions (1) and (4) in Section 12.2. Initially these reactions proceed uniformly over the entire surface including the creviced area. After a short period the oxygen within the crevice is depleted because of the restricted flow and oxygen reduction stops in this area. However, initially, the decrease in the overall rate of oxygen reduction (cathodic reaction) is negligible because of the small area of crevice involved and consequently corrosion of the metal both inside and outside the crevice continues at the same

rate. Eventually, however, the cessation of oxygen reduction in the crevice tends to produce an excess of positively charged metal ions (M^+) within the crevice which is necessarily balanced by the migration of chloride ions (Cl^-) into that area (Figure 19). Hydroxide ions can also migrate from the outside but are of less consequence because of their lower mobility.

The resulting metal chlorides which form in the crevice hydrolyze in water to insoluble metal hydroxides and free acid according to:

$$M^+Cl^- + H_2O \rightarrow MOH\downarrow + H^+Cl^- \qquad (7)$$

Both chlorides and low pH enhance metal dissolution in the crevice, resulting in a rapidly accelerating or autocatalytic process, while the reduction reaction (4) cathodically protects the regions outside the crevice. Active-passive metals which depend on passive layers for corrosion resistance are particularly susceptible to crevice corrosion because chlorides and low pH (H^+ ions) destroy their passive films.

Crevice corrosion should be of prime consideration when selecting candidate materials for irradiated fuel containers.

12.4.3 Pitting

This is a form of extremely localized corrosion that results in holes in the metal and causes components to fail by perforation, with only a small percent of metal loss of the entire component. Pitting may occur on any metal but it is the prevalent form of corrosion experienced with passive alloys and the passive metals such as aluminum, iron, nickel and chromium. Pitting is most likely to occur in the presence of chloride ions combined with such depolarizers as oxygen or oxidizing salts. Most buried components suffer from pitting corrosion which increases with increasing temperature, acidity and concentration of

damaging anions (e.g., Cl^-) in the soil solution. Pits may require a long time (several months or a year) to show up in service. Pits will initiate when the rate of metal dissolution is momentarily high at one point as a result of the breakdown of passive films. Local dissolution may be high because of the presence of crevices, chlorides, differential aeration cells due to oxygen, metal-ion concentration cells, inclusions and scratches or other surface defects. Once initiated, the mechanism of pit growth is virtually identical to that of crevice corrosion, i.e., the process is autocatalytic and propagation is associated with an acid mechanism (Figure 19). Because of this, pitting is felt to be a special case of crevice corrosion since alloy systems which show pitting attack are particularly susceptible to crevice corrosion. The reverse is not always true; many systems which show crevice attack do not suffer pitting attack on freely exposed surfaces.

The susceptibility of a material to pitting can be judged from its experimentally determined pitting potential, E_{pit} (Figure 16). Materials which exhibit a more noble pitting potential show less tendency for pit initiation and growth. Variables that influence pitting, such as solution composition, pH, temperature and alloying, do so by causing shifts in the pitting potential in either the noble or active direction.

Most pitting is associated with halide ions, with chlorides, bromides and hypochlorites being the most prevalent. Fluorides and iodides have comparatively few pitting tendencies. Oxidizing metal ions with chlorides are aggressive pitters. Cupric, ferric and mercuric halides are extremely aggressive. Halides of the non-oxidizing metal ions (e.g., NaCl, $CaCl_2$) cause pitting but are less aggressive. Cupric and ferric chlorides do not require the presence of oxygen because their cations can be cathodically reduced according to equations (5) and (6), and this is one reason why ferric chloride solutions are widely used in pitting studies[130]. It has been shown that nitrates, chromates, sulfates, hydroxides, chlorates, carbonates and silicates can act as

pitting inhibitors in many instances when added in appropriate concentrations[131-133]. However, the presence of hydroxide, chromate, or silicate salts may accelerate pitting when present in small concentrations[121]. In general, the presence of unaggressive anions produces three different effects: an increase of E_{pit}, a prolongation of the induction period and a lowering of the number of pits.

Pitting corrosion is also affected by pH. It has long been known that alkalis have an inhibiting effect. Although the pitting potential is not affected appreciably in the acid pH range[133], it moves markedly in the noble direction at a pH greater than about 7 for stainless steels[134] exposed to sodium chloride solutions.

Increasing temperature generally shifts the pitting potential to more active values, thus increasing the tendency for pitting corrosion[134]. However, there is some evidence that, at higher temperatures, a reversal occurs and the pitting potential begins to increase with increasing temperature[135-137]. This reversal in temperature dependence is accompanied by a change in the nature of the pitting corrosion from well-defined pitting to a more shallow pitting and general attack[136]. Although this phenomenon is not well understood, it appears that the reversal temperatures for austenitic stainless steels are generally below 200°C in alkaline chloride-containing solutions. However, in near-neutral solutions containing 100 - 3000 mg/L chloride ions, reversal temperatures greater than 200°C have been reported[136-138], with evidence of well-defined pitting attack at temperatures as high as 289°C[138].

Alloying can decrease susceptibility to pitting by shifting the pitting potential to more noble values. Various review articles have detailed the effects of minor and major alloying elements[131,133,134]. Their effects on pitting potential are shown graphically for stainless steels in Figure 20. Also included are the resulting shifts which these alloying elements create in the various regions of the polarization

curve for active-passive metals. Of the major alloying elements, chromium and nickel[111] impart improved resistance to pitting. Of the minor alloying elements, nitrogen (up to ~ 0.4%) and molybdenum (~ 2-3%) are the most significant. Generally elements which tend to be austenite stabilizers are beneficial.

Pitting corrosion is an important consideration for container material selection.

12.4.4 Intergranular Corrosion

This is localized attack at, and adjacent to, grain boundaries, with relatively little corrosion of the grains. Intergranular corrosion can be caused by impurities at the grain boundaries, enrichment of one of the alloying elements or depletion of one of these elements in the grain boundary areas. Intergranular corrosion of austenitic stainless steels is a common occurrence when they are heated in the temperature range 425 to 820°C. In this temperature range, chromium carbide has a low solubility and precipitates preferentially at the grain boundaries if the carbon content is about 0.02% or higher. The result is metal with lower chromium content in the area adjacent to the grain boundaries. The chromium-depleted zone is corroded because it does not contain the required chromium content ($\geq$ 12%) for resistance to corrosive attack. This phenomenon is called sensitization and is often associated with corrosion failures at welds (weld decay) due to heating in the sensitizing range. The methods used to overcome sensitization and hence minimize susceptibility to intergranular corrosion in austenitic stainless steels were discussed in Section 5.2.

Ferritic stainless steels, like the austenitics, can be susceptible to intergranular corrosion but their behaviour is quite different from the austenitic grades. The sensitization treatment for a ferritic steel involves heating above about 925°C. In the welded condition the weld metal itself and the high temperature heat-affected zone

become sensitized when, with the austenitic grades, parent metal on either side of the weld becomes sensitized. Slow cooling from the sensitizing temperature or annealing sensitized material at about 790°C will usually eliminate the problem in ferritic stainless steels.

High nickel alloys containing up to 80% nickel and more than 15% chromium are also susceptible to intergranular corrosion. Alloys such as Inconel and Incoloy behave like austenitic stainless steels, in that sensitization treatments which cause attack usually involve grain boundary carbide and/or intermetallic compound precipitation in the range 427 to 871°C. Control of intergranular corrosion in these alloy systems is similar to that for austenitic stainless steel, in that materials in the annealed and water-quenched conditions are resistant to intergranular attack. Nickel-chromium alloys containing more than 15% molybdenum for resistance to aqueous chloride environments can also become sensitized when heated in the temperature range 593 to 1149°C for short times, making welds susceptible to intergranular attack. Like the stainless steels, high nickel alloys can be made more resistant to intergranular corrosion by using material with very low carbon contents or stabilizing alloying elements.

Other alloys which depend on precipitated phases for strengthening may also be susceptible to intergranular attack. Duralumin-type alloys (Al-Cu) are examples of high strength aluminum alloys which can corrode intergranularly due to copper-depleted areas around grain boundary precipitates. Some magnesium- and copper-based alloys which form precipitates along grain boundaries or slip lines fall into the same category. This form of attack commonly occurs as a result of welding of some metal alloy systems, since the localized high heat treatments lead to one or more of the above conditions. Since welding will be employed during container fabrication, candidate materials should be resistant to intergranular corrosion.

1.4.3 Stress corrosion cracking

This refers to cracking caused by the simultaneous presence of tensile stress and a specific corrosion medium. During stress corrosion cracking, the metal or alloy is virtually unattacked over most of its surface, while fine cracks propagate intergranularly or transgranularly through it. The most important variables affecting SCC are tensile stress, solution composition, temperature, metal composition and structure. The time to failure for SCC increases with decreasing threshold stress. Stress raisers play an important part in crack initiation since high stresses can be generated locally at a surface flaw in a relatively low stressed component. Stress corrosion cracks are often found at the base of corrosion pits. The critical threshold stress for SCC is generally around the yield stress of the material but may be considerably less when an aggressive environment is present. The presence of oxidizers, particularly when chloride ions are present, has a pronounced influence on cracking. The synergistic effects of oxygen and chloride on SCC in aqueous media are well documented, particularly for the iron and nickel-based alloys. As with most chemical reactions, SCC is accelerated by increasing temperature. Cracking in magnesium alloys occurs readily at room temperature; in other alloy systems boiling temperatures may be required. The susceptibility to SCC can be reduced by changes in metal composition and structure. Increasing the nickel content of Fe-Cr alloys decreases to a minimum their cracking susceptibility as a function of composition[56]. The presence of ferrite in stainless steels retards SCC and, in fact, completely ferritic stainless steels are generally immune to SCC in most environments. It has generally been accepted that pure metals are not susceptible to SCC, although more and more information is being published which challenges this belief.

Although the container may be subjected to compressive stresses in the event of vault reflooding, residual tensile stresses are also possible after welding which could lead to SCC failures, particularly

chlorides and oxygen are present. Containers must be resistant to stress-corrosion cracking in the repository environment.

Of the three forms of localized corrosion considered to be most important for container material selection, the likelihood of initiating each of these forms in a particular environment decreases in the following order: crevice > pitting > SCC. Clearly, then, crevice corrosion will be the major consideration in selecting candidate materials.

12.4.6 Galvanic Corrosion

This is not a major consideration when selecting candidate materials for a corrosion-resistant container in a vault environment. If the irradiated fuel inside the container is invested in some low-melting-point metal such as lead, zinc or aluminum, galvanic corrosion may become a concern, but only when the first level of containment has been breached.

12.4.7 Erosion Corrosion

In the near stagnant environment of the vault, erosion corrosion will not be a factor.

12.4.8 Selective Leaching

This refers to the selective removal of an element from an alloy by corrosion. It has been observed in only a few two-phase alloy systems, e.g., Cu-Zn, Cu-Al, and is not a problem in pure metals or solid-solution alloys.

13. GROUNDWATER CHEMISTRY

The exact nature of the groundwater chemistry is unknown. Originally the composition of the Swedish tunnel water was considered to resemble closely the expected groundwater composition of deep groundwater in plutonic rock[139,140]. Recently, a more complete estimate of groundwater composition was provided by Bottomley[141] and is reproduced in Table 18, although there is a possibility that the actual groundwater chemistry may deviate from that specified in Table 18. Factors such as contamination introduced during repository construction, water radiolysis, solute concentration effects and intentional modifications of the water chemistry in the vault to make it benign, have already been discussed[142]. Further examination of these effects is required and their potential implications on container material selection is not directly considered here. The approach used in this report is to select potential materials which will be compatible with a moist backfill with water chemistry no worse than the maximum impurity concentrations indicated in Table 18. In addition, a maximum container surface temperature of 150°C is assumed.

The corrosivity of soils cannot be quantitatively defined because of its dependence on such factors as electrical resistivity, acidity, aeration and the corrosion product form (soluble vs. insoluble). However, some general correlations between each of the above factors and corrosion in soils have been suggested. Since underground corrosion is an electrochemical process, the conductivity or resistivity of the soil has long been recognized as a measure of its corrosivity. Table 19 shows the relation between soil resistivity and its corrosiveness towards steel pipe[143]. Romanoff[17] suggests that soils with resisitivities above 30 Ω·m are only moderately corrosive (see Table 19). The probable range of resistivities calculated from Table 18 for groundwater in crystalline rocks is 17 to 25 Ω·m. It is most likely that soils containing this groundwater (i.e., moist backfill) would have a

higher resistivity than the groundwater alone, and thus, tentatively, the corrosivity of the backfill could be considered to be in the moderate class (Table 19). It is worth noting that steel pipelines buried in soils with resistivities > 100 Ω·m generally do not require any form of cathodic protection. Cathodic protection is normally only justifiable when resistivities are < 100 Ω·m. Soil corrosivity also increases with increasing soil acidity (decreasing pH of the soil solution). This correlation generally holds for both high and low resistivity soils. The classification of soils with respect to acidity is shown in Table 20[17]. Aeration factors are those that affect the access of oxygen and moisture to the metal and thereby affect the corrosion process. Oxygen from atmospheric sources or oxidizing salts or compounds, stimulates corrosion by combining with metal ions to form oxides, hydroxides or salts of the metal. If these corrosion products are soluble, corrosion proceeds. However, if the products accumulate, they may form a protective layer which can reduce corrosion, or they may stimulate and localize corrosion if the products are more noble than the bare metal. Local differences in aeration may develop oxygen concentration cells, leading to rapid localized corrosion at oxygen-depleted areas.

Although the groundwater composition in Table 18 does not appear overly aggressive, it certainly cannot be considered benign. A measurable chemical oxygen demand (COD) is a definite indication of a reducing environment. Species such as carbonates (most abundant constituent), nitrates, phosphates and (to a lesser extent) sulphates are recognized to be effective inhibitors of ferrous alloy corrosion. Generally, most construction materials (Fe- and Ni-based alloys) exhibit minimums in their corrosion rates under mildly alkaline conditions like that of the model groundwater. On the other hand, the water conductivity is such that it would maintain electrochemical corrosion reactions which may be initiated in the form of localized corrosion. The chloride content, one of the main factors which determines the corrosivity of water to Fe- and Ni-based alloys, is appreciable. The synergistic effects of oxygen and chloride on localized forms of corrosion

have already been mentioned and, although the probable range of oxygen levels is reasonably low (< 0.01 mg/L), the probability of high oxygen levels existing at the time of emplacement cannot be ignored.

In selecting a suitable container material for underground disposal, one would opt for materials which would be either immune to the groundwater or form stable passive films, ensuring an exceptionally low corrosion rate. In general, the chemical nature of the groundwater appears conducive to passive film formation on most active-passive materials; however, the breakdown of passive films due to the presence of damaging chlorides often leads to localized forms of corrosion. Localized corrosion would be the major life-limiting factor and materials should be selected on the basis of their resistance to localized corrosion in the vault environment.

14. SELECTION OF CANDIDATE MATERIALS

Part I discussed the physical metallurgy, mechanical properties and weldability of the following groups of commercial metals and alloys:

1. Aluminum- and magnesium-base alloys.
2. Plain carbon and low-alloy ferritic steels.
3. Stainless steels.
4. Superalloys and high-alloy austenitics.
5. Titanium and its alloys.
6. Copper and its alloys.

This section discusses the corrosion behaviour of these materials with the specific vault environment in mind. Each group will be reviewed with respect to any specific attributes or drawbacks they have in the assumed environment. The review will concentrate on the potential

problems with localized forms of corrosion, particularly crevice and pitting corrosion, which appear to be the life-limiting factors for potential container materials.

14.1 ALUMINUM- AND MAGNESIUM-BASE ALLOYS

14.1.1 Aluminum and Aluminum-Base Alloys

Aluminum is a very reactive metal with a high affinity for oxygen. The cathodic reaction controlling aluminum corrosion in near-neutral aqueous media is oxygen reduction according to equations (3) and (4). In the presence of oxygen, aluminum reacts with water at temperatures below 75°C to form aluminum hydroxide ($Al(OH)_3$) initially, which ages with time to form a hydrated oxide or mixed oxides, the most common being bayerite ($Al_2O_3 \cdot 3H_2O$). Above 25°C the predominant oxide formed is boehmite (α-$Al_2O_3 \cdot H_2O$)[144]. The high corrosion resistance of aluminum in near-neutral water is due to the formation of these strongly adherent, protective oxide films. Generally, the higher the degree of purity, the greater the corrosion resistance, but a number of aluminum alloys have been developed for improved mechanical properties, particularly at higher temperatures (Section 3). However, certain elements such as magnesium, manganese and zinc, in amounts up to about 1%, can be alloyed with refined aluminum without substantially reducing the corrosion resistance of the pure metal in many environments. At temperatures less than about 90°C the most commonly encountered form of aluminum corrosion is pitting, between 90° and 250°C corrosion attack is generally uniform, and at temperatures greater than 250°C attack is intergranular.

The major compositional factors which influence the corrosivity of water to aluminum are pH, copper, bicarbonate, chloride and oxygen. The potential pH diagram for aluminum in water (Figure 21)[127] shows that the passivity domain extends over the entire potential range where water is thermodynamically stable. The passive oxide film is generally stable in solutions having a pH between 4.5 and 8.5. However,

because the film is soluble outside the range, attack can be quite severe in strong alkaline or acid solutions. In low temperature water, the optimum pH for minimizing the corrosion of aluminum is about 5.0 to 6.0[145] and is related to the effect of pH on the solubility of the oxide film (Figure 22)[146]. In general, high-strength (heat-treatable) aluminum alloys are not as corrosion-resistant as moderate-strength (non-heat-treatable) alloys.

Aluminum-base alloys are very susceptible to pitting attack in solutions containing heavy metal ions since the reaction of these ions introduces an additional cathodic reaction (Reaction (6)). Copper is by far the most notorious of the heavy metal ions, but mercury, lead, nickel, cobalt, tin and silver have also caused pitting attack[147]. Copper in most natural waters is less than 0.2 mg/L and thus is usually not determined in conventional water analyses. On the basis of case histories, Godard[144] believes that 0.1 mg/L copper in distilled water is sufficient to cause pitting in aluminum alloys. However, others[148] feel that as little as 0.02 mg/L copper can initiate pitting in hard waters. This is probably the result of the synergistic effects of copper, chloride and bicarbonate on pitting of aluminum. The combination of the three is more damaging than if they are present singly or if one of them is absent. Godard cites numerous references on this effect which is illustrated in Figure 23. In the presence of all three ions, pits up to 0.25 mm deep were seen after 24 days[144]. At higher temperatures, the effect can be more dramatic and pitting can be induced in solutions containing "pairs" of ions (copper + chloride, copper + bicarbonate, bicarbonate + chloride) (Figure 24). Oxygen can also affect pit initiation by setting up oxygen-concentration cells on the surface, particularly at crevices. Godard has observed pit initiation in oxygen-saturated tap water but not in oxygen-free tap water[144]. Moreover, it has been reported that the exclusion of air in water containing copper, chloride and bicarbonate reduced pitting by about one-third[144].

Romanoff has shown that aluminum alloys are susceptible to pitting and crevice attack in soils[17], and it is generally desirable to use some form of protection for aluminum materials buried in soils except where there is previous experience of satisfactory service in a given soil[148].

Stress corrosion cracking occurs in aluminum alloys developed for moderate and high-strength applications because of the precipitation of separate phases in the microstructure. Cracking is nearly always intergranular. SCC has not been observed in pure aluminum. Aluminum alloys are most susceptible to SCC when moisture is present and, in fact, crack velocities are similar in both moist atmospheres and water. The presence of halides such as Cl^-, Br^- and I^- can increase crack propagation by as much as 100 times. Lowering the pH also increases the susceptibility to SCC. Reference to SCC of particular aluminum alloys has already been made in Part I. It appears that the high probability of chloride and bicarbonate being present in the groundwater will make the vault environment aggressive to aluminum alloys, particularly since small amounts of copper cannot be tolerated. The probability of pitting or crevice corrosion is particularly high. Additionally, the presence of oxygen, which is unavoidable during container emplacement, will aggravate the situation.

14.1.2 Magnesium and Magnesium-Base Alloys

Magnesium has a high chemical reactivity and therefore it does not have a high degree of corrosion resistance. The potential pH diagram in Figure 25 shows a large corrosion domain which extends well into the neutral range of water[127]. A passive $Mg(OH)_2$ film can be formed under strongly alkaline conditions but it can be readily destroyed in the presence of chloride ions. The corrosion resistance of magnesium is inferior to that of aluminum and its alloys and hence it will not be considered further.

14.2 PLAIN CARBON AND LOW-ALLOY FERRITIC STEELS

Plain carbon and low-alloy steels are probably the most widely used materials for construction because of their availability, low cost and adequate mechanical properties. When iron corrodes, the rate is usually controlled by reaction (2) in deaerated acidic solutions but more commonly by reactions (3) or (4) in oxygen-containing aqueous media. When iron is exposed to water, hydrous ferrous oxide ($FeO \cdot nH_2O$) or ferrous hydroxide ($Fe(OH)_2$) forms a diffusion barrier layer next to the iron surface through which oxygen must diffuse. This layer is normally green to greenish-black in appearance. At the outer surface of the film, access to dissolved oxygen converts ferrous hydroxide to hydrous ferric oxide or ferric hydroxide ($Fe(OH)_3$). Hydrous ferric oxide is orange to red-brown in colour and comprises most of ordinary rust. The potential-pH diagram in Figure 17 shows the regions in which these compounds are thermodynamically stable at 25°C[127]. Biernat and Robins have presented potential-pH diagrams for the iron-water system at temperatures up to 300°C[149]. At temperatures above about 90°C, $Fe(OH)_3$ will form well-defined crystals of $FeOOH^-$ which on further heating to above 130°C decompose to Fe_2O_3. The hydroxide $Fe(OH)_2$ decomposes to Fe_3O_4 above 150°C.

The main environmental factors that effect carbon steel corrosion are oxygen, temperature, pH and halide (Cl^-) concentration. At normal temperatures, oxygen is necessary for appreciable corrosion of carbon steel and corrosion increases almost linearly with oxygen concentration. At higher concentrations (> 13 cm^3/L at 25°C), the corrosion rate decreases with increasing oxygen concentration due to passivation of the steel by the oxygen. The linear dependence of the corrosion rate on oxygen concentration is extended to higher oxygen concentrations when chlorides are present or when the temperature is increased. The combination of higher temperature and chlorides causes the passive film to break down, leading to severe pitting. In appreciable chloride concentrations (e.g., sea water), passivity is not established at all.

When corrosion is controlled by oxygen diffusion, the corrosion rate approximately doubles for every 30°C rise in temperature[150]. In open systems, corrosion increases to a maximum at about 80°C and then falls off, due to a decrease in oxygen solubility in the water with increasing temperature. In a closed system, however, the corrosion rate continues to increase with temperature. The effect of pH on the corrosion of mild steel is shown in Figure 26[151]. Corrosion is independent of pH within the range of about 4 to 10. At pH < 4, the ferrous oxide film is dissolved whereas at pH > 10 the steel becomes increasingly passive in the presence of alkalis and dissolved oxygen. At higher temperatures, however, the corrosion rate at high pH's is excessive since the corrosion products are unstable, the stable species being the $HFeO_2^-$ ion. At 300°C, carbon steel shows a minimum in the corrosion rate at a pH of about 11 to 12.

By far the most damaging combination of the environmental variables in the vault would be temperature (up to 150°C) and chlorides (up to 400 mg/L). At low temperature and high chloride concentrations (e.g., sea water), the corrosion of carbon steel is typically about 0.13 mm/a, but pitting corrosion rates can be as high as about 0.5 to 0.8 mm/a[152]. The effect of both temperature and chloride concentration on the uniform corrosion of mild steel is shown in Table 21[153]. The susceptibility of steel to pitting in chloride solutions at ambient temperature has already been illustrated in the experimentally determined potential-pH diagram (Figure 18). Certainly the presence of crevices on the outside surfaces of the containers would aggravate the situation. Results from the National Bureau of Standards soil tests show that in the more corrosive soils the maximum pitting rate of carbon steel after 12 years exposure ranged from about 0.2 to 0.4 mm/a. Corrosion rates of this magnitude would lead to failure of a container with a 25 mm wall thickness within 100 years. Low alloy ferritic steels do not offer any substantial increase in resistance to pitting corrosion. In soils, the pitting rates are typically about 0.15 mm/a after 12 years exposure[17]. Of the low alloy steels, chromium steels containing

molybdenum performed the best but, even in the less aggressive soils, the pitting rates were of the order of 0.1 mm/a.

In conclusion, the aggressiveness of the vault environment precludes the use of plain carbon and low alloy steels for container materials.

14.3 STAINLESS STEELS

By far the most corrosion-resistant of the iron-base alloys are the stainless steels. Their high degree of corrosion resistance in water is due to alloying with at least 12% chromium, which results in the formation of a stable passive oxide film in most aqueous media. The film is generally a mixture of hydrated chromium, iron and nickel oxides usually referred to as spinels, with chromium being the major component.

The five main classes of stainless steels as discussed in Part I are martensitic, ferritic, austenitic, precipitation-hardened and duplex (or austenitic-ferritic). The advantages and disadvantages of these steels with respect to their physical and mechanical metallurgy were discussed in detail in Section 5, and the increase in susceptibility of these alloys to intergranular corrosion and SCC as a result of welding was also pointed out. In this section crevice corrosion, pitting corrosion and SCC will be discussed in greater detail with particular emphasis on crevice and pitting attack.

The passive films on stainless steels offer excellent resistance to uniform corrosion. For this reason, stainless steels are used for many nuclear power reactor components because of their low uniform corrosion rates (< 0.0025 mm/a) in high-temperature (250° to 300°C) water[145]. Even in superheated steam at temperatures up to 732°C, the corrosion rates are less than 0.025 mm/a. These rates indicate that, on the basis of uniform corrosion, stainless steels would be acceptable candidate materials for containers. However, as with other alloys that

exhibit passivity under oxidizing conditions, stainless steels may suffer from localized attack, particularly when aggressive anions such as chlorides are present in the water. In this sense, the martensitic stainless steels are generally the least resistant of the stainless steels. They are used in applications requiring moderate corrosion resistance plus high strength or hardness. They are not often used for process equipment such as tanks and pipelines and are considered to be unsuitable for service in sea water applications[154].

The higher chromium content of the ferritic stainless steels provides some improvement in corrosion resistance over the martensitic grades, but the ferritic structure introduces some limitations in mechanical properties and fabrication. These steels are particularly attractive in applications requiring good corrosion resistance, particularly where heat resistance is required such as in furnace parts or heat-treating equipment. One of the unique aspects of ferritic stainless steels is their resistance to SCC, particularly in chloride-containing waters.

The precipitation-hardened (PH) stainless steels are strengthened by solution-quenching followed by heating for substantial periods at temperatures in the approximate range 425° to 535°C. The more common PH stainless steels find their widest application in the aircraft and missile industry under relatively mild corrosive conditions and in applications requiring good wear resistance. Their corrosion resistance to severe environments is generally less than that of the austenitic stainless steels.

Duplex steels which contain controlled amounts of ferrite and austenite were developed primarily for increased strength over that for single-phase austenitic grades. In addition to improving the strength, the ferrite contributes to increased resistance to chloride SCC compared to austenitic stainless steels. The resistance to general and pitting corrosion, however, is comparable to that of the austenitic grades.

The austenitic stainless steels possess better corrosion resistance than the straight chromium grades. For this reason they are widely specified for the more severe corrosion conditions such as those encountered in the process industries. The austenitics themselves can be divided into major groups according to alloying constituents.

The addition of significant amounts of manganese to chromium-nickel stainless steels (e.g., AISI 200 series, Nitronics, Tenelon) increases the strength but reduces the pitting and SCC resistance. Those steels with a maximum of 2% manganese (e.g., AISI 304) are more resistant to SCC, but a large number of service failures still occur.

The stabilized grades contain small amounts of titanium (e.g., AISI 321) or niobium (e.g., AISI 347) to suppress intergranular corrosion and weld cracking problems. Stabilization may be helpful against intergranular SCC but will not deter transgranular SCC. Low carbon (L) grades have the carbon limit lowered from the customary 0.08% to less than 0.03 or 0.02% carbon to reduce the risk of intergranular corrosion.

Specialty austenitic stainless steels contain large amounts of the major alloying elements such as chromium, nickel, molybdenum or manganese and are used where particular corrosion resistance or mechanical properties are required. In our case, resistance to localized forms of corrosion in water which contains chlorides is of prime importance. In Section 13 it was pointed out that crevice corrosion would be the major consideration in selecting candidate materials, since it is easier to initiate than either pitting or chloride SCC. Evidence of this is given in Figure 27 for type 304 SS in neutral sodium chloride solutions. The temperature-chloride concentration envelopes defining the initiation of pitting and cracking were produced by Truman from long-term immersion tests in air-saturated solutions[44]. Although the envelope labelled by Truman as "pitting" includes some results for pits initiated at glass/metal contacts (i.e., crevices) in his apparatus, for the most part localized corrosion defined by this envelope was in the form of pitting

on crevice-free surfaces. However, this anomaly in reporting the data suggests that the conditions for pitting, as reported by Truman, may be somewhat conservative. The temperature-chloride concentration envelope defining the occurrence of crevice corrosion in long-term immersion tests was produced by Kovach[155]. Although the overlap with Truman's curve for pitting corrosion is most likely associated with the uncertainties in constructing such curves, it may also reflect some degree of conservatism in Truman's results. In any event, these data indicate that it is easier to initiate crevice corrosion than either pitting or chloride SCC in the same environment.

Some reservations have been expressed about using electrochemical techniques to predict the crevice corrosion behaviour of metals and alloys in different environments. One of the more significant advances in the development of such techniques was made by Wilde and Williams[156] who conducted cyclic anodic polarization measurements on samples containing crevices. They found that the occurrence of hysteresis in the polarization curves was related to the susceptibility to crevice corrosion. Moreover, the extent of hysteresis could be directly related to the severity of crevice corrosion.

Alternative techniques for generating anodic polarization data have been used which involve rapid scan rates[157,158] and crevices different from those recommended by Wilde and Williams[156]. However, there are reservations about the reliability of rapid scan techniques in predicting the conditions under which crevice corrosion will occur[159]. To illustrate this, the results of Efird and Moller's electrochemical tests using a rapid scan technique, without a controlled artificial crevice, are compared with crevice corrosion data from immersion tests in Figure 27. It is evident that the electrochemical data fails to correctly predict the conditions for crevice corrosion, and hence can be misleading, although the electrochemical predictions in this case are conservative. This indicates that electrochemical data alone should not be relied on to determine the susceptibility to localized corrosion and,

even when more accepted test procedures are used[160], should be backed up with data from immersion tests under conditions representative of the service environment.

Lowering the pH to more acid conditions causes a shift in the temperature-chloride envelopes of Figure 27 downward and to the left. Figure 28 illustrates the effect of pH, in solutions which contain chlorides, on localized corrosion of type 316 L stainless steel. These data were taken from a summary of INCO corrosion tests in power plant flue gas scrubbing processes[161]. The scrubbing liquors acquire acidity during absorption of SO_2 (and some SO_3) and contain chloride introduced from the fuel (especially coal). The exposure temperatures at which the data in Figure 28 were obtained were generally within the range 50° to 60°C. The data indicate a strong dependence of localized corrosion on solution pH and provide some confirmation of the immersion test results in Figure 27.

Steels with greater resistance to crevice/pitting corrosion than type 316 SS are those with higher chromium and molybdenum contents. Increases in nickel and nitrogen are also beneficial (Figure 20) since they increase the pitting potential to more noble values but to a lesser degree than do chromium and molybdenum. The influence of the latter additions on pitting and crevice corrosion is best illustrated in Figures 29 - 31. Figures 29 and 30 show the relationship between the critical pitting potential of Fe-Cr-Mo alloys measured in deaerated synthetic sea water at 90°C and pH 7.2, and their resistance to crevice attack in synthetic sea water at 121°C and $\sim$ 60 mg/L oxygen[162]. The effect of molybdenum is clearly evident. These and other data, principally by Streicher[163], led to the development of the alloy 29-4 (29Cr-4Mo), a stress corrosion resistant ferritic stainless steel with good resistance to crevice and pitting corrosion in saline environments. Figure 31 shows the critical temperature required to initiate crevice corrosion on some experimental and commercial austenitic stainless steels in a 10% $FeCl_3$ solution as a function of molybdenum content[164].

The 10% $FeCl_3$ test is an accelerated test believed to be an indicator of the susceptibility of materials to localized corrosion in sea water. The data are consistent with the beneficial effects of molybdenum shown in Figures 29 and 30 for ferritic stainless steels. Al-6X (20Cr-24Ni-6.5Mo) was specifically developed for sea water applications and its behaviour in sea water at ambient temperatures is considered to be comparable to Hastelloy-C or even titanium. Electrochemical tests in chloride solutions at ambient temperatures show that the pitting potential is high (Table 22)[165]. Furthermore, its resistance to crevice corrosion in the 10% $FeCl_3$ test is excellent and similar to Hastelloy-C and titanium (Table 23)[165]. Al-6X is receiving much attention for condenser applications, and a number of U.S. utilities are currently using or have committed themselves to AL-6X tubing for condensers where sea water cooling is required.

Most of the molybdenum-bearing steels have been developed to combat crevice/pitting corrosion in applications where either the temperature or chloride concentrations (but not both) are high. Several review articles have been published that compare the different grades in various chloride-containing media[166-169]. All articles stress the significance of Cr+Mo additions to stainless steel for sea water service and substantiate the alloy ranking shown in Tables 22 and 23. Application for service in high-temperature, high-chloride media is generally reserved for molybdenum-bearing high nickel alloys.

14.4 SUPERALLOYS AND HIGH-ALLOY AUSTENITICS

Nickel-base alloys primarily used for corrosion-resistance applications are typically those referred to as Monel, Inconel, Incoloy and Hastelloy. The composition of these alloy systems has already been discussed in Section 6 (Table 7). The uniform corrosion rate of these alloys in high-temperature water is very low (< 2.5 µm/a) due to the formation of a passive oxide or hydrated oxide film (Figure 32)[127]. Even in 2% NaCl solutions at 140°C the Hastelloys only corrode at

< 2.5 μm/a[170]. It is important to distinguish between the solid-solution-strengthened (SSS) and the precipitation-hardened (PH) nickel alloys. The SSS alloys are important because of their excellent corrosion resistance, especially when alloyed with chromium and molybdenum or copper, and are used in the chemical industry, power generating industry and in marine engineering. Precipitation-hardened nickel alloys are used where high-temperature corrosion resistance is required, such as in gas turbines. At ambient and slightly elevated temperatures, PH nickel alloys are more susceptible to SCC than pure nickel or SSS nickel alloys. Monel, Inconel, Incoloy and Hastelloy are all SSS alloys.

Susceptibility to chloride SCC is greatly reduced in Fe-Ni-Cr alloys containing greater than ~ 50% Ni[56]. Figure 33 shows that high nickel alloys are virtually immune to SCC in the boiling $MgCl_2$ test at 154°C[171], an accelerated test used to rank the susceptibility of materials to chloride SCC. At higher temperatures (280° to 350°C), dilute chloride solutions containing oxygen will cause cracking in high nickel alloys containing greater than about 70% Ni, such as Inconel 600[171]. The optimum composition for resistance to SCC in solutions containing oxygen, chlorides or free hydroxide appears to be at a Cr/Ni ratio of about 30%/60%. A decrease in the chromium content of Inconel 600 is believed to be partly responsible for its increase in susceptibility. At temperatures of about 150°C, the high nickel alloys are generally more resistant to SCC than the austenitic stainless steels or the lower nickel-bearing alloys such as Incoloy 800, Incoloy 825 and Inconel 718.

The significance of chromium and molybdenum additions to nickel alloys with respect to crevice and pitting corrosion is identical to that for stainless steels. Table 24 shows that the higher the molybdenum content of the nickel-base alloy, the higher the oxidizing potential required to initiate localized attack[159]. For this reason alloys which do not contain molybdenum (such as the Monels, Inconel 600 and Incoloy 800) are no more resistant to crevice/pitting attack in water containing chloride than the 300-series austenitic stainless steels.

The pitting potential of Inconel 600 is virtually the same as that for type 316 SS in 90°C synthetic sea water (Figure 29). Under the same conditions, the pitting potential of Incoloy 825 (∿ 3% Mo) is somewhat higher but not as high as that for Inconel 625, which contains about 9% Mo (Figure 29). This difference is further shown from results of two-year corrosion tests on nickel alloys in quiet and low-velocity sea water given in Table 25[172]. Alloys most susceptible to both general corrosion and localized attack include the Monels. Those which showed neither general nor localized attack were those containing appreciable Cr+Mo additions such as Hastelloy-C, Inconel 625 and Rene 41. However, Rene 41 is generally less resistant to SCC since it is a PH alloy.

The excellent corrosion resistance of the molybdenum-bearing nickel alloys to both high temperature and high chloride-containing solutions is best demonstrated by results of autoclave and pilot plant corrosion tests on materials considered for use in sewage treatment plants[173]. These plants are based on the wet air oxidation (WAO) principle and materials of construction are an important design factor due to the high operating temperatures (∿ 200°C), the complex composition of the sewage sludge and the presence of soluble chlorides. Results of these tests on a variety of materials are given in Table 26 and show that Hastelloy C-276 and Inconel 625 can tolerate at least 1000 mg/L chloride and the 28Cr-4Mo alloys at least 600 mg/L chloride, whereas Incoloy 825 and other specialty stainless steels suffered from localized corrosion at lower chloride concentrations. Commercially pure titanium was resistant even at 3000 mg/L chloride. For comparison, both 304 and 316 austenitic stainless steels were resistant to localized corrosion in sludge containing 200 mg/L chloride, but suffered from crevice corrosion at both 300 mg/L and 400 mg/L chloride. However, the performance of 304 and 316 stainless steels in sewage sludge is better than would be predicted from the tests reported in Figure 27. It was suggested that this tolerance to chloride may be due to the presence of naturally occurring inhibiting components in sewage sludge[173].

Of the various grades of Hastelloy, alloy C-276 with extra low carbon is the most resistant, showing excellent resistance to crevice and SCC even in the sensitized condition (Table 27)[64]. Alloy C is equally resistant but only in the solution-annealed condition. Alloy C-4 resists SCC in either condition but is susceptible to crevice corrosion in a 50°C ferric chloride test in all conditions.

As with most other alloy systems, nickel alloys may suffer from intergranular corrosion when sensitized as a result of welding[174]. The nature of the grain boundary precipitation phenomenon in Ni-Cr-Mo alloys is more complex than in Ni-Cr-Fe alloys (see Part I). It seems probable that two different mechanisms of intergranular corrosion operate in the former, one involving attack on the depleted regions adjacent to the grain boundaries (e.g., in hydrogen-evolving acidic solutions), and the other in which the intermetallic precipitate is preferentially attacked (e.g., in more highly oxidizing acidic media). Limiting the silicon and carbon contents to very low levels reduces the tendency for formation of the intermetallic phase during welding and this led to the development of the improved alloy Hastelloy C-276. More recently a composition possessing even greater thermal stability, i.e., Hastelloy C-4, has been introduced, in which iron and tungsten have been replaced by nickel, and small amounts of titanium ($\sim$ 0.5%) have been added to stabilize carbon. However, its resistance to crevice corrosion is somewhat inferior to that of a low carbon grade of Hastelloy C-276[64].

Of the nickel-based alloys, only Hastelloy C-276 and Inconel 625 seem to offer any substantial improvements in corrosion resistance over that of the specialty stainless steels for the application of a corrosion-resistant container.

14.5 TITANIUM AND TITANIUM ALLOYS

Titanium is intrinsically very reactive so that, whenever the metal surface is exposed to water or any environment containing available

oxygen, a thin tenacious surface film of oxide is formed. The potential-pH diagram for titanium (Figure 34) shows this, since the domain of thermodynamic stability of the oxide (TiO_2) is common with the domain of thermodynamic stability of water at 25°C[127]. The film resists attack by oxidizing solutions, in particular those containing chloride ions, and thus has outstanding resistance to corrosion and pitting in marine environments.

Of the three main types of titanium alloys (see Part I), single-phase α-Ti alloys are used most often where corrosion resistance is of extreme importance. These include C.P. titanium (ASTM Grades 1 to 4), Ti-Pd alloys (ASTM Grades 7 and 11) and Ti-Mo-Ni alloys (ASTM Grade 12). The strong passive film is responsible for the extremely low uniform corrosion rates measured in aqueous media at ambient and elevated temperatures. The corrosion rate in sea water is typically < 1 μm/a.

In their survey of titanium for use as a container material for nuclear waste, the Swedes report corrosion rates generally less than 2 μm/a for unalloyed titanium exposed at temperatures up to 400°C with a maximum value of 5.6 μm/a quoted in one reference (Table 28)[70,81,175]. Even at this rate and assuming a linear corrosion process, only 5-6 mm of titanium would be consumed in 1000 years. The final Swedish assessment assumed that a rate of 0.25 μm/a was a conservative value and, based on this, estimated a lifetime of ≥ 10 000 years for a 6 mm thick container[70,81]. Additional conservatism is implied if a logarithmic oxide growth is also assumed. Similar low corrosion rates were recently reported by Braithwaite et al. for titanium corrosion in brine and sea water at 250°C[46]. The resistance of titanium to crevice corrosion and pitting is superior to that of iron- and nickel-base alloys because of the tolerance of the oxide film to chloride. This has been demonstrated repeatedly in 10% ferric chloride crevice corrosion tests (e.g., Table 23). Electrochemical tests in 1 mol/L NaCl solutions showed that the pitting potential of C.P. titanium at 25°C is about 9 V_{SCE} and at 150°C it is still as high as 2 V_{SCE}[176].

The resistance of titanium and its alloys to crevice corrosion has been the subject of many investigations. It is generally agreed that increasing chloride concentration, temperature and pH all increase the susceptibility to crevice corrosion. However, the effect of increasing oxygen (solution aeration) is still the subject of some controversy, some data indicating that it causes an increase in susceptibility[177-179], and other data suggesting the opposite effect[180-182]. These differences in observations may be due, in part, to the varying types of crevice used. For example, Schlain and Kenahan[183] reported that crevice corrosion was most severe when the crevice opening was between 75 and 100 μm. In addition, it is known that metal to metal and metal to non-metal crevices can produce different susceptibilities to crevice corrosion for given conditions.

For many years, the generally accepted behaviour of titanium and its alloys in aqueous chloride environments was that determined by the titanium industry based on laboratory data and industrial experience[184,185]. This indicates that the upper temperature limit for corrosion-free service in sea water is about 130°C for C.P. titanium (ASTM grade 2) and about 170°C for the Ti-0.2% Pd alloy (ASTM grade 7), as shown in Figure 35[185]. However, recent work by Shimogori et al. (see Figure 35) in solutions containing chloride in the range 10^2-10^5 mg/L suggests a lower temperature limit for immunity of C.P. titanium to crevice corrosion[179]. The same authors found a higher temperature limit for the Ti-0.2% Pd alloy, i.e., no crevice corrosion up to 250°C in water containing 10^5 mg/L chloride. These conflicting results indicate the need for a more systematic study of crevice corrosion of titanium alloys in aqueous chloride solutions, using specimens with carefully controlled crevice geometries.

Corrosion tests related to the WAO process for sewage treatment (mentioned in Section 14.4) have shown C.P. titanium to be resistant to crevice, pitting and SCC at 204°C in solutions containing 3000 mg/L chloride (Table 26). In similar applications, a Japanese

study has found no evidence of any corrosion of titanium in their sewage treatment plants after 5 years of service at 232°C and chloride concentrations up to 5000 mg/L (~ 1% as NaCl)[173]. The test results and service experience in sewage sludge indicate that the resistance of C.P. titanium to localized corrosion is greater than would be predicted from the data of Shimogori et al., discussed above[179]. However, an appreciable chemical oxygen demand (COD) of the sewage sludge suggests mildly reducing conditions during these exposures.

The increase in crevice corrosion resistance with increasing pH is shown in Figure 36 for C.P. titanium (Ti-50A) and the new Ti-0.3% Mo-0.8% Ni (TiCode-12) alloy in 24% NaCl (brine) solution[72]. TiCode-12 was developed as a low cost alternative to the Ti-0.2% Pd alloy with about equivalent crevice corrosion resistance and increased strength. It is evident that under more acid conditions TiCode-12 and Ti-0.2% Pd are superior to Ti-50A. This conclusion is supported by the results of Braithwaite, who reported no evidence of crevice corrosion on samples of TiCode-12 exposed to 250°C oxygenated brine (4.2×10^4 mg/L Cl^-) at a pH of about 3.4[46]. One disadvantage of these alloys, however, is that they are more susceptible to hydrogen absorption than unalloyed titanium, particularly when coupled with non-precious metals[81].

Crevice corrosion has not been observed on titanium in brines with pH values greater than about nine, although, as indicated in Figure 36, hydriding of titanium may occur at pH values greater than 10 and temperatures exceeding about 200°C. However, rapid hydriding would not be anticipated in titanium containers in a disposal vault because of the specified maximum temperature limit of 150°C. At this temperature, pH values exceeding about 12 (which at this time appears highly improbable) are required to promote hydriding.

Despite their excellent corrosion resistance, titanium alloys have been found to be susceptible to SCC in aqueous solutions. Two suggestions have been proposed for the damaging species responsible for

aqueous SCC. These are (a) Cl^-, Br^- and I^- derived from solutions or, in some cases, from impurities in the titanium alloy itself, as described by Beck[186] and (b) hydrogen derived from the interaction of titanium alloy with water, as postulated by Scully[187]. Either of these agents appears to be sufficient by itself, and a definitive statement as to which is the damaging species in aqueous solutions, as yet, cannot be made.

The resistance of titanium alloys to stress corrosion lies mainly in the extreme protectiveness of the oxide film which, in preventing pit initiation, also prevents crack initiation[188]. This resistance is demonstrated from results of tests in which specimens of titanium alloys, which have been plastically deformed while immersed in chloride solutions, fail to develop cracks unless the strain rate is high. By comparison, other susceptible materials such as the austenitic stainless steels crack readily when they are strained dynamically at low rates. In titanium alloys emergent slip planes are repassivated too rapidly for any significant corrosion attack to occur.

Precracked titanium alloys appear to be more susceptible to SCC in sea water if they contain aluminum, tin, manganese, cobalt and/or oxygen. Alloys containing more than 6% aluminum are particularly susceptible. On the other hand, the presence of beta stabilizers such as molybdenum, niobium or vanadium reduces or eliminates the susceptibility to cracking. Of the C.P. alloys, only those with a high oxygen content (i.e., 0.3% oxygen) cracked in ambient sea water in laboratory tests on pre-cracked specimens. As a result, there have been no reports, to our knowledge, of SCC failures of C.P. titanium or Ti-0.2 Pd alloys in service.

In view of the above, C.P. titanium (ASTM Grade 2), Ti-0.2% Pd (ASTM Grade 7) or Ti-0.8% Ni-0.3% Mo (ASTM Grade 12) would all appear to have adequate corrosion resistance for service as a container material in a disposal vault. Although Grades 7 and 12 are more corrosion

resistant, they are also more susceptible to hydrogen adsorption and hence to potential embrittlement (see Part I).

14.6 COPPER AND COPPER ALLOYS

Since copper is not an inherently reactive metal, the general rate of corrosion in water even in the absence of corrosion films or insoluble corrosion products is usually low. Nevertheless, in practice, the good behaviour of copper and its alloys often depends to a considerable extent on the maintenance of a protective oxide film. When copper corrodes in near-neutral or alkaline water, the controlling cathodic reaction is one of oxygen reduction according to equation (4). The oxide film formed in water is generally cuprous oxide (Cu_2O) but, under more oxidizing conditions, cupric oxide (CuO) is the stable form (Figure 37)[127].

Copper and copper alloys are used in large quantities for handling both fresh and salt waters, fresh water being in general less corrosive towards copper than sea water. The uniform corrosion rate in sea water can vary from 5 to 50 μm/a and up to several times these rates in contaminated waters[189].

There are several types of corrosion that copper and its alloys may undergo, particularly in sea water, but also on occasion in fresh waters. Dezincification of brasses occurs when regions of the brass become replaced by a porous mass of copper, and although the original structure is retained, it has virtually no strength. The mechanism is either selective corrosion of the zinc in the brass, which leaves the copper behind, or complete dissolution of the brass followed by redeposition of the copper, or both. Generally the rate of dezincification increases with increasing zinc content. Other factors that cause higher rates are high temperature, high chloride content and stagnant conditions. Dezincification is likely to occur preferentially beneath deposits or in crevices where there is a low degree of aeration.

Additions of antimony or phosphorus in α-β brasses can reduce the attack but will not render them immune under all conditions of exposure.

Selective attack analogous to dezincification can occur in other copper alloys, particularly in aluminum bronzes and less frequently in tin bronzes and cupro-nickels. Dealuminification of aluminum bronzes increases with aluminum content while the lower alloyed α-phase alloys are less susceptible. Pitting of copper in fresh water can be classified into two major types[190]. Type 1 pitting is usually associated with certain hard or moderately hard well waters. It is more likely to occur in cold water than in hot water and may cause perforation in domestic plumbing in only one or two years. It is characterized by the formation of fairly large well-defined pits usually containing soft crystalline cuprous oxide (and often cuprous chloride) beneath hard grey mounds of calcium carbonate or basic copper carbonate (Figure 38). Type 2 pitting occurs only in certain soft waters and is practically unknown at water temperatures below 60°C. It is characterized by deep pits of small cross section containing very hard crystalline cuprous oxide and capped by small black or greenish mounds of cuprous oxide or basic copper sulphate. Type 2 pitting in sea water has not been reported, even for sea water that has been acidified and used at high temperatures, as in desalination plants.

Crevice corrosion is also known to occur in copper and its alloys, and the mechanism has been attributed to either differential aeration or metal-ion concentration cells. The crevice corrosion resistance of copper and some of its alloys compared to other alloys in sea water is shown in Table 29[191]. Efird et al.[192] suggest that a crevice protection potential exists for copper alloys in NaCl solutions which is in close proximity to the intersection of the general corrosion region and the primary passivation line (circled in Figure 39). More noble corrosion potentials support crevice attack whereas more active potentials favour repassivation within the crevice by a second more protective film. Since this crevice protection potential is dependent

on the nature of the potential-pH diagram for copper, they suggest that this concept might be applicable to all copper-base alloys having the same general features in their experimental potential-pH diagrams.

Most of the development of copper-base alloys was related to service in sea water because of their low corrosion rates and inherent resistance to marine fouling. The main environmental factors which influence copper alloy corrosion in sea water are oxygen, temperature, pH, chloride and contamination by sulphide. Oxygen, one of the most important factors, can affect the corrosion reaction by depolarizing cathodic areas, oxidizing cuprous ions to the more corrosive cupric state and promoting the formation of a protective film. In high-temperature sea water, acceptably low corrosion rates are only attainable under low oxygen (dearated) conditions (Figure 40)[193]. The effect of increasing temperature on the corrosion rate has been reported as being adverse, of no effect or beneficial[193,194]. The reduction in corrosion rates observed with increasing temperature is probably a result of the reduced oxygen solubility in water at higher temperature. In the presence of oxygen, increasing temperature increases the corrosion rate. Results from tests in desalting environments indicate that useful high-temperature service of copper alloys in desalination plants can only be assured if the oxygen content is kept low[194].

The influence of pH is obvious from the potential-pH diagram of Figure 37. In acidic solutions, the controlling cathodic reaction is one of oxygen reduction according to reaction (3). Low pH prevents copper-base alloys from developing protective films, resulting in high corrosion rates. High oxygen levels, in combination with low pH, further accelerate corrosion. Chloride tends to promote localized forms of corrosion. Dezincification and dealuminification are more likely to occur in warm or hot waters with relatively high chloride concentrations. A high $SO_4^{=}:Cl^-$ ratio favours pitting in copper alloys[195], which is opposite to the conditions which favour pitting attack in stainless steels. Chloride, in combination with free carbon dioxide,

sulphate and high temperature, also promotes high dissolution rates in aqueous media. The formation of carbonic acid, even though very weak, prevents the formation of protective films ordinarily developed on copper.

Water becomes very aggressive to copper and its alloys when contaminated with sulphides, and a number of reports have dealt with investigations specifically related to this problem[196-201]. In sulphide-containing waters, a copper sulphide film is formed on the surface which is more cathodic than the corrosion film developed in clean waters. Breaks in the sulphide film greatly stimulate local attack by pitting because of the large cathodic area. Sulphide concentrations as low as 0.01 mg/L have been observed to cause accelerated attack on copper alloys[198], and vigorous attack has been observed on 90/10 Cu-Ni alloys at sulphide concentrations of 0.2 mg/L in ambient sea water. Maximum pit depths of 0.5 mm were measured after 15 days exposure. The effects of oxygen on sulphides are synergistic and combinations of 0.06 mg/L sulphide and 0.87 mg/L O_2 can increase normal corrosion rates in pure water by a factor of 10[199]. Electrochemical measurements have shown a noble (electropositive) shift in corrosion potential for 90/10 Cu-Ni electrodes exposed to sea water with sulphide concentrations ranging from 0.05 to 0.2 mg/L, which supports a pitting mechanism based on the local potential difference between freshly exposed Cu-Ni and the surrounding sulphide-modified filmed areas[198].

From experience obtained to date on copper alloys exposed to sea water and desalting environments, the following general comments can be made with regard to the corrosion resistance of various alloys. Qualitatively, the most favourable experience with copper alloys has been at service temperatures of 90°C or less. Pure copper is generally not suitable in hot sea water and its use would be limited to deaerated water at low velocities. The brasses and bronzes are somewhat more resistant, but their uses are generally restricted to conditions where oxygen content is known to be low (deaerated water). They also suffer

from dealloying (dezincification and dealuminification), especially in chloride media. The copper-nickel alloys (90/10 Cu-Ni and 70/30 Cu-Ni) are probably the most resistant of the copper-base alloys for sea water service. Table 30 shows the corrosion rates of various copper alloys in quiescent sea water and indicates the superior resistance of the copper-nickel alloys[201]. However, as pointed out earlier, they are susceptible to sulphide-induced pitting in contaminated waters.

The suitability of copper or copper-base alloys as a corrosion-resistant container is questionable. A low $SO_4^{=}:Cl^-$ ratio in the groundwater would certainly favour resistance to the normal Type 1 pitting previously discussed. However, the combination of oxygen, chloride, sulphide and high surface temperature of the container does raise the question of container integrity due to localized corrosion processes such as dealloying and sulphide-induced pitting, particularly when crevices are present. For pure copper, of course, dealloying is not a problem. Moreover, the Swedish KBS assessment concluded that, in the absence of γ-irradiation effects, a 200 mm thick copper container for fuel immobilization would have a lifetime of hundreds of thousands of years[3,202]. Certainly there is considerable historical and archeological evidence to indicate that copper would be acceptable in some environments for at least 500 years[203]. Thus, although there is some uncertainty about the corrosion performance of copper, in the absence of more specific information on the groundwater chemistry and radiolysis effects on the production of oxidants, it is recommended that copper be included as a candidate container material.

15. SUMMARY OF PART II

The preceding assessment eliminated low-alloy steels, aluminum and magnesium alloys from present consideration for container materials on the basis of their corrosion susceptibility under the temperature and

chemistry conditions currently envisaged in a deep underground disposal vault. In addition, some concern was expressed as to the suitability of copper alloys in such an environment, although it was recommended that pure copper be included for further evaluation. Of the remaining alloy systems discussed, the commercial alloys considered as most promising can be ranked according to their crevice corrosion behaviour in aqueous chloride solutions.

Ideally, the proper ranking of these materials should be made from results of immersion tests over the expected range of temperature and chloride concentrations in near neutral solutions. However, only a limited amount of data from such tests exists over a sufficiently broad range of chloride-temperature conditions. This includes the long-term field data of Kovach[155] for types 304 and 316 stainless steel condenser tubing, and the data for titanium and its alloys, produced by the titanium suppliers[185] and Shimogori et al.[179]. The discrepancy between the titanium data from these two sources has already been discussed in Section 14.5. In addition, some of the materials of interest have been evaluated under wet air oxidation conditions in sewage sludge containing 200 to 3000 mg/L chloride ion at 204°C[173]. However, the behaviour of many of these materials, including the high-molybdenum austenitic and ferritic stainless steels and the nickel-base alloys (Inconel 625 and Hastelloy C-276), has not been evaluated in immersion tests in chloride solutions in the temperature range 50-150°C. In the absence of such data, the likely corrosion performance of these materials must be inferred from other short-term tests used to predict the corrosion performance in aqueous chloride solutions. Results from electrochemical tests may not be particularly suitable for this purpose since, as demonstrated in Section 14.3, they are not truly representative of a long-term immersion test, although the electrochemical data appear to be somewhat conservative. Of the available ranking tests, the 10% $FeCl_3 \cdot 6H_2O$ immersion test has been used most successfully to rank alloys with respect to their expected behaviour in sea water. Garner[204] has demonstrated that this test is a good indicator of susceptibility to

crevice corrosion in sea water by comparing the crevice corrosion temperature in 10% $FeCl_3 \cdot 6H_2O$ with the behaviour of the same materials in long-term tests in sea water. He concluded that, for stainless steels, crevice corrosion in sea water will only occur at temperatures higher than the crevice corrosion temperature determined in the 10% $FeCl_3 \cdot 6H_2O$ test (Figure 41). All but one of the 122 data points in his survey demonstrated this behaviour. Thus, it can be inferred that the behaviour of other alloys (e.g., Inconel 625, Hastelloy C-276, titanium) in the ferric chloride test may also give a valid indication of their susceptibility to crevice corrosion in sea water although, unlike the stainless steels, detailed comparisons with long-term sea water exposures have not been made on these alloys.

Crevice corrosion temperatures in ferric chloride tests from a number of sources are summarized in Table 31. The lowest temperature at which crevice corrosion has been reported to occur is noted and, for conservatism, these values will be used for ranking purposes.

Figure 42 attempts to rank the materials with respect to their susceptibility to crevice corrosion in aqueous chloride solutions. The solid lines represent data determined from immersion tests, excluding ferric chloride tests. Crevice corrosion has been observed at temperatures and chloride concentrations to the right of the solid lines, and it is reasonable to suggest that this represents the possible behaviour of these materials in a vault environment. Where no long-term immersion data exist, alloy performance has been inferred (dashed lines) from the ranking observed in ferric chloride tests and from data obtained under wet air oxidation conditions in sewage sludge immersion tests. Clearly much more work is required for materials which fall into this category.

From Figure 42 the suggested ranking of materials in order of increasing resistance to crevice corrosion is as follows:

austenitic stainless steel,
austenitic and ferritic stainless steels containing molybdenum,
high nickel-base alloys containing molybdenum,
titanium and dilute titanium alloys.

The effectiveness of chromium and molybdenum additions in improving the resistance of iron- and nickel-base alloys to crevice corrosion becomes evident from this ranking. Moreover, Figure 42 clearly indicates those areas requiring more thorough investigation:

1. Although the immersion test data on types 304 and 316 stainless steels are reasonably consistent with the high temperature data from wet air oxidation (WAO) tests, more information is required in the critical temperature range 100° to 200°C.

2. Although Figure 42 indicates that the austenitic and ferritic stainless steels containing molybdenum (up to 6%) are more resistant to chlorides than types 304 and 316 stainless steels, more investigations are required over a broad range of temperature and chloride concentration.

3. For the high nickel-base alloys containing molybdenum (Inconel 625, Hastelloy C-276), there is a paucity of data in the range of temperature and chloride content expected in a disposal vault.

4. Although immersion tests have been done on titanium and its alloys over the temperature and chloride concentrations of interest, it is evident from Figures 35 and 42 that there is some disagreement between the results of various investigators. For example, the ferric chloride test results on grade 2 titanium appear to be in reasonable agreement with the data of Shimogori et al.[179], although the data obtained in sewage sludge under WAO conditions is in closer agreement with the immersion data quoted by the titanium suppliers[185].

There is, however, general agreement that the Ti-0.2% Pd alloy (ASTM grade 7) is more resistant to crevice corrosion than C.P. titanium. Most of the reported data indicate that, of the alloy systems considered, titanium and its dilute alloys should be the most resistant to crevice corrosion in aqueous chloride solutions. However, it is recommended that additional tests be carried out to resolve the discrepancy in the reported performance of C.P. titanium.

Of the materials reviewed, the Ti-0.2% Pd alloy is the most resistant to crevice corrosion in chloride solutions. However, it is at least a factor of two more expensive than C.P. titanium. The recently developed alloy Ticode-12 (ASTM grade 12) is also reported to be more resistant to localized corrosion in chloride solutions than C.P. titanium[72], although comprehensive data on its performance over a range of chloride concentration and temperature does not appear to be available in the literature.

If future hydrogeological studies establish that the groundwater in the vault will be relatively benign (< about 100 mg/L chloride, and no salt-concentrating mechanisms), an austenitic stainless steel, such as 316 L, could be considered as a candidate container material. However, it is most unlikely that such conditions will prevail, or could be guaranteed over long periods of time. At higher chloride concentrations, nickel-base alloys, stainless steels with high molybdenum content, and titanium alloys would have to be seriously considered.

In conclusion, it is recommended that the following specific alloys or groups of alloys be further evaluated as candidate container materials for fuel immobilization:

316 L stainless steel,

copper,

Inconel 625,

Hastelloy C-276,
dilute titanium alloys.

A final selection can only be made on the basis of further experimental assessment and when the chemistry conditions likely to exist in the vault are more closely defined.

16. CONCLUSIONS

In the summaries to Parts I and II of this report (Sections 10 and 15), certain alloy groups are recommended for further consideration for the fabrication of containers in which to immobilize nuclear fuel wastes for subsequent disposal in a deep hard-rock vault. Both parts of the report arrive at similar recommendations even though their respective bases for assessment are different. The main groups of materials recommended and the preferred choice of alloys within each group are shown below. Where more than one alloy in a group is considered, a recommended ranking is given.

Alloy Group	Specific Alloys
AISI 300 stainless steels	316
High nickel-base alloys	1. Inconel 625 2. Hastelloy C-276
Dilute titanium-base alloys	1. ASTM grade 2 2. ASTM grade 12 (Ticode-12) 3. ASTM grade 7 (Ti-0.2% Pd)

The final choice of alloy group will be primarily dictated by the vault environment, and especially the groundwater chemistry.

In general, because of their acknowledged susceptibility to crevice corrosion and SCC in chloride-containing environments, the AISI 300 stainless steels would only be suitable for very benign groundwater conditions. Quantitative limits are difficult to define, but it is suggested that these materials not be used if the chloride content of the groundwater exceeds ∿ 100 mg/L, or if salt concentration mechanisms are likely.

The high nickel-base and dilute titanium-base alloys are suitable for service in a moderately agressive vault environment, and should be resistant to crevice corrosion in the groundwater compositions considered in this report. Based on the data used in this assessment, Inconel 625, titanium grade 2 and Ticode-12 are the cheapest alloys in the two groups and are also comparable in cost. The final choice would depend on the prevailing materials costs and an assessment of the ease of fabrication and the costs associated with the preferred container design.

With increase in chloride content of the groundwater, the titanium-base alloys would be preferred since they have the greatest resistance to crevice corrosion. Primarily because of its higher strength, Ticode-12 would appear marginally cheaper than grade 2 (for a given design stress), and it is reported to have greater resistance to crevice corrosion. However, Ticode-12 is a recently developed alloy, so there is only limited commerical experience with its use and potential limitations compared with grade 2. Titanium grade 7 (Ti-0.2% Pd) has the greatest resistance to crevice corrosion but is at least twice as expensive as grade 2; indeed it is the most expensive of all the alloys considered in this assessment.

The above materials are recommended both for containers in which the container shell alone is designed to support the possible stresses during service (e.g., the potential hydrostatic pressure due to vault flooding), and container designs in which the shell is internally supported by periodic bracing, continuous solid matrixing, particulates or other means.

For the supported-shell container design, it is suggested that phosphorus deoxidised copper also be included for further evaluation as a potential container material. Although some reservations about the localised corrosion behaviour of copper alloys in certain environments were expressed in Part II, there is considerable historical evidence to indicate that copper would be acceptable in some environments for at least 500 years[203].

Finally, as with any major new application for engineering materials, it is recommended that a comprehensive test program be carried out to further evaluate the ease of fabrication and performance of the candidate alloys.

ACKNOWLEDGEMENTS

The authors acknowledge with gratitude the many discussions with their colleagues during preparation of this report. They also thank Mr. J.L. Crosthwaite for the use of unpublished data on container thicknesses.

REFERENCES

1. "The AECL Program on the Safe Immobilization and Disposal of Radioactive Materials from Canadian Nuclear Reactors", brief presented by Atomic Energy of Canada Limited to the Standing Committee on National Resources and Public Works (1978).

2. "Management of Radioactive Fuel Wastes: The Canadian Disposal Program", J. Boulton (Ed.), Atomic Energy of Canada Limited Report, AECL-6314 (1978).

3. "Handling of Spent Nuclear Fuel and Final Storage of Vitrified High Level Reprocessing Waste", Vols. I-IV, prepared by KBS, Stockholm, Sweden (1978).

4. Aluminum Standards and Data, Aluminum Association (1976).

5. Aluminum, Vol. 1, K.R. Van Horn (Ed.), American Society for Metals, Metals Park, Ohio (1967).

6. P.C. Varley, "The Technology of Aluminum and its Alloys", CRC Press, Cleveland, Ohio, 1970.

7. Fundamentals of Welding, Welding Handbook Section 1, A.L. Phillips (Ed.), American Welding Society, New York, 1963.

8. Metals and Their Weldability, Welding Handbook Section 4, A.L. Phillips (Ed.), American Welding Society, New York, 1966.

9. D.O. Sprowls and R.H. Brown, "Stress Corrosion Mechanisms for Aluminum Alloys", Proceedings of Conference on Fundamental Aspects of Stress Corrosion Cracking, R.W. Staehle, A.J. Forty and D. Van Rooyen (Eds.), NACE-1, 466 (1969).

10. E.H. Dix, Jr., W.A. Anderson and M.B. Shumaker, "Development of Wrought Aluminum-Magnesium Alloys", Alcoa Research Laboratories Technical Paper No. 14 (1958).

11. D.O. Sprowls and H.C. Rutemiller, "Susceptibility of Aluminum Alloys to Stress Corrosion", Materials Protection 2,62 (1963).

12. E.H. Cook, quoted in reference (9), unpublished research at Alcoa Research Laboratories (1959).

13. E.F. Emley, "Principles of Magnesium Technology", Pergamon Press, London, 1966.

14. G.V. Raynor, "The Physical Metallurgy of Magnesium and its Alloys", Pergamon Press, New York, 1959.

15. P.A. Fisher, "Production, Properties and Industrial Uses of Magnesium and its Alloys", International Metals Review 23(6), 269 (1978).

16. Metals Handbook Vol. 1, 9th Edition, American Society for Metals, Chicago, 1978.

17. M. Romanoff, "Underground Corrosion", National Bureau of Standards Circular 579, United States Government Printing Office, 1957.

18. G.M. Gordon, "Physical Metallurgy of Fe-Cr-Ni Alloys", Proceedings of Conference on Stress Corrosion Cracking and Hydrogen Embrittlement of Iron-Base Alloys, R.W. Staehle, J. Hochman, R.D. McCright and J.E. Slater (Eds.), NACE-5, 893 (1977).

19. F.B. Pickering, "Physical Metallurgy of Stainless Steel Developments", International Metals Review 21,227 (1976).

20. L. Colombier and J. Hochmann, "Stainless and Heat Resisting Steels", Edward Arnold Ltd., London, 1967.

21. R.F. Steigerwald, A.P. Bond, H.J. Dundas and E.A. Lizlovs, "The New Fe-Cr-Mo Ferritic Stainless Steels", Corrosion 33,279 (1977).

22. "Stainless Steel '77", Proceedings of Conference sponsored by Climax Molybdenum Company, London, September, 1977.

23. "Intergranular Corrosion of Stainless Alloys", R.F. Steigerwald (Ed.), ASTM STP 656, 1978.

24. E. Baerlecken, W.A. Fischer and K. Lorenz, "Investigations on the Transformation Behaviour, Impact Strength, and Susceptibility to Intergranular Corrosion of Iron-Chromium Alloys with Chromium Contents up to 30%", Stahl u. Eisen 81,768 (1961).

25. F.B. Pickering, "Some Aspects of the Heat Treatment of Welded Corrosion- and Heat-restisting Steels" in Heat-Treatment Aspects of Metal-joining Processes, The Iron and Steel Institute, London, 84, 1972.

26. M. Semchyshen, A.P. Bond and H.J. Dundas, "Effects of Composition on Ductility and Toughness of Ferritic Stainless Steels", Proceedings of symposium on Towards Improved Ductility and Toughness, Kyoto, Japan, 239, 1972.

27. R.O. Williams, "Further Studies of the Iron-Chromium System", Trans. Met. Soc. AIME 212,497 (1958).

28. R. Lagneborg, "Deformation in an Iron-30%Chromium Alloy Aged at 475°C", Acta Met 15,1737 (1967).

29. S.H. Bush and R.L. Dillon, "Stress Corrosion in Nuclear Systems", Proceedings of Conference on Stress Corrosion Cracking and Hydrogen Embrittlement of Iron-Base Alloys, R.W. Staehle et al. (Eds.), NACE-5, 61 (1977).

30. R.A. Lula, "Ferritic Stainless Steels: Corrosion Resistance and Economy", Metal Progress 110(2),24 (1976).

31. D.C. Ludwigson and H.S. Link, "Further Studies on the Formation of Sigma in 12 to 16% Chromium Steels", in Advances in the Technology of Stainless Steels and Related Alloys, ASTM STP 369, p. 299 (1963).

32. A.J. Lena and M.F. Hawkes, "475°C Embrittlement in Stainless Steels", J. Metals 6, AIME Trans. 200, 607 (1954).

33. A.P. Bond and H.J. Dundas, "Stress Corrosion Cracking of Ferritic Stainless Steels", Proceedings of Conference on Stress Corrosion Cracking and Hydrogen Embrittlement of Iron-Base Alloys, R.W. Staehle, J. Hochman, R.D. McCright and J.E. Slater (Eds.), NACE-5, 1136 (1977).

34. R.F. Steigerwald, "New Molybdenum Stainless Steels for Corrosion Resistance: A Review of Recent Developments", Materials Performance 13(9),9 (1974).

35. I.A. Franson, Allegheny Ludlum Steel Corporation, personal communication.

36. R.F. Steigerwald, Climax Molybdenum Company, personal communication.

37. R.L. Cowan and C.S. Tedmon, "Intergranular Corrosion of Iron-Nickel-Chromium Alloys", Advances in Corrosion Science and Technology 3,293 (1973).

38. F.G. Wilson, "Mechanism of Intergranular Corrosion of Austenitic Stainless Steels: Literature Review", British Corrosion Jnl. 6,100 (1971).

39. W.J. Mecham, W.B. Seefeldt and M.J. Steindler, "An Analysis of Factors Influencing the Reliability of Retrievable Storage Containers for Containment of Solid High-Level Radioactive Waste", Argonne National Laboratory, ANL-76-82 (1976).

40. "Retrievable Surface Storage Facility Conceptual System Design Description", Atlantic Richfield Hanford Company and Kaiser Engineers, ARH-LD-140 Rev., pp. 3-12 (1977).

41. R.M. Latanision and R.W. Staehle, "Stress Corrosion Cracking of Iron-Nickel-Chromium Alloys", Proceedings of Conference on Fundamental Aspects of Stress Corrosion Cracking, R.W. Staehle, A.J. Forty and D. Van Rooyen (Eds.), NACE-1, 214 (1969).

42. G.J. Theus and R.W. Staehle, "Review of Stress Corrosion Cracking and Hydrogen Embrittlement in Fe-Cr-Ni Alloys", Proceedings of Conference on Stress Corrosion Cracking and Hydrogen Embrittlement in Iron-Base Alloys, R.W. Staehle, J. Hochman, R.D. McCright and J.E. Slater (Eds.), NACE-5, 845 (1977).

43. R.W. Staehle, "Stress Corrosion Cracking of the Iron-Chromium-Nickel Alloys System", Proceedings of Conference on the Theory of Stress Corrosion Cracking in Alloys, J.C. Scully (Ed.), NATO, Brussels,223 (1971).

44. J.E. Truman, "The Influence of Chloride Content, pH and Temperature of Test Solution on the Occurrence of Stress Corrosion Cracking with Austenitic Stainless Steel", Corrosion Science 17,737 (1977).

45. J.E. Truman, "Problems of Stress Corrosion Cracking of Steel in Customer Usage", Proceedings of Conference on Stress Corrosion Cracking and Hydrogen Embrittlement in Iron-Base Alloys, R.W. Staehle, J. Hochman, R.D. McCright and J.E. Slater (Eds.), NACE-5, 111 (1977).

46. J.W. Braithwaite and M.A. Molecke, "High-Level Waste Canister Corrosion Studies Pertinent to Geologic Isolation", Nuclear and Chemical Waste Management 1,37 (1980).

47. Properties and Applications of Special Stainless Steels, Datasheet Metal Progress 110(5),72 (1976).

48. Quick Reference Guide to High Nickel Alloys, Huntington Alloys publication, Huntington, West Virginia.

49. Huntington Alloys publication on Inconel 600, 601, 625 and Incoloy 800, 801, 825 Alloys, Huntington, West Virginia.

50. Cabot Corporation publications on Hastelloy Alloys, F30526D, F30356E, F30267D, 1978.

51. Sandvik Steel Catalogue 4.00E, 1972.

52. Allegheny Ludlum Industries datasheet on Al-6X.

53. J.W. Pugh and J.D. Nisbet, "A Study of the Iron-Nickel-Chromium Ternary System", J. Metals 188(2) Trans. 268 (1950).

54. J.L. Everhart, "Engineering Properties of Nickel and Nickel Alloys", Plenum Press, New York - London, 1971.

55. "Joining Huntington Alloys", Huntington Alloy Products Division, Huntington, West Virginia.

56. H.R. Copson, "Effect of Composition on Stress Corrosion Cracking of Some Alloys Containing Nickel", Physical Metallurgy of Stress Corrosion Fracture (Met. Soc. Conf), Interscience, New York, 227 (1959).

57. R.L. Cowan and G.M. Gordon, "Intergranular Stress Corrosion Cracking and Grain Boundary Composition of Fe-Ni-Cr Alloys", Proceedings of Conference on Stress Corrosion Cracking and Hydrogen Embrittlement of Iron-Base Alloys, R.W. Staehle, J. Hochman, R.D. McCright and J.E. Slater (Eds.), NACE-5, 1023 (1977).

58. H. Coriou, R. Grall, M. LeGall and S. Vettier, "Stress Corrosion Cracking of Inconel in High-Temperature Water", Colloque de Metallurgie Corrosion, Centre d'Etudes Nucleaires de Saclay, North Holland, Amsterdam, 161 (1960).

59. H.R. Copson and G. Economy, "Effect of some Envirormental Conditions on Stress Corrosion Behaviour of Ni-Cr-Fe Alloys in Pressurized Water", Corrosion 24(3), 55 (1968).

60. M.H. Brown, "The Relationship of Heat Treatment to the Corrosion Resistance of Stainless Alloys", Corrosion 25(10), 438 (1969).

61. H. Coriou, L. Grall, C. Mahieu and M. Pelas, "Sensitivity to Stress Corrosion and Intergranular Attack of High-Nickel Austenitic Alloys", Corrosion 22(10), 280 (1966).

62. E.L. Raymond, "Mechanisms of Sensitization and Stabilization of Incoloy Ni-Fe-Cr Alloy 825", Corrosion 24(6), 180 (1968).

63. R.B. Leonard, "Thermal Stability of Hastelloy Alloy C-276", Corrosion 25(5), 222 (1969).

64. M.A. Streicher, "Effect of Composition and Structure on Crevice, Intergranular, and Stress Corrosion of Some Wrought Ni-Cr-Mo Alloys", Corrosion 32(3), 79 (1976).

65. F.G. Hodge, "Improved Stability Nickel-Base Alloys Meet New CPI Requirements", Metal Progress 113(2),22 (1978).

66. J.S. Armijo, "Intergranular Stress Corrosion Cracking of Austenitic Stainless Steels in Oxygenated High Temperature Water", Corrosion 24(10),319 (1968).

67. A.D. McQuillan and M.K. McQuillan, "Titanium", Metallurgy of the Rarer Metals, No. 4, Academic Press, New York, 1956.

68. R.I. Jaffee and H.M. Burte, "Titanium Science and Technology", Proceedings of 2nd International Conf. on Titanium, Plenum Press, New York - London, 1973.

69. R.I. Jaffee and N.E. Promisel, "The Science, Technology and Application of Titanium", Proceedings of an International Conference, Pergamon Press, Oxford, 1970.

70. Corrosion Resistance of Lead-lined Titanium Canister for Final Disposal of Reprocessed and Vitrified Nuclear Fuel Waste, KBS Technical Report 107, Sweden, 1978.

71. ASTM Standard Specification for Titanium and Titanium Alloy Strip, Sheet and Plate, B-265, 1978.

72. Publication on Ticode-12, Timet, Titanium Metals Corporation of America.

73. Designers Guide to Timet Code Roll Standard Size Titanium Sheet and Plate, Titanium Metals Corporation of America, publication EP-2-77-2M.

74. W.W. Minkler, "Titanium for Chemical Processing Equipment", Metal Progress 113(2), 27 (1978).

75. D. Durham, Timet, personal communication to K. Nuttall, 1979.

76. N.G. Feige and R.L. Kane, "Experience with Titanium Structures in Marine Service", Materials Protection and Performance 9(8), 13 (1970).

77. J.A. McMaster, "The Use of Titanium in Pressure Vessels and Piping Construction", Symposium on Titanium and Zirconium for the Chemical Process Industries, New Orleans, Nov., 1975.

78. "Titanium Welding Techniques", Titanium Engineering Bulletin No. 6, publication of Titanium Metals Corporation of America.

79. R.E. Goosey, "Heat Treatment Aspects of Joining Titanium-Based Materials", in Heat Treatment Aspects of Metal-Joining Processes, The Iron and Steel Institute, London, 61, 1972.

80. L.C. Covington, "Titanium Solves Corrosion Problems in Petroleum Processing", Metal Progress 111(2), 38 (1977).

81. S. Henriksson and K. Pettersson, "Suitability of Titanium for a Corrosion Resistant Canister Containing Nuclear Waste", KBS Report No. 11, Sweden, 1977.

82. N.G. Feige and L.C. Covington, "Overview of Corrosion Cracking of Titanium Alloys", in Stress Corrosion Cracking of Metals - A State of the Art", ASTM STP 518, 119, 1971.

83. M.J. Blackburn, J.A. Feeney and T.R. Beck, "Stress Corrosion Cracking of Titanium Alloys", Advances in Corrosion Science and Technology 3,67 (1973).

84. J.C. Scully and D.T. Powell, "The Stress Corrosion Cracking Mechanism of α-Titanium Alloys at Room Temperature", Corrosion Science 10 719 (1970).

85. J.C. Scully and T.A. Adepoju, "Stress Corrosion Crack Propagation in a Ti-O Alloy in Aqueous and Methanolic Solutions", Corrosion Science 17,789 (1977).

86. R.E. Curtis, R.R. Boyer and J.C. Williams, "Relationship Between Composition, Microstructure, and Stress Corrosion Cracking (in Salt Solution) in Titanium Alloys", Trans. ASM 62,457 (1969).

87. I.R. Lane, J.L. Cavallaro and A.G.S. Morton, "Sea Water Embrittlement of Titanium", in Stress-Corrosion Cracking of Titanium, ASTM STP 397, 246 (1966).

88. P. Cotterill, "The Hydrogen Embrittlement of Metals", Progress in Materials Science 9,205 (1961).

89. N.E. Paton and J.C. Williams, "Effect of Hydrogen on Titanium and its Alloys", Hydrogen in Metals, Proceedings of an International Conference, American Society for Metals, 409 (1974).

90. N.E. Paton, B.S. Hickman and D.H. Leslie, "Behaviour of Hydrogen in α-Phase Ti-Al Alloys", Metallurgical Transactions 2,2791 (1971).

91. D.N. Williams, "The Hydrogen Embrittlement of Titanium Alloys", Journal of the Institute of Metals 91,147 (1962).

92. G.A. Lenning, C.M. Craighead and R.I. Jaffee, "Constitution and Mechanical Properties of Titanium-Hydrogen Alloys", Trans. Amer. Inst. Min. Met. Eng. 200,367 (1954).

93. C.J. Beevers and D.V. Edmonds, "The Deformation and Fracture of Titanium-Oxygen-Hydrogen Alloys", Trans. of the Metallurgical Society of AIME 245,2391 (1969).

94. N.E. Paton, unpublished research quoted in reference (89).

95. D.N. Williams, "Subcritical Crack Growth Under Sustained Load", Metallurgical Transactions 5,2351 (1974).

96. D.N. Williams, "Effects of Hydrogen in Titanium Alloys on Subcritical Crack Growth under Sustained Load", Materials Science and Engineering 24,53 (1976).

97. D.A. Meyn, "Effect of Hydrogen on Fracture and Inert-Environment Sustained Load Cracking Resistance of α-β Titanium Alloys", Metallurgical Transactions 5,2405 (1974).

98. N.E. Paton and R.A. Spurling, "Hydride Habit Planes in Titanium-Aluminum-Alloys", Metallurgical Transactions 7A,1769 (1976).

99. R.R. Boyer and W.F. Spurr, "Characteristics of Sustained-Load Cracking and Hydrogen Effects in Ti-6Al-4V", Metallurgical Transactions 9A,23 (1978).

100. E.C.W. Perryman, "Pickering Pressure Tube Cracking Experience", Nuclear Energy 17(2), 95 (1978).

101. R. Dutton, K. Nuttall, M.P. Puls and L.A. Simpson, "Mechanisms of Hydrogen Induced Delayed Cracking in Hydride Forming Materials", Metallurgical Transactions 8A,1553 (1977).

102. C.E. Coleman and J.F.R. Ambler, "Susceptibility of Zirconium Alloys to Delayed Hydrogen Cracking", in Zirconium in the Nuclear Industry, ASTM STP 633, p. 589 (1977).

103. K. Nuttall and A.J. Rogowski, "Some Fractographic Aspects of Hydrogen-Induced Delayed Cracking in Zr-2.5 wt.% Nb Alloys", J. Nuc. Mat. 80,279 (1979).

104. J.L. Waisman, G. Sines and L.B. Robinson, "Diffusion of Hydrogen in Titanium Alloys Due to Composition, Temperature and Stress Gradients", Metallurgical Transactions 4,291 (1973).

105. R.P. Marshall, "The Thermal Diffusion of Hydrogen in Titanium", Trans. of the Metallurgical Society of AIME 233,1449 (1965).

106. M.R. Louthan, Jr., "Stress Orientation of Titanium Hydride in Titanium", Trans. of the Metallurgical Society of AIME 227, 1166 (1963).

107. H.G. Nelson, "Aqueous Chloride Stress Corrosion Cracking of Titanium - A Comparison with Environmental Hydrogen Embrittlement", Hydrogen in Metals, Proceedings of an International Conference, American Society for Metals, 445 (1974).

108. H.G. Nelson, "A Film Rupture Model of Hydrogen Induced Slow Crack Growth in Acicular Alpha-Beta Titanium", Met. Trans. 7(A), 621 (1976).

109. T.B. Cox and J.P. Gudas, "Investigation of the Fracture of Near-Alpha Titanium Alloys in High Pressure Hydrogen Environments", in Effects of Hydrogen on Behaviour of Materials, A.W. Thompson and I.M. Bernstein (Eds.), AIME, 287 (1976).

110. Standards Handbook, Wrought Mill Products, Alloy Data/2, Copper Development Association Inc., New York, 1973.

111. Properties and Applications of Widely Used Wrought Coppers and Copper Alloys, Metal Progress Databook 110(1), 100 (1976).

112. Copper and Copper Alloys, Metals Handbook Vol. 1, 8th Edition, American Society for Metals, Chicago, 1961.

113. R.J. Dawson, "Gas Shielded Arc Welding of Copper and Copper Alloys", Technical Note TN2, Copper Development Association, London, 1970.

114. "Corrosion Resistance of Copper Canisters for Final Disposal of Spent Nuclear Fuel", KBS Technical Report 90, 1978.

115. P.J. Macken and A.A. Smith, "The Aluminum Bronzes", Publication No. 31, Copper Development Association, London, 1966.

116. A.A. Smith, "An Assessment of the Aluminum Bronzes for Corrosive Environments", Corrosion Prevention and Control 10(6), 29 (1963).

117. D.H. Thompson, "Stress Corrosion Cracking of Copper Metals", in Stress Corrosion Cracking of Metals - A State of the Art, ASTM STP 518, 39, 1971.

118. E.N. Pugh, J.V. Craig and A.J. Sedricks, "The Stress Corrosion Cracking of Copper, Silver and Gold Alloys", Proceedings of Conference on Fundamental Aspects of Stress Corrosion Cracking, R.W. Stachle, A.J. Forty and D. Van Rooyen (Eds.), NACE-1, 118 (1969).

119. T.H. White and R.V.V. Davis, "Weld Overlaying for Marine Corrosion Resistance", Welding and Metal Fabrication 46(5), 353 (1978).

120. "What's the State-of-the-Art in Stainless Overlay", Iron Age, p. 91, July 31 (1978).

121. M.G. Fontana and N.D. Greene, "Corrosion Engineering", Second Edition, McGraw-Hill, 1978.

122. L.L. Shreir, "Corrosion", Vol. 1, Second Edition, Newnes-Butterworths, 1976.

123. H.H. Uhlig, "The Corrosion Handbook", Eighth Edition, John Wiley and Sons., Inc., 1963.

124. J. O'M. Bockris and A.K.N. Reddy, "Modern Electrochemistry", Plenum Press, 1970.

125. L.L. Shreir, "Corrosion", Vol. 2, Second Edition, Newnes-Butterworths, 1976.

126. H.H. Uhlig, "Corrosion and Corrosion Control", Second Edition, John Wiley and Sons., Inc., 1971.

127. M. Pourbaix, "Atlas of Potential/pH Diagrams", Pergamon, Oxford, 1962.

128. M. Pourbaix, "Lectures on Electrochemical Corrosion", Plenum Press, New York, 1973.

129. E.D. Verink and M. Pourbaix, "Use of Electrochemical Hysteresis Techniques in Developing Alloys for Saline Exposures", Corrosion 27(12), 495 (1971).

130. R.J. Brigham, "Pitting and Crevice Corrosion Resistance of Commercial 18% Cr Stainless Steels", Materials Performance 13(11) 29, (1974).

131. J.M. Kolotyrkin, "Pitting Corrosion of Metals", Corrosion 19(8), 261 (1963).

132. W. Schwenk, "Theory of Stainless Steel Pitting", Corrosion 20(4), 129 (1964).

133. Z. Szklarska-Smialowska, "Review of Literature on Pitting Corrosion Published Since 1960", Corrosion 27(6), 223 (1971).

134. O. Steensland, "Contribution to the Discussion on Pitting Corrosion of Stainless Steels", Uddeholms Aktiebolag Research Laboratory, Sweden, Report No. 75, 1967.

135. J. Postlethwaite, R.A. Brierley, M.J. Walmsley and S.C. Goh, "Pitting at Elevated Temperatures", Proceedings of Conference on Localized Corrosion, NACE-3, p. 415 (1974).

136. W.F. Bogaerts et al., "Pitting Behaviour of Austenitic Stainless Steel at Elevated Temperature", Proceedings of the Seventh International Congress on Metallic Corrosion, ABRACO, Rio de Janeiro, p. 526 (1978).

137. Tetsuo Fujii, "Electrochemical Study on the Corrosion Behaviour of Metals and Alloys in Aqueous Solutions at High Temperature and Pressure", Transactions of National Research Institute for Metals 18(3), 101 (1976).

138. P.E. Manning and D.J. Duquette, "The Effect of Temperature (25-289°C) on Pit Initiation in Single Phase and Duplex 304L Stainless Steels in 100 ppm Cl^- Solution", Corrosion Science 20(4), 597 (1980).

139. H.Y. Tammemägi, Atomic Energy of Canada Limited, unpublished data, 1977.

140. J. Cherry, Atomic Energy of Canada Limited, unpublished data, 1977.

141. D.J. Bottomley, National Hydrology Research Institute, unpublished data, 1978.

142. D.J. Cameron and G.G. Strathdee, "Materials Aspects of Nuclear Waste Disposal in Canada", in Proceedings of Ceramics in Nuclear Waste Management, International Symposium of the American Ceramic Society at Cincinnati, Ohio, p. 4 (1979).

143. J.D. Palmer, "Soil Resistivity - Measurements and Analysis", Materials Performance 13(1) 41 (1974).

144. H.P. Godard, W.B. Jepson, M.R. Bothewell and R.L. Kane, "The Corrosion of Light Metals", John Wiley and Sons, Inc., pp. 3 - 208, 1967.

145. W.E. Berry, "Corrosion in Nuclear Applications", John Wiley and Sons, Inc., p. 141, 1971.

146. V.H. Troutner, "Uniform Aqueous Corrosion of Aluminum - Effects of Various Ions", USAEC Report HW-50133 (1957).

147. J. Vaccari, "Wrought Aluminum and its Alloys", Materials and Design Engineering 61(6), 117 (1965).

148. L.L. Shreir, Corrosion, Volume 1, Second Edition, Newnes-Butterworths, pp. 4 - 22, 1976.

149. R.J. Biernat and R.G. Robins, "High-Temperature Potential/pH Diagrams for the Iron-Water-Sulphur Systems", Electrochimica Acta 17,1261 (1972).

150. H.H. Uhlig, "Corrosion and Corrosion Control", John Wiley and Sons, Inc., Second Edition, p. 97, 1971.

151. H.H. Uhlig, "The Corrosion Handbook", Eighth Edition, John Wiley and Sons, Inc., p. 129, 1963.

152. M.G. Fontana and N.D. Greene, "Corrosion Engineering", McGraw-Hill, pp. 269 - 270, 1967.

153. H.H. Uhlig, "Corrosion and Corrosion Control", Second Edition, John Wiley and Sons, Inc., p. 263, 1971.

154. L.L. Shreir, Corrosion, Volume 1, Second Edition, Newnes-Butterworths, pp. 3 - 50, 1976.

155. C.W. Kovach et al., "Crevice Corrosion Performance of a Ferritic Stainless Steel Designed for Saline Water Condenser and Heat Exchanger Applications", Paper No. 95, presented at NACE - Corrosion/80, Chicago (1980).

156. B.E. Wilde and E. Williams, "The Use of Current/Voltage Curves for the Study of Localized Corrosion and Passivity Breakdown on Stainless Steels in Chloride Media", Electrochimica Acta 16, 1971 (1971).

157. P.E. Morris, "Use of Rapid Scan Potentiodynamic Techniques to Evaluate Pitting and Crevice Corrosion Resistance of Chromium-Nickel Alloys", in Galvanic and Pitting Corrosion - Field and Laboratory Studies, ASTM STP 576, pp. 261-275 (1976).

158. K.D. Efird and G.E. Moller, "Electrochemical Characteristics of 304 and 316 Stainless Steels in Fresh Water as Functions of Chloride Concentration and Temperature", Paper No. 87, presented at NACE, Corrosion/78, Houston (1978).

159. A.I. Asphahani, "Localized Corrosion of High Performance Alloys", Paper No. 248, presented at NACE, Corrosion/79, Atlanta, Ga. (1979).

160. American Society for Testing and Materials Recommended Procedure ASTM-G61-79, "Practice for Conducting Cyclic Potentiodynamic Polarization Measurements for Localized Corrosion", Annual Book of ASTM Standards, 1979.

161. E.C. Hoxie and G.W. Tuffnell, "A Summary of INCO Corrosion Tests in Power Plant Flue Gas Scrubbing Processes", in Resolving Corrosion Problems in Air Pollution Control Equipment, NACE, pp. 65 - 71 (1976).

162. N. Pessall and J.I. Nurminen, "Development of Ferritic Stainless Steels for Use in Desalination Plants", Corrosion 30(11), 381 (1974).

163. M.A. Streicher, "Development of Pitting Resistant Fe-Cr-Mo Alloys", Corrosion 30(3), 77 (1974).

164. A. Garner, "Molybdenum in Stainless Steels", The Metallurgical Society of CIM, Annual Volume, 1977.

165. J.R. Maurer, "Controlling Corrosion Problems with the New High Technology Stainless Steels", Paper presented at the 38th Annual Meeting, International Water Conference, Pittsburg, Penn., 1977, p. 55 (Publ. 1978).

166. R.F. Steigerwald, "New Molybdenum Stainless Steels and Alloys for Corrosion Resistance", Paper presented at NACE, Corrosion/74, Chicago, Ill., 1974, Paper No. 44.

167. G.B. Coulter and G. Aggen, "New High Chromium Ferritic Stainless Steels", Paper presented at NACE, Corrosion/74, Chicago, Ill., 1974, Paper No. 42.

168. J.R. Maurer, "Stainless Steel Condenser Tubes: Economy, Reliability, Performance", Paper presented at the INCO Power Conference, Lausanne, Switzerland, 1977.

169. H.E. Deverell and J.R. Maurer, "Stainless Steels in Sea Water", Materials Performance 17(3), 15 (1978).

170. A.I. Asphahani, "Effect of Acids on the Stress Corrosion Cracking of Stainless Materials in Dilute Chloride Solutions", Paper No. 142, presented at NACE, Corrosion/79, Atlanta, Ga. (1979).

171. M.O. Spiedel, Chapter on "Stress Corrosion Cracking of Nickel Alloys", ARPA Handbook on Stress Corrosion Cracking, to be published.

172. R.B. Niederberger, R.J. Ferrara and F.A. Plummer, "Corrosion of Nickel Alloys in Quiet and Low Velocity Sea Water", Materials Protection and Performance 9(8), 18 (1970).

173. T.P. Oettinger and M.G. Fontana, "Austenitic Stainless Steels and Titanium for Wet Oxidation of Sewage Sludge", Materials Performance 15(11), 29 (1976).

174. M. Henthorne, "Intergranular Corrosion in Iron and Nickel Base Alloys", in Localized Corrosion - Cause of Metal Failure, ASTM STP 516, p. 66, 1972.

175. E. Mattsson, The Corrosion Institute and Reference Group, "Corrosion Resistance of Canister Materials for Nuclear Waste: Interim Report 1977-09-27 and Comments", KBS Technical Report No. 31, 1977.

176. T.R. Beck, "A Review: Pitting Attack of Titanium Alloys", Proceedings of U.R. Evans Conference on Localized Corrosion, NACE-3, p. 625 (1974).

177. J.C. Griess, "Crevice Corrosion of Titanium in Aqueous Salt Solutions", Corrosion 24(4), 96 (1968).

178. G.R. Wallwork and J.M. Newburn, "Crevice Corrosion in Titanium", Proceedings of Conference on High Temperature High Pressure Electrochem. Aqueous Solutions, NACE-4, p. 474 (1976).

179. K. Shimogori, H. Sato and H. Tomari, "Crevice Corrosion of Titanium in NaCl Solutions in the Temperature Range 100 to 250°C", Journal of the Japan Institute of Metals 42,567 (1978).

180. P.B. Needham, Jr., S.D. Cramer, J.P. Carter and F.X. McCawley, "Corrosion Studies in High Temperature, Hypersaline Geothermal Brines", Paper No. 59, presented at NACE, Corrosion/79, Atlanta, Ga. (1979).

181. E.G. Bohlmann and F.A. Posey, "Aluminum and Titanium Corrosion in Saline Waters at Elevated Temperatures", Proceedings of the First International Symposium on Water Desalination, Vol. 1, 306 (1965).

182. J.D. Jackson and W.K. Boyd, "Crevice Corrosion of Titanium", in Applications Related Phenomena in Titanium Alloys, ASTM STP 432, 218, 1968.

183. D. Schlain and C.B. Kenahan, "The Role of Crevices in Decreasing the Passivity of Titanium in Certain Solutions", Corrosion 12(8),68 (1956).

184. L.C. Covington, "Pitting Corrosion of Titanium Tubes in Hot Concentrated Brine Solutions", in Galvanic and Pitting Corrosion - Field and Laboratory Studies, ASTM STP 576, p. 147 (1976).

185. Imperial Metal Industries (Kynoch) Ltd., "Titanium Heat Exchangers for Service in Sea Water, Brine and Other Natural Aqueous Environments", Titanium Information Bulletin IMI 5020/220, 1970.

186. T.R. Beck, "Electrochemical Models for SCC of Titanium", in The Theory of Stress Corrosion Cracking in Alloys, Dr. J.C. Scully (Ed.), Published by NATO Scientific Affairs Division, p. 64 (1971).

187. G. Sanderson, D.T. Powell and J.C. Scully, "Metallographic Studies of the Stress Corrosion Cracking of Titanium Alloys in Aqueous Chloride Solutions", Proceedings of Conference on Fundamental Aspects of Stress Corrosion Cracking, R.W. Staehle et al. (Eds.), NACE-1, p. 638 (1969).

188. J.A. Feeney and M.J. Blackburn, "The Status of Stress Corrosion Cracking of Titanium Alloys in Aqueous Solutions", in The Theory of Stress Corrosion Cracking in Alloys, Dr. J.C. Scully (Ed.), Published by NATO Scientific Affairs Division, p. 355 (1971).

189. F.L. La Que and H.R. Copson, "Corrosion Resistance of Metals and Alloys", Second Edition, Reinhold Publishing Company, 1963.

190. H.S. Campbell, "A Review: Pitting Corrosion of Copper and its Alloys", Proceedings of U.R. Evans Conference on Localized Corrosion, NACE-3, p. 625 (1974).

191. W.D. France, "Crevice Corrosion of Metals", General Motors Research Publication GMR-1105 (1971).

192. K.D. Efird and E.D. Verink, "The Crevice Protection Potential for 90-10 Copper Nickel", Corrosion 33(9), 328 (1977).

193. W.K. Boyd and F.W. Fink, "Corrosion of Metals in Marine Environments", Metals and Ceramics Information Center, Battelle Columbus Laboratories, MCIC-75-245R (1975).

194. C.F. Schrieber and F.H. Coley, "Behaviour of Metals in Desalting Environments: Seventh Progress Report (Summary)", Paper presented at NACE, Corrosion/75, Toronto, Canada, 1975, Paper No. 36.

195. L.L. Shreir, Corrosion, Volume 1, Second Edition, Newnes-Butterworths, p. 1:165, 1976.

196. J.M. Schluter, "Copper Alloy Tube Failures in Sea Water Condensers (Case History)", Materials Performance 17(2), 25 (1978).

197. H.P. Hack and J.P. Gudas, "Inhibition of Sulfide-Induced Corrosion of Copper-Nickel Alloys with Ferrous Sulfate", Materials Performance 18(3), 25 (1979).

198. J.P. Gudas and H.P. Hack, "Sulfide Induced Corrosion of Copper Nickel Alloys", Corrosion 35(2), 67 (1979).

199. B.C. Syrett, "Accelerated Corrosion of Copper in Flowing Pure Water Contaminated with Oxygen and Sulfide", Corrosion 33(7), 257 (1977).

200. D.C. Vreeland, "Review of Corrosion Experience with Copper-Nickel Alloys in Sea Water Piping Systems", Materials Performance 15(10), 38 (1976).

201. T.J. Lennox, M.H. Peterson and R.E. Groover, "De-Alloying of Copper Alloys and Response to Cathodic Protection in Quiescent Sea Water", Materials Protection and Performance 10(7), 31 (1971).

202. "Corrosion Resistance of Copper Canisters for Final Disposal of Spent Nuclear Fuel", Swedish Corrosion Institute, KBS Technical Report No. 90 (1978).

203. R.F. Tylecote, "Durable Materials for Sea Water: The Archeological Evidence", BNFL Report 314(R) (1977).

204. A. Garner, "Crevice Corrosion of Stainless Steels in Seawater: Correlation of Field and Laboratory Tests", Paper No. 35, presented at NACE, Corrosion/80, Chicago (1980).

205. F.L. LaQue, "Qualification of Stainless Steel for OTEC Heat Exchanger Tubes", Argonne National Laboratories Report, ANL/OTEC-001 (1979).

206. R.L. Tapping, Chalk River Nuclear Laboratories, unpublished work (1981).

TABLE I

SERIES DESIGNATION AND CORRESPONDING ALLOYING ADDITIONS IN COMMERCIALLY AVAILABLE ALUMINUM ALLOYS[4]

Series	Major alloy additions (wt.%)	Treatment
1000	< 1% total	non H.T.
2000	Cu (4-6%)	H.T.
3000	Mn (1.2%)	non H.T.
4000	Si (5-12%)	non H.T.
5000	Mg (0.8-5%)	non H.T.
6000	Mg (0.6-1.1%), Si (0.5-1.4%)	H.T.
7000	Zn (1-7.5%), Mg (2.5-3.3%)	H.T.

TABLE 2

RANGE* OF MECHANICAL PROPERTIES OBTAINABLE IN SOME COMMON ALUMINUM ALLOYS[4]

Alloy Designation	Yield stress min (MPa)	Ultimate tensile strength min (MPa)	Elongation (%)
1060	17-83	55-110	25-4
2024	262-393	400-455	~ 5
3003	34-165	97-186	25-4
5154	76-241	207-310	18-4
5454	66-220	172-270	18-4
6061	110-241	207-290	16-8
7075	360-440	440-530	~ 6

* For the non-heat-treatable alloys only, the range includes the annealed condition

TABLE 3

TYPICAL COMPOSITIONS AND MECHANICAL PROPERTIES OF FERRITIC STAINLESS STEELS[19,30]

Typical Compositions

Designation	Analysis, wt.%							
	C	Si	Mn	Cr	Al	Mo	Nb	Ti
AISI 405	0.06	0.25	0.40	13.5	0.20	-	-	-
AISI 409	0.06	0.25	0.40	11.0				0.40
AISI 429	0.06	0.40	0.40	15.0				
AISI 430	0.06	0.40	0.40	17.0				
AISI 430 Ti	0.07	0.25	0.40	17.0				0.50
AISI 430 Nb	0.05	0.25	0.40	17.0			0.50	
AISI 434	0.05	0.25	0.40	17.0		0.90		
AISI 436	0.05	0.25	0.40	17.0		0.80	0.50	
AISI 442	0.08	0.25	0.40	21.0				
AISI 446	0.08	0.25	0.40	25.0				
18/2	0.02	0.40	0.40	18.0		2.0		
E-Brite 26-1*	0.02	-	-	26.0		1.0		

Mechanical Properties

Designation	Yield stress (MPa)	Tensile strength (MPa)	Elongation (%)
AISI 405	280-380	400-510	20-30
AISI 409	250-280	450-480	25-30
AISI 430	280-450	450-580	20-35
AISI 430 Nb	340	550	30
AISI 434	340-450	490-570	25-27
AISI 436	340-370	520-560	27-30
AISI 422	310-420	520-580	20-30
AISI 446	340	550	23
439, 18-2	280-410	450-590	25-35
26-1S, E-Brite 26-1*	340-380	520-550	25-35
29 Cr-4 Mo, 29 Cr-4 Mo-2 Ni	480-550	520-590	25-35

* Allegheny-Ludlum Industries Inc.

TABLE 4

COMPOSITIONS AND PROPERTIES OF STANDARD AUSTENITIC STAINLESS STEELS[19]

Composition (wt.%)	AISI Type								
	301*	302*	304*	310*	316*	321*	347*	201+	202+
C	0.15 max.	0.15	0.08	0.25	0.08	0.08	0.08	0.15 max.	0.15 max.
Mn								5.7-7.5	7.5-10.0
Cr	16-18	17-19	18-20	24-26	16-18	17-19	17-19	16-18	17-19
Ni	6-8	8-10	8-12	19-22	10-14	9-12	9-13	3.5-5.5	4.0-6.0
Mo					2-3				
Ti						5xC			
Nb							10xC		
N_2	0.03	0.03	0.03	0.03	0.3	0.03	0.3	0.25 max.	0.25 max.
Typical properties (solution-treated material)									
Tensile strength, MPa	571	541	541	571	571	541	556	806	741
0.2% proof stress, MPa	247	247	247	247	247	247	247	386	371
Elongation, %	50	50	50	50	50	50	50	48	50

* Standard 300 series of Cr-Ni steels

\+ Low Ni, 200 series, Mn + N replacing some nickel

TABLE 5

COMPOSITIONS (wt.%) OF SOME STANDARD GRADES OF MARTENSITIC STAINLESS STEEL[18]

Designation or Type Number	C	Mn (max)	Si (max)	P (max)	S (max)	Cr	Ni	Other Elements
403	0.15 max	1.00	0.50	0.040	0.030	11.50-13.00		
410	0.15 max	1.00	1.00	0.040	0.030	11.50-13.50		
414	0.15 max	1.00	1.00	0.040	0.030	11.50-13.50	1.25-2.50	
416	0.15 max	1.25	1.00	0.06	0.25 min	12.00-14.00		Mo: 0.60 max
416 Se	0.15 max	1.25	1.00	0.06	0.06	12.00-14.00		Se: 0.15 min
420	Over 0.15	1.00	1.00	0.040	0.030	12.00-14.00		
431	0.20 max	1.00	1.00	0.040	0.030	15.00-17.00	1.25-2.50	
440 A	0.60-0.75	1.00	1.00	0.40	0.030	16.00-18.00		Mo: 0.75 max
440 B	0.75-0.95	1.00	1.00	0.040	0.030	16.00-18.00		Mo: 0.75 max
440 C	0.95-1.20	1.00	1.00	0.040	0.030	16.00-18.00		Mo: 0.75 max

TABLE 6

COMPOSITION AND TYPICAL PROPERTIES OF PRECIPITATION-HARDENABLE STAINLESS STEELS[18,19,46]

Alloy	Major Elements (wt.%)*								(c) 0.2% Y.S. (MPa)	(c) U.T.S. (MPa)	(c) Elongation (%)
MARTENSITIC ALLOYS											
	C	Cr	Ni	Mo	Al	Cu	Ti				
PH 13-8 Mo	0.03	12.75	8.2	2.2	1.1				1470	1575	12
17-4 PH	0.04	16	4.3			3.3			1295	1400	14
15-5 PH	0.04	15	4.6			3.3			1225	1330	14
Custom 450	0.05	15	6	0.8					1285	1365	14
Custom 455	11.75	8.5				2.25	1.2		1540	1610	12
SEMI AUSTENITIC ALLOYS											
	C	Cr	Ni	Mo	Al						
17-7 PH	0.07	17	7		1.2				1330	1435	9
15-7 PH	0.07	15.1	7.1	2.2	1.2				1435	1505	7
AM 350[a]	0.1	16.5	4.25	2.75					1225	1442	13
AM 355[a]	0.13	15.5	4.25	2.75					1220	1470	14
AUSTENITIC ALLOYS											
	C	Cr	Ni	Mn	Si	P	Cu	Mo			
17-10 PH	0.12	16.7	10.2	0.75	0.5	0.28			610	950	25
HNM	0.3	18.5	9.5	3.5	0.5	0.25			830	1120	18
17-14 Cu Mo	0.12	16	14	0.75	0.5		3	2.5	-	-	-
A 286[b]	0.5	26	15					1.2	700	1000	25
21-4-9	0.4	21	4	9					650	1050	14

* balance iron
(a) 0.1% N
(b) 2% Ti, 0.15% Al γ'-forming
(c) properties in fully-aged condition

TABLE 7

COMPOSITIONS (wt.%) OF SPECIAL STAINLESS STEELS AND NICKEL-BASE SUPERALLOYS[47-52]

Alloy	C	Cr	Ni	Fe	Mn	Al	Co	Mo	Nb + Ta	Cu	Ti	W
Ni-base												
Inconel 600	0.08	15.5	76	8	0.5	-	-	-	-	-	-	-
Inconel 601	0.05	23	60.5	14	0.5	1.35	-	-	-	-	-	-
Inconel 625	0.05	21.5	61	2.5	0.25	0.2	-	9	3.65	-	0.2	-
Hastelloy C-276	0.02+	15.5	Bal.	5.5	1+	-	2.5+	16	-	-	-	3.8
Hastelloy C-4	0.15+	16.3	Bal.	3+	-	0.2	2+	15	-	-	0.5	-
Hastelloy G	0.05+	22.3	Bal.	19.8	1.5	-	2.5+	6.5	2	2	-	1+
Monel 400	0.2	-	66.5	2.5	2	-	-	-	-	31.5	-	-

Alloy	C	Cr	Ni	Fe	Mo	Mn	Cu	Al	Nb	Ti
Fe-base										
Incoloy 800	0.05	21	32.5	Bal.	-	0.75	0.38	0.38	-	0.38
Incoloy 801**	0.05	20.5	32	Bal.	-	0.75	0.25	-	-	1.13
Incoloy 825	0.03	21.5	42	Bal.	3	0.5	2.25	0.1	-	0.9
AL 6X	0.03	20	24	Bal.	6	1.5	-	-	-	-
Sandvik 2RK65	0.02	19.5	25	Bal.	4.5	1.8	1.5	-	-	-
Sandvik 2RE10	0.02	24.5	20	Bal.	-	1.8	-	-	-	-
Sandvik 2RE69*	0.02	25	22	Bal.	2.1	1.7	-	-	-	-
UHB 904L	0.02	20	25	Bal.	4.5	1.75	1.5	-	-	-
JS 700	0.03	21	25	Bal.	4.5	1.7	-	-	0.3	-
AISI 310	0.25+	25	20	Bal.	-	2+	-	-	-	-
Carpenter 20 Cb-3	0.06+	20	34	Bal.	2.5	2+	3.5	-	++	-
Uniloy-332	0.05+	20.5	32.5	Bal.	-	1	-	-	-	-

\+ maximum

* contains 0.12% N

++ Nb + Ta stabilized

** γ'-strengthened

TABLE 8

TYPICAL MECHANICAL PROPERTIES OF SPECIAL STAINLESS STEELS AND NICKEL-BASE SUPERALLOYS[47-52]

Alloy		0.2% Yield strength† (MPa)	Ultimate tensile strength† (MPa)	Elongation (%)
Ni-base				
Inconel 600 H.F.*	(1)	241 - 621	586 - 820	50 - 25
A*		207 - 345	552 - 690	55 - 35
Inconel 601 H.F.	(1)	241 - 690	586 - 830	60 - 15
A		207 - 415	552 - 790	70 - 40
Inconel 625 H.F.	(1)	415 - 760	830 -1100	60 - 30
A		415 - 655	830 -1035	60 - 30
Hastelloy C-276	(2)	365	785	59
Hastelloy C-4	(2)	335	805	63
Hastelloy G	(2)	310	690	62
Monel 400 A	(1)	175 - 350	490 - 630	60 - 35
Fe-base				
Incoloy 800 H.F.*	(1)	241 - 620	552 - 830	50 - 25
A		207 - 415	517 - 690	60 - 30
Incoloy 801 **	(1)	207 - 550	890	30
Incoloy 825	(1)	242 - 415	586 - 725	50 - 30
AL 6X	(3)	276	586	45
Sandvik 2RK65	(4)	214 (min)	490 - 740	40 (min)
Sandvik 2RE10	(4)	235 (min)	490 - 690	30
Sandvik 2RE69	(4)	255	540 - 740	30 (min)
UHB 904L	(5)	248	586	50
JS 700	(6)	270	586	45
Carpenter 20 Cb-3	(7)	330	760	40
Uniloy-332	(8)	262	614	35

Producers Code:
(1) Huntington Alloys Inc.
(2) Stellite Div., Cabot Corp.
(3) Allegheny Ludlum Industries Inc.
(4) Sandvik Steel Inc.
(5) Uddeholm Steels
(6) Jessop Steel Co.
(7) Carpenter Technology Corp.
(8) Universal-Cyclops, Cyclops Corp.

† the lower values are typical of the annealed or solution annealed condition

* H.F. - hot-finished; A - annealed

** can be strengthened by γ' precipitation

TABLE 9

COMPOSITIONS OF SOME COMMONLY USED TITANIUM ALLOYS[71-73]

ASTM Grade	COMPOSITION (wt.%)										
	N*	C*	H*	Fe*	O*	Al	V	Sn	Pd	Mo	Ni
1	0.03	0.1	0.015	0.2	0.18	-	-	-	-	-	-
2	0.03	0.1	0.015	0.3	0.25	-	-	-	-	-	-
3	0.05	0.1	0.015	0.3	0.35	-	-	-	-	-	-
4	0.05	0.1	0.015	0.5	0.4	-	-	-	-	-	-
5	0.05	0.1	0.015	0.4	0.2	5.5-6.75	3.5-4.5	-	-	-	-
6	0.05	0.1	0.02	0.5	0.2	4.0-6.0	-	2.0-3.0	-	-	-
7	0.03	0.1	0.015	0.3	0.25	-	-	-	0.12-0.25		
11	0.03	0.1	0.015	0.2	0.18	-	-	-	0.12-0.25		
12†	0.03	0.08	0.015	0.3	0.25	-	-	-	-	0.2-0.4	0.6-0.9

* maximum

† e.g. Ticode-12

TABLE 10

MECHANICAL PROPERTIES OF SOME COMMONLY USED TITANIUM ALLOYS[71-73]

ASTM Grade	0.2% Y.S. (MPa)		U.T.S. (MPa)	Elongation (%)
	Min.	Max.	Min.	Min.
1	170	310	240	24
2	275	450	345	20
3	380	550	450	18
4	485	655	550	15
5	830	-	895	10
6	795	-	830	10
7	275	450	345	20
11	170	310	240	24
12	345	-	483	18

TABLE 11

STRENGTH AND FRACTURE PROPERTIES OF α-TITANIUM ALLOYS IN THE MILL ANNEALED CONDITION[86]

Alloy	0.2% Yield (MPa)	U.T.S. (MPa)	K_{IC} (MPa$\sqrt{m}$)	K_{ISCC}^{*} (MPa$\sqrt{m}$)
Ti-50A	293	454	66.4	66.4
Ti-70	582	705	126	60
Ti-5Al-2.5Sn	892	954	80	29

* Taken as the value of applied stress intensity at 360 minutes of testing.

TABLE 12

NOMINAL COMPOSITIONS OF SOME COMMONLY USED WROUGHT COPPERS AND COPPER ALLOYS[110]

C.D.A.#	Name	Nominal Composition (wt.%)										
		Cu	O	P	Be	Zn	Sn	Si	Ni	Fe	Al	Mn
102	Oxygen-free copper	99.95										
110	Electrolytic tough-pitch copper	99.90	0.04									
122	Phosphorus deoxidised copper	99.40		0.02								
170	Beryllium copper	99.5			1.7							
220	Commercial bronze	90.0				10.0						
260	Cartridge brass	70,0				30.0						
280	Muntz metal	60.0				40.0						
505	Phosphor bronze	98.75					1.25					
524	Phosphor bronze	90.0					10.0					
651	Low-silicon bronze	98.5						1.5				
655	High-silicon bronze	97.0						3.0				
706	Copper-nickel 10%	88.7							10.0	1.3		
715	Copper-nickel 30%	70.0							30.0			
614	Aluminum bronze, D	91.0								2.0	7.0	
632	Aluminum bronze	82.0							5.0	4.0	9.0	
674	Manganese brass	58.5				36.5	1.0				1.2	2.8
675	Manganese bronze, A	58.5				39.0	1.0					0.1

TABLE 13

RANGE OF MECHANICAL PROPERTIES IN THE ANNEALED CONDITION FOR COMMONLY USED WROUGHT COPPERS AND COPPER ALLOYS[110]

C.D.A. Series	Name	0.5% Y.S. (MPa)	U.T.S. (MPa)	Elongation (%)
100	Coppers	70	220	45-55
100	High copper alloys	70-220	203-490	32-55
200	Brasses	70-147	240-380	45-66
300	Leaded brasses	84-140	260-370	45-65
400	Tin brasses	70-175	270-390	40-65
500	Phosphor bronzes	98-196	280-460	48-70
600	Aluminum bronzes	210-378	525-640	18-45
600	Silicon bronzes	105-147	280-392	55-60
700	Copper-nickel	90-210	300-490	35-45
700	Copper-nickel zinc	126-189	340-420	40-50
	Manganese brass	84-240	320-490	28-60
	Manganese bronze	210	455	33
	Aluminum brass	190	420	55

TABLE 14

COMPARATIVE CREEP RATES OF PURE COPPERS AT 150°C [16]

Type of Copper	Stress* (MPa)
Electrolytic tough-pitch	66
Oxygen-free	58
Phosphorus deoxidised	147

* Stress to produce a creep rate of 0.0001% per hour

TABLE 15

MINIMUM MECHANICAL PROPERTIES SPECIFIED FOR ANNEALED PLATE BY ASTM

Alloy	Condition	0.2% Y.S.* (MPa)	U.T.S.* (MPa)	Elongation* (% on 50 mm)	Normalized Y.S.	ASTM Specification
Austenitic stainless						
steels 304L	Annealed	170	485	40	1	A167
316L	Annealed	170	485	40	1	A167
317L	Annealed	205	515	35	0.83	A167
347	Annealed	205	515	40	0.83	A167
310	Annealed	205	515	40	0.83	A167
Ferritic stainless						
steels 446	Annealed	275	515	20	0.62	A176
444	Annealed	310	415	20	0.55	A176
Titanium grade 1	Annealed	170	240	24	1	B265
grade 2	Annealed	275	345	20	0.62	B265
grade 3	Annealed	380	450	18	0.45	B265
grade 12	Annealed	345	483	18	0.49	B265
Aluminum alloys						
1100	Annealed	25	75	28	6.8	B209
3003	Annealed	34	97	23	5	B209
5086	Annealed	95	240	16	1.8	B209
5456	Annealed	124	283	16	1.37	B209
Incoloy 825	Annealed	240	586	30	0.71	B424
Incoloy 800	Annealed	205	520	30	0.83	B409
	As-rolled	240	550	25	0.71	B409
	Soln. Treated	170	450	30	1	B409
Inconel 625	Annealed	414	827	30	0.41	B443
Inconel 600	Annealed	240	550	30	0.71	B168
Hastelloy C-276	Annealed	315	690	30	0.54	B334
Monel	Annealed	195	485	35	0.87	B402
	As-rolled	275	515	25	0.62	B402
Copper (ETP)	Annealed	70	205	-	2.43	B152
Aluminum bronze C614	Annealed	205	485	30	0.83	B169
Copper-nickel C706	Annealed	105	275	30	1.62	B402
C715	Annealed	140	345	30	1.21	B402
Copper-silicon C655	Annealed	125	345	40	1.36	B96
C658	Annealed	125	345	40	1.36	B96
Phosphor bronze C51	Annealed	-	295	-	-	B103

* minimum values

TABLE 16

VARIOUS COST COMPARISONS FOR ENGINEERING ALLOYS

Alloy	Cost ($/kg)	Cost of fabricated pipe ($/kg)	Cost ratio on the basis of Y.S.
A36 mild steel	0.75 P	1.17	0.13
Copper	3.81 B	5.57**	2.53
Copper-10% nickel	4.75 B	7.10**	2.1
Aluminum bronze	4.40 B	6.60**	1.0
304L stainless steel	2.29	5.28	0.88
316L stainless steel	3.61 P	6.01	1.00
310 stainless steel	-	9.60	1.32
321 stainless steel	5.06 P	5.52	0.76
347 stainless steel	5.19 P	5.79	0.80
26 Cr-1 Mo ferritic stainless steel	5.57	-	-
20 Cb 3 stainless steel	8.18	-	-
Incoloy 825	7.96	13.1*	1.55
Incoloy 800	5.35 P	10.5	1.43
Inconel 600	9.04	13.20	1.65
Inconel 625	11.88 P	19.23	1.38
Hastelloy C-276	17.16	23.43	2.22
Monel 400	8.18	12.76	2.04
Grade 2 titanium	11.88 P	27.2	1.58
Ticode-12	15.40 P	30.7*	1.41
Aluminum alloy 1100	5.17 P	7.87**	3.14
Aluminum alloy 5086	4.77 P	7.12**	0.73
Lead	0.77	-	-

† based on quotations for pipe 91.4 cm O.D. x 2.54 cm w.t.

B based on quotations for billets

P based on quotations for plate

* assumes same fabrication costs as for similar alloys

** assumes fabrication cost is 50% of base metal price

TABLE 17

RELATIVE COSTS OF EXTRUDED AND SEAM WELDED PIPE
BASED ON QUOTATIONS FOR 91.4 cm O.D. x 2.54 cm W.T.

Material	Extruded Pipe ($/m)	Seam Welded Pipe ($/m)
AISI 304L	5 802	2 998
AISI 316L	6 157	3 430
AISI 310	7 495	5 484
AISI 321	6 262	3 152
Incoloy 800	10 791	5 982
Inconel 600	16 199	8 318

TABLE 18

PROBABLE GROUNDWATER COMPOSITIONS OF CRYSTALLINE ROCKS OF THE CANADIAN SHIELD[141]

Analysis	Units	Probable Range	Maximum*
Conductivity	µS/cm	400-600	1 100
$KMnO_4$ consum.	mg/L	5-35	50
COD_{Mn}	O_2 mg/L	1.2-9	12.5
Ca^{2+}	mg/L	20-60	100
Mg^{2+}	mg/L	15-30	150
Na^{+}	mg/L	(∿ 20-40)	200
Fe-total	mg/L	1-20	30
Fe^{2+}	mg/L	0.5-15	30
Mn^{2+}	mg/L	0.1-0.5	3
HCO_3^-	mg/L	150-400	500
CO_2	mg/L	0-25	50
Cl^-	mg/L	20-100	400
SO_4^{2-}	mg/L	20-40	100
NO_3^-	mg/L	0.1-2	10
PO_4^{3-}	mg/L	0.1-0.6	1
F^-	mg/L	0.5-3	8
SiO_2	mg/L	15-40	60
HS^-	mg/L	< 0.2-5	10
NH_4^+	mg/L	0.1-0.4	5
NO_2	mg/L	0.01-0.1	0.5
$^0_{dH}$	$^0_{dH}$	6-15	50
O_2	mg/L	<0.01	1
pH	∿ 8 (Swedish tunnel water)		

* 95% Estimated probability that the maximum will not be exceeded.

TABLE 19

SOIL RESISTIVITY CLASSIFICATIONS*(143)

Resistivity Range (Ω·cm)	Corrosivity
0 - 1 000	Very severe
1 001 - 2 000	Severe
2 001 - 5 000	Moderate
5 001 - 10 000	Mild
10 001 +	Very mild

* refers to steel pipe.

TABLE 20

SOIL ACIDITY CLASSIFICATIONS[17]

Classification	pH
Extremely acid	< 4.5
Very strongly acid	4.5 - 5.0
Strongly acid	5.1 - 5.5
Medium acid	5.6 - 6.0
Slightly acid	6.1 - 6.5
Neutral	6.6 - 7.3
Mildly alkaline	7.4 - 7.8
Moderately alkaline	7.9 - 8.4
Strongly alkaline	8.5 - 9.0
Very strongly alkaline	> 9.0

TABLE 21

EFFECT OF TEMPERATURE AND CHLORIDE CONCENTRATION ON MILD STEEL CORROSION[153]

% NaCl	Temperature (°C)	Corrosion Rate (mm/a)
0	20	0.53
	75	0.91
0.002	20	0.66
	75	1.70
0.05	20	0.79
	75	2.16
3.5	20	0.61

TABLE 22

PITTING POTENTIALS OF VARIOUS ALLOYS IN A 1000 mg/L CHLORIDE SOLUTION AT AMBIENT TEMPERATURE[165]

Alloy	Minimum Breakthrough Potential (Volts vs. SCE)
AL-6X	1.0+ (beyond range tested)
29Cr-4Mo	1.0+ (beyond range tested)
Hastelloy C	1.0+ (beyond range tested)
26-1S	0.98
216	0.95
$20Cb_3$	0.55
18-2	0.40
316	0.33
439	0.30
304	0.22
430	0.05

TABLE 23

RELATIVE RESISTANCE OF VARIOUS ALLOYS TO CREVICE CORROSION IN 10% FERRIC CHLORIDE RUBBER BAND TEST[165]

72 Hours - Room Temperature

ASTM G-48

Alloy	Weight Loss (g/cm^2)	Rating
Al-6X 29-4 29-4-2 Hastelloy C Titanium	0	Excellent Resistance
216 E Brite 26-1 26-1S	0.0010-0.0040	Good Resistance
317 3Re60 316 439 304 $20Cb_3$	0.010-0.035	Fair Resistance

TABLE 24

EFFECT OF MOLYBDENUM CONCENTRATION ON THE OXIDIZING POTENTIAL REQUIRED TO INITIATE LOCALIZED CORROSION[C-99]

24-h Exposure - Constant Applied Potential; 3.5% $FeCl_3$ at 70°C					
Potential mV (SCE)	(2-3% Mo) Type 316 Stainless Steel	(3% Mo) Incoloy Alloy 825	(6.5% Mo) Hastelloy Alloy G	(9% Mo) Haynes Alloy No. 625	(16% Mo) Hastelloy Alloy C-276
+ 800	*	*	*	*	o
+ 700	*	*	*	*	o
+ 600	*	*	*	*	o
+ 500	*	*	*	*	o
+ 400	*	*	*	o	o
+ 300	*	*	*	o	o
+ 200	*	*	o	o	o
+ 100	*	*	o	o	o
0	*	*	o	o	o
- 100	*	o	o	o	o
- 200	o	o	o	o	o

* Localized corrosive attack

o No attack.

TABLE 25

CORROSION RATING OF NICKEL ALLOYS AFTER TWO YEARS EXPOSURE TO QUIESCENT SEA WATER[172]

Rating Group	Corrosion Behaviour	Alloy	Major Alloy Content
No General Corrosion			
1A	No attack	N	54Ni-19Cr-10Mo-11Co (René 41)
		R	62Ni-22Cr-9Mo-3Fe (Inc. 625)
		T	56Ni-16Cr-16W-6Fe-4W (Hastelloy C)
1B	Little or no pitting on boldly exposed areas, minor attack in crevices	O	47Ni-22Cr-9Mo-18Fe
		P	69Ni-7Cr-16Mo-4Fe (Hastelloy X)
		Q	42Ni-21Cr-3Mo-30Fe (Incoloy 825)
		S	66Ni-20Cr-5Mo-6Fe
1C	Little or no pitting on boldly exposed surfaces, moderate to severe attack in crevices	U	53Ni-18Cr-3Mo-18Fe
		V	42Ni-12Cr-6Mo-35Fe
1D	Moderate to severe attack in boldly exposed surfaces and in crevices	G	63Ni-35Cr-2Fe
		I	76Ni-20Cr-3Fe
		J	73Ni-15Cr-7Fe
		K	30Ni-20Cr-47Fe
1E	Consistently severe attack by pitting and crevice corrosion	F	77Ni-16Cr-7Fe (In.600)
		H	60Ni-19Cr-17Co
		L	32Ni-20Cr-47Fe (In.800)
		A	97Ni-2Be
General Corrosion			
1I	General corrosion plus moderate localized attack	M	65Ni-27Mo (Hastelloy B)
		B	65Ni-35Cu (Monel 400)
		C	60Ni-40Cu
		D	45Ni-55Cu
		E	65Ni-30Cu-3Al (Monel K500)

TABLE 26

LOCALIZED CORROSION OF ALLOYS EVALUATED UNDER WET AIR OXIDATION CONDITIONS[173]

Material	Autoclave 204°C			Pilot Plant 177°C
	600 mg/L Cl^-	1000 mg/L Cl^-	3000 mg/L Cl^-	1000 mg/L Cl^-
Titanium	NC	NC	NC	NC
Hastelloy Alloy C-276	NC	NC	P	NC
Inconel 625	NC	NC	P	NC
Hastelloy Alloy G	NC	P,C	P,C	-
28Cr-4Mo	NC	P,C	P,C	P
28Cr-4Mo-2Ni	NC	P,C	P,C	-
Incoloy 825	P,C	P,C	P,C	P
Carpenter 20Cb-3	P,C	P,C	P,C	P
Sandvik 2RN65	-	P,C,SCC	P,C,SCC	P,SCC
E-Brite 26-1	P,C	P,C	P,C	P
Sandvik 3RE60	P,C	P,C,SCC	P,C,SCC	P,SCC
Carpenter 7-Mo (329)	P,C	P,C,SCC	P,C,SCC	P,SCC
Type 316 Stainless Steel	P,C,SCC	P,C,SCC	-	P,SCC

Note: NC = no corrosion; P = pitting; C = crevice corrosion; SCC = stress corrosion cracking.

TABLE 27

RESISTANCE OF VARIOUS GRADES OF HASTELLOY-C TO INTERGRANULAR, CREVICE AND STRESS CORROSION[64]

	Alloy			Heat Treatment[1]	Intergranular Corrosion Test Ratios[2]		Crevice Corrosion in 10% Ferric Chloride[3]	Stress Corrosion Cracking[4] 45% $MgCl_2$
	Code	Analysis (wt.%)			Ferric Sulfate	"Pure" Sulfuric Acid	50°C	155°C
		C	Si		(24 h)	(5 h)		
Alloy C	46	0.03	0.70	Solution Annealed	1.0	1.0	None	None
				1 h at 705°C	6.1	15.0	Yes	Yes
				1 h at 820°C	14.3	4.6	Yes	Yes
				1 h at 1035°C	[illegible]	4.8	Yes	Yes
				Furnace Cooled	2.6	2.2	Yes	Yes
				Agglomerating	2.0	2.4	Yes	Yes
Alloy C-276	3006	0.01	0.01	Solution Annealed	1.0	1.0	None	None
				1 h at 705°C	1.5	1.2	None	None
				1 h at 820°C	13.8	3.1	None	Yes
				1 h at 1035°C	7.3	1.5	None	None
Alloy C-276	3101	0.008	0.004	Solution Annealed	1.0	1.0	None	None
				1 h at 705°C	1.0	1.1	None	Yes
				1 h at 820°C	11.4	1.9	None	Yes
				1 h at 1035°C	10.6	1.3	None	Yes
Alloy C-276	3100	0.004	0.01	Solution Annealed	1.0	1.0	None	None
				1 h at 705°C	1.0	1.0	None	None
				1 h at 820°C	14.2	1.9	None	None
				1 h at 1035°C	3.5	1.2	None	None
				Furnace Cooled	2.4	1.0	None	None
				Agglomerating	2.0	1.0	None	None
Alloy C-4	7137	0.006[5]	0.04	Solution Annealed	1.0	1.0	Yes	None
				1 h at 820°C	2.4-7.4	1.3	Yes	None
				Furnace Cooled	1.0	1.0	Yes	None

(1) Heat Treatments: Furnace cooled from 1200 or 1225°C to 540°C in 1.5 h.
Agglomerating: Heat in 4 h to 1170°C, hold 1 h, cool to 1120°C and hold 3 h, then cool to below 565°C in 0.5 h.

(2) Ratio of rate of given specimen divided by rate of solution annealed specimen in boiling 50% H_2SO_4, with and without ferric sulfate.

(3) Specimen with six crevices.

(4) U-bend specimens.

(5) Alloy contains 0.43% Ti to stabilize carbon.

TABLE 28

SUMMARY OF OXIDATION DATA FOR UNALLOYED TITANIUM[81]

Temp. °C	Environment	Ti-Consumption µm/a	Reference No in ref. (81)
60	3.5% NaCl+96.5% H_2O, air-saturated solution	0.24	29
	3.5% NaCl+96.5% H_2O, Ar-saturated, Exposure time 146 d	0.24	
120	Steam, 120°C, pH 7, Exposure time 2 a	0.0025	20
130	3.5 NaCl+96.5% H_2O, air-saturated solution	1.6	29
	3.5% NaCl+96.5% H_2O, Ar-saturated, Exposure time 146 d	5.6	*
200	3.5% NaCl+96.5% H_2O, air-saturated	3.2	29
	3.5% NaCl+96.5% H_2O, Ar-saturated, Exposure time 146 d		
252	Boiler water, pH 10-11, Exposure time 234 d	0.007	10
315	Simulated PWR-water, pH 10 Exposure time 80 d	0.2 - 1.6	10**
360	Degasified H_2O, pH 9.5 Exposure time 107 d	0.16	10
400	Steam 400°C, 10 MPa Exposure time 417 d	0.35	45

* Based on weight loss. All other values were re-calculated on the basis of a weight gain.

** No hydrogen absorption or effect on mechanical characteristics.

TABLE 29

RELATIVE CREVICE CORROSION RESISTANCE OF METALS AND ALLOYS IN QUIET SEA WATER[191]

Metal or Alloy	Resistance
Hastelloy C Titanium	Inert
90Cu-10Ni-1.5Fe 70Cu-30Ni-0.5Fe Bronze Brass	Best
Austenitic Nickel Cast Iron Cast Iron Carbon Steel	Neutral
Incoloy 825 Carpenter 20 Ni-Cu Alloy Copper	Less
316 Stainless Steel Ni-Cr Alloys 304 Stainless Steel Series 400 Stainless Steels	Pit Initiation At Crevices

TABLE 30

DEPTH OF ATTACK AND CORROSION RATES OF COPPER AND COPPER ALLOYS AFTER 735 DAYS IN QUIESCENT SEA WATER WITHOUT CATHODIC PROTECTION[201]

Alloy Name	CDA No.	Depth of Attack (mils)*				Average Corrosion Rate (mpy)*
		Crevice[2]		Surface[3]		
		Deepest	Average	Deepest	Average	
Copper	-	4	3	1	<1	0.37
Copper-Beryllium	172	9	6	<1	<1	0.46 (d)
Copper-Cobalt-Beryllium	175	3	2	2	1	0.10 (d)
Commercial Bronze, 90%	220	6	2	4	3	0.08 (d)
Red Brass, 85%	230	2	2	0[5]	0[5]	0.07 (d)
Cartridge Brass, 70%	260	12[6]	7[6]	13[6]	12[6]	0.31 (d)
Yellow Brass, 66%	268	22[6]	11[6]	15[6]	12[6]	0.31 (d)
Muntz Metal, 60%	280	-[6]	-[6]	-[6]	-[6]	0.63 (d)
Admirality, Arsenical	443	4	2	2	1	0.34 (d)
Naval Brass, Uninhibited (Grade A)	464	2[6]	2[6]	-[6]	-[6]	0.26 (d)
Phosphor Bronze, 10% D	524	7	5	6	4	0.24 (d)
Aluminum Bronze, 5% Al	608	0	0	0	0	0.13 (d)
Aluminum Bronze, 9% Al	612	<1	<1	0	0	0.07 (d)
Aluminum Bronze, D, 7% Al, 2% Fe	614	<1	<1	<1	<1	0.05 (d)
High Silicon Bronze A	655	12	6	3	2	0.74 (d)
Copper-Nickel, 10%	706	0	0	0	0	0.06
Copper-Nickel, 30%	715	0	0	0	0	0.07
Copper-Nickel, 30% Ni, 5% Fe	716	43	26	4	1	0.14 (d)

(1) There were no measurable pits and no detectable weight loss on specimens which were cathodically protected with zinc anodes.

(2) The deepest and average of the ten deepest points of attack associated with a crevice.

(3) The deepest and average of the ten deepest points of attack on the surface not associated with any known crevice.

(4) The average corrosion rate is given for comparison only. Since uniform attack is assumed in its calculation, the average corrosion rate is applicable only to those alloys which did not experience localized attack or de-alloying. (d) = de-alloyed.

(5) Alloy pitted on surfaces, but pits were too narrow for accurate measurement of depth of attack.

(6) Copper deposits from de-alloying made accurate measurement of depth attack impractical.

* 1 mil = 0.001 in = 0.025 mm
mpy = mils per year.

TABLE 31

CREVICE CORROSION TEMPERATURES (°C) OF VARIOUS ALLOYS IN 10% $FeCl_3 \cdot 6H_2O$ SOLUTION

Alloy / Reference	304 S.S.	316 S.S.	Alloy 216	26Cr-1Mo	A1-6X	29Cr-4Mo	Inconel 625	Hastelloy C-276	C.P. Ti Grade 2	Ti-0.2Pd Grade 7
Streicher (163)				<RT		<50	RT-50*	65-75*	65-75*	
Steigerwald (166)	<RT	<RT	<RT	<50	RT-50	>50	RT-50*	>50	>50	
Garner (204)	-2.5	-2.5			30/35**					
Brigham (130)					28-30					
La Que (205)	-2.5	0		20-22.5	17.5-20					
Kovach et al. (155)	<0	<0			23	50				
Coulter et al. (167)				<RT		>50				
Timet (72)									<100	>100
Tapping (206)	0				>48		45		>48	
Lowest Reported	-2.5	-2.5	<RT	<RT	17.5	<50	45	65	65	>100

* (T_1-T_2) = resistant at T_1 but not at T_2

** Welded/not welded

RT = room temperature

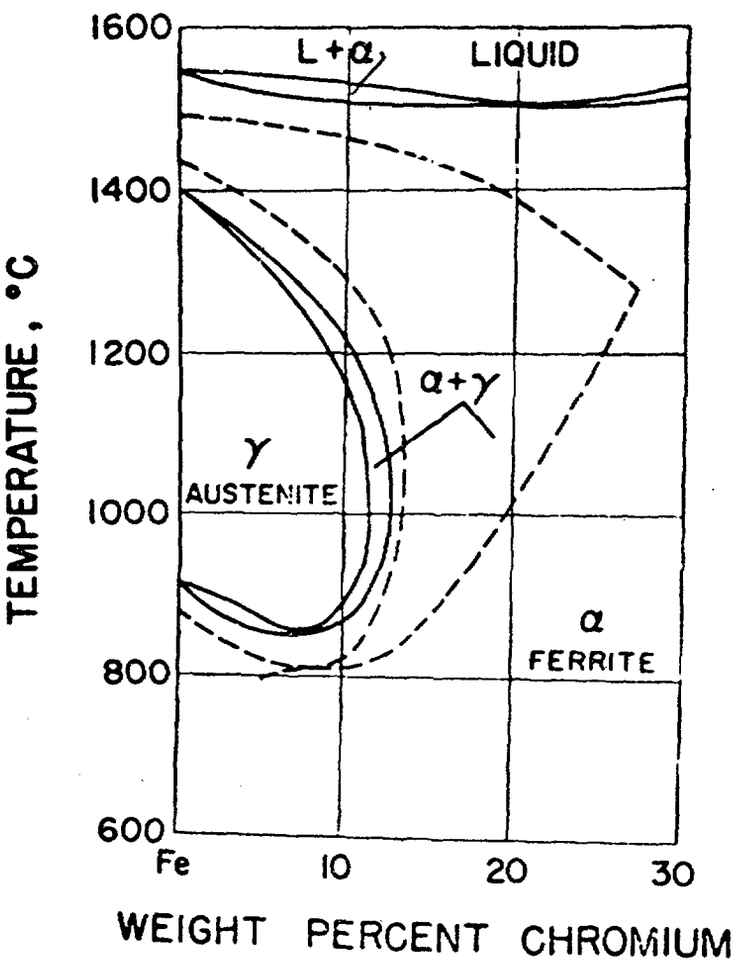

FIGURE 1: Phase Diagram Showing γ-Loop in Fe-Cr Alloys Containing Less Than 0.01% Carbon or Nitrogen (Solid Lines) and Alloys Containing 0.1 to 0.2% Carbon or Nitrogen (Dotted Lines)[18]

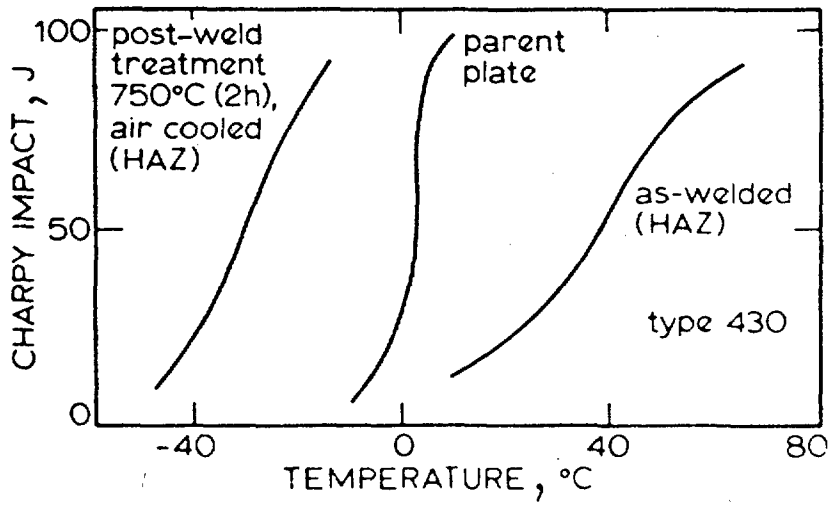

FIGURE 2: Effect of Post-Weld Annealing on the Impact Properties of 17% Chromium Steel[25]

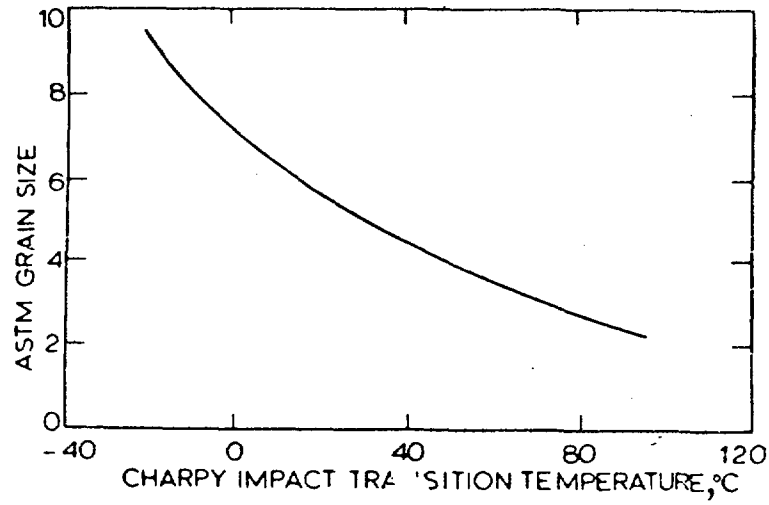

FIGURE 3: Effect of Ferritic Grain Size on the Impact Transition Temperature of Commercial 17% Chromium Steels[25]

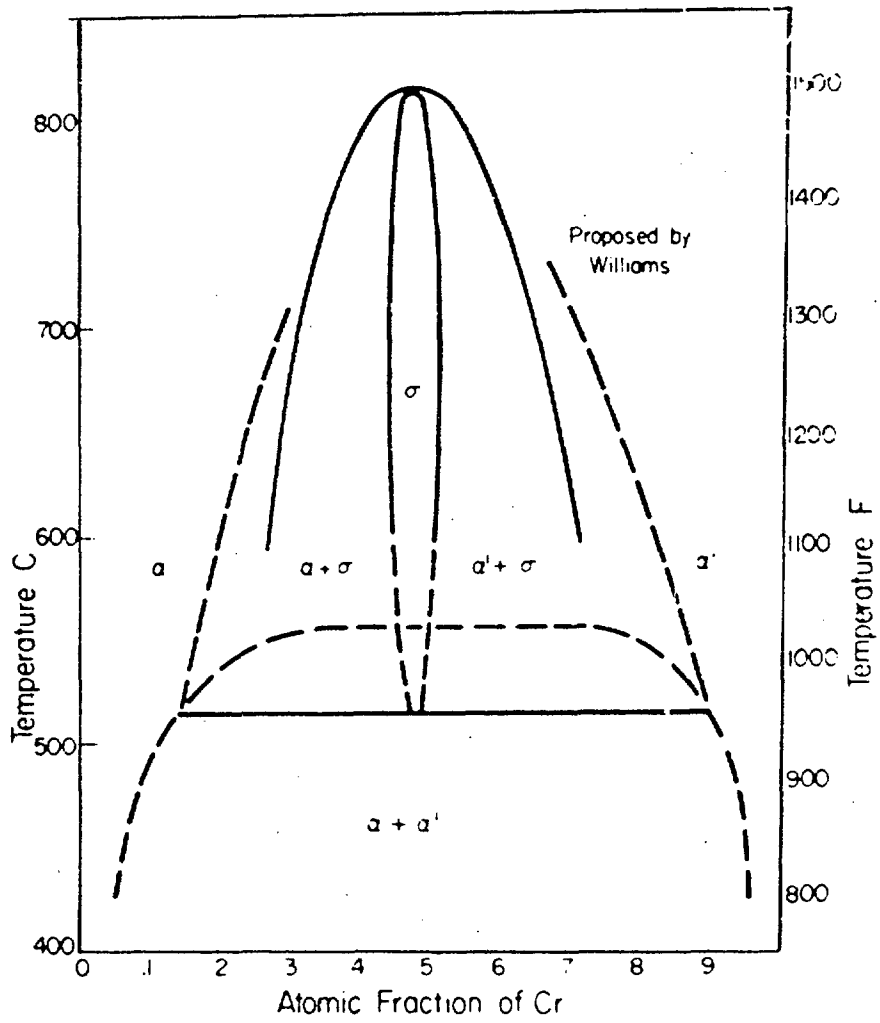

FIGURE 4: Lower Temperature Portion of the Fe-Cr Phase Diagram(18)

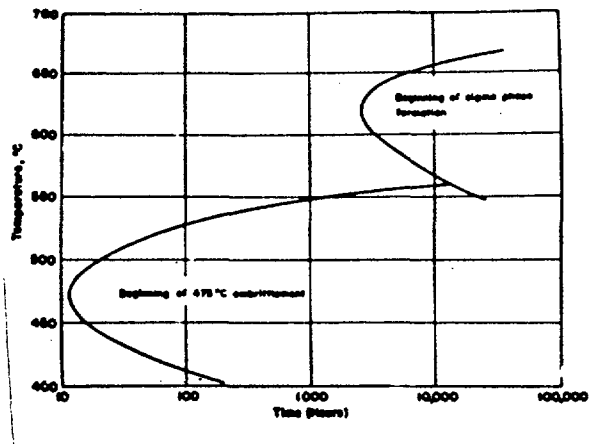

FIGURE 5: Time-Temperature Dependence of σ-Phase Formation and 475°C Embrittlement in Fe-Cr Alloys[18]

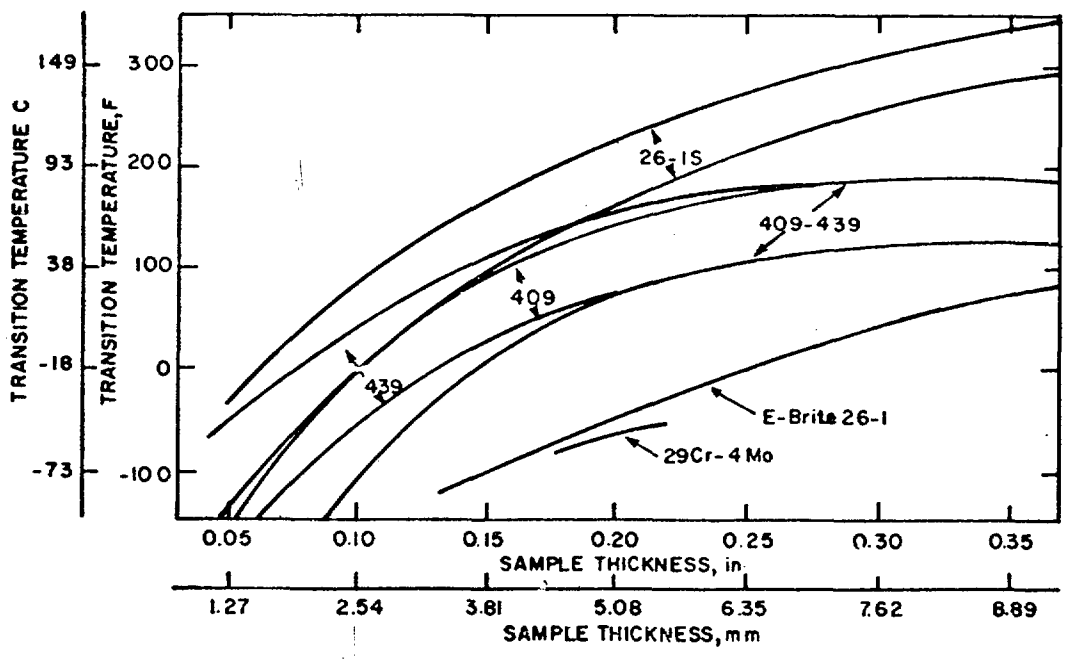

FIGURE 6: Effect of Section Thickness on Ductile to Brittle Transition Temperature for Ferritic Stainless Steels. Bands for 26-1s, 409 and 439 indicate data scatter[30]

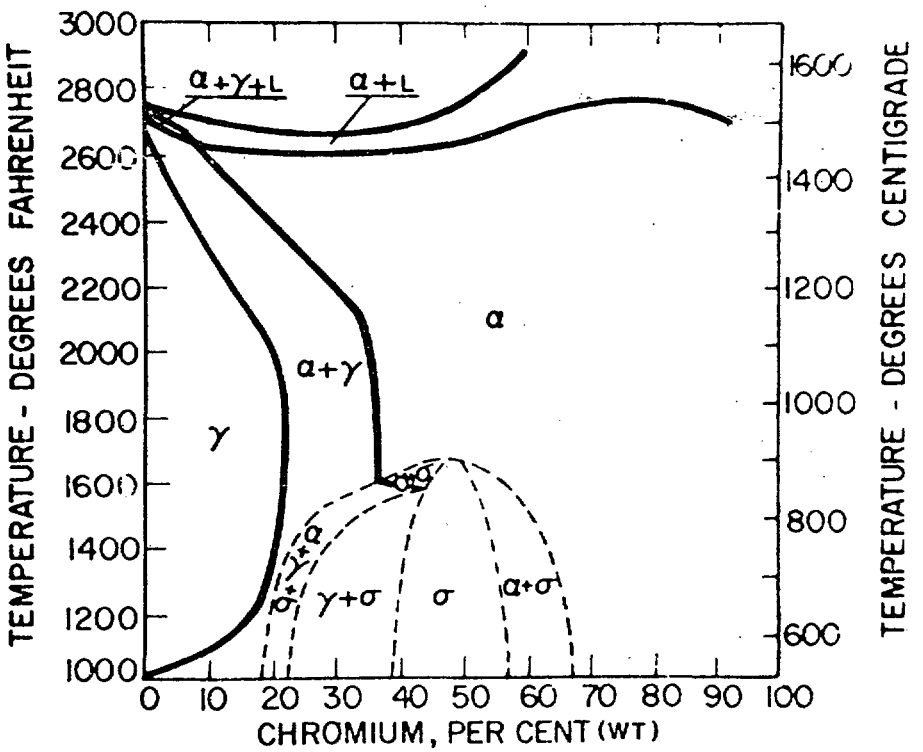

FIGURE 7: Phase Diagram for Fe-Cr Showing the Effect of 8% Nickel[18]

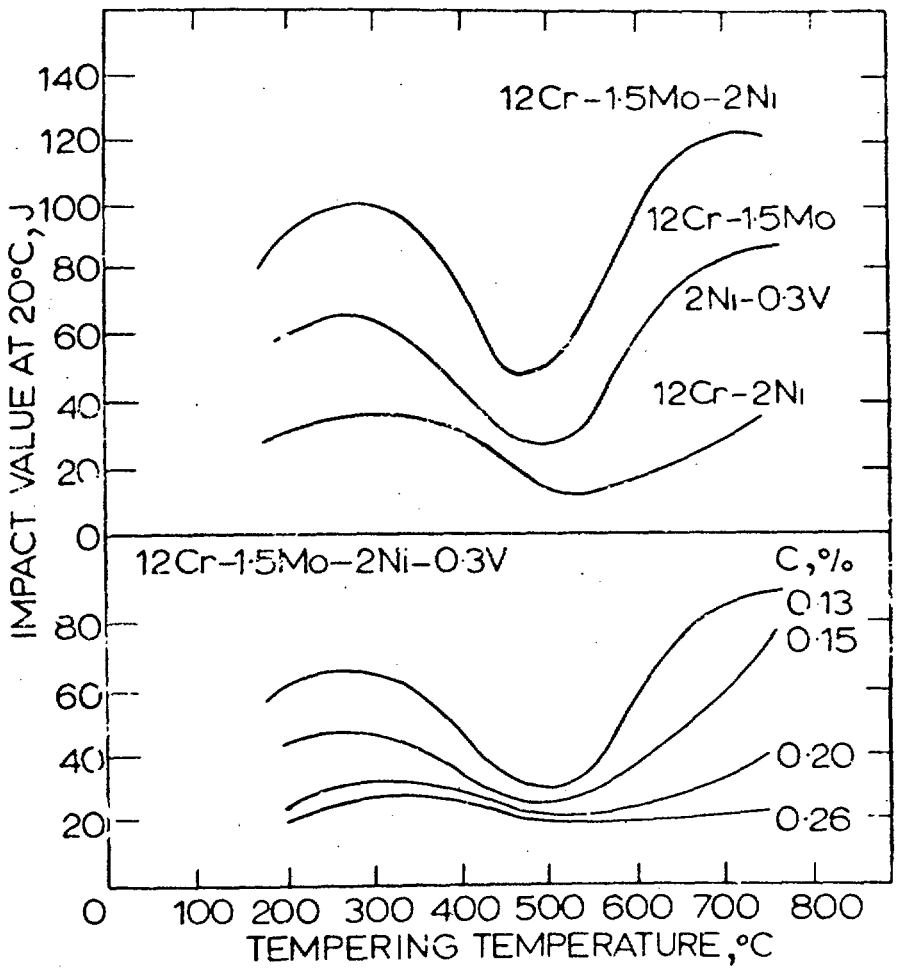

FIGURE 8: Effect of Tempering on Impact Resistance Showing a Minimum in the Temperature Range of Maximum Secondary Hardening (450 - 550°C[19])

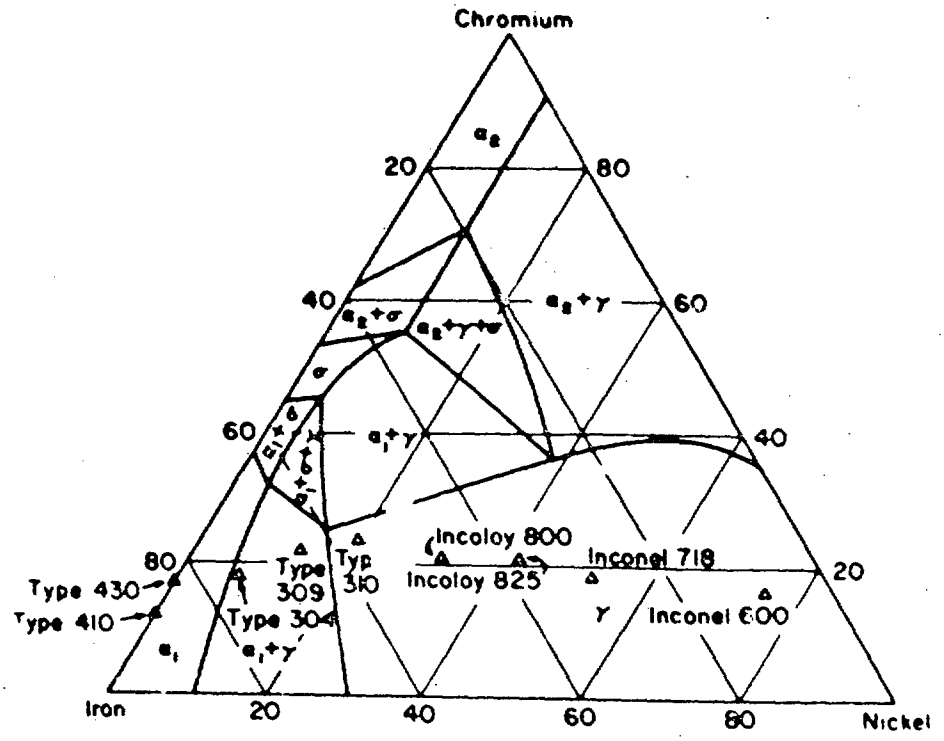

FIGURE 9: The Fe-Cr-Ni Phase Diagram, Isothermal Section at 400°C(18)

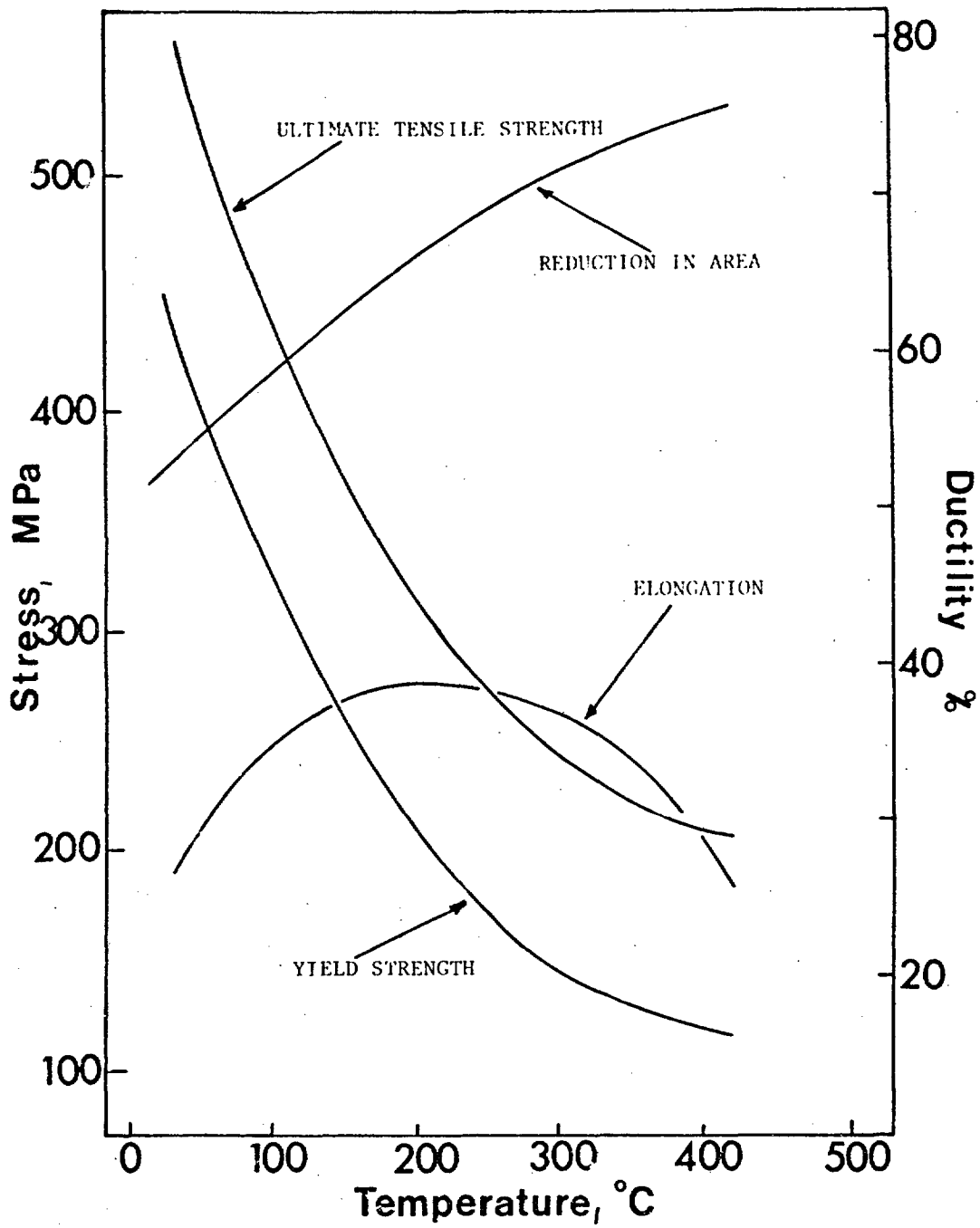

FIGURE 10: Effects of Temperature on Strength and Ductility of Mill-annealed Unalloyed Titanium (ASTM Grade 3)[8].

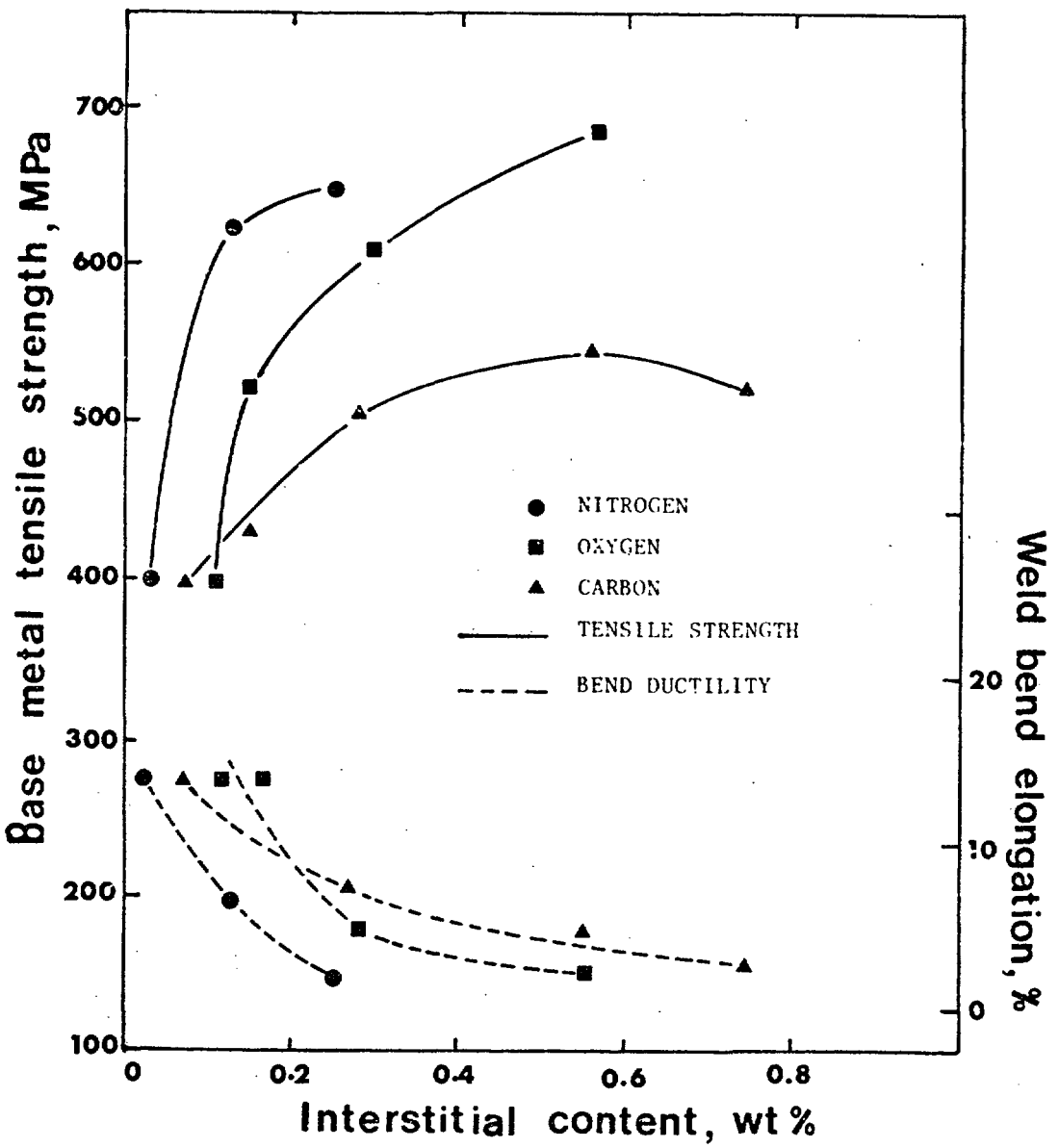

FIGURE 11: Effects of Carbon, Oxygen and Nitrogen on the Base-metal Tensile Strength and Bend Ductility of Arc Welds in Unalloyed Titanium[8].

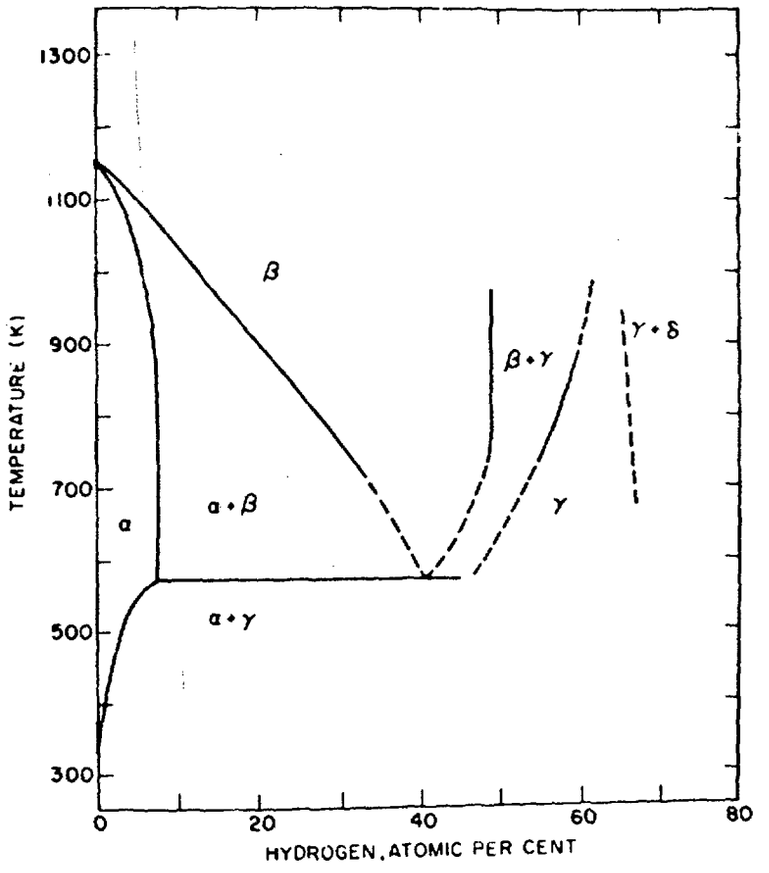

FIGURE 12: Titanium-Hydrogen Phase Diagram at one Atmosphere Pressure(92)

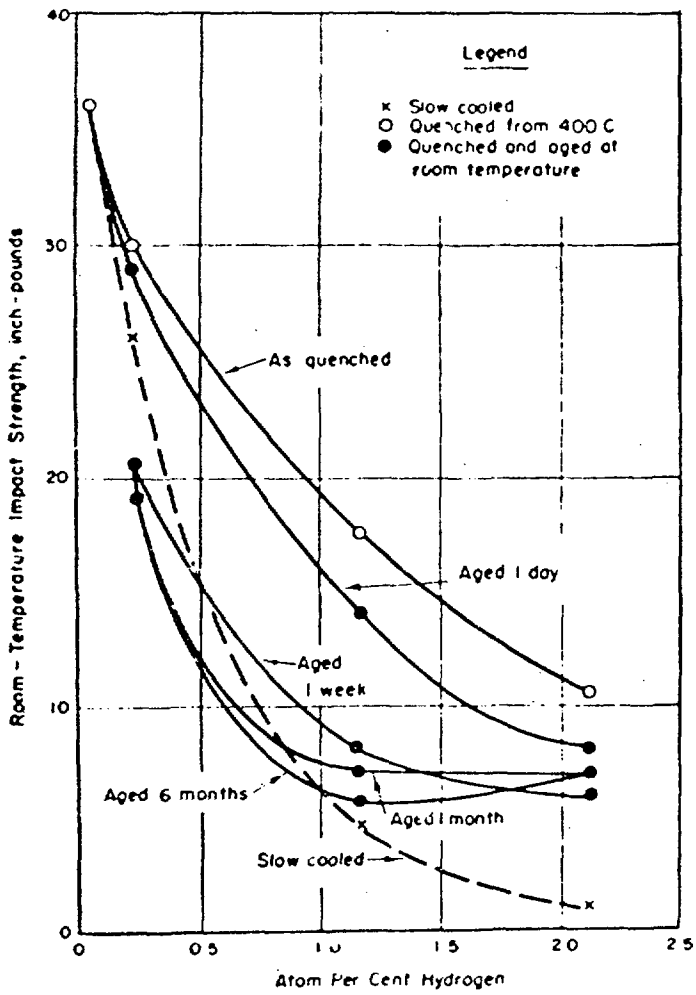

FIGURE 13: Embrittlement of Titanium With Variation in Hydride Size and Dispersion[92]

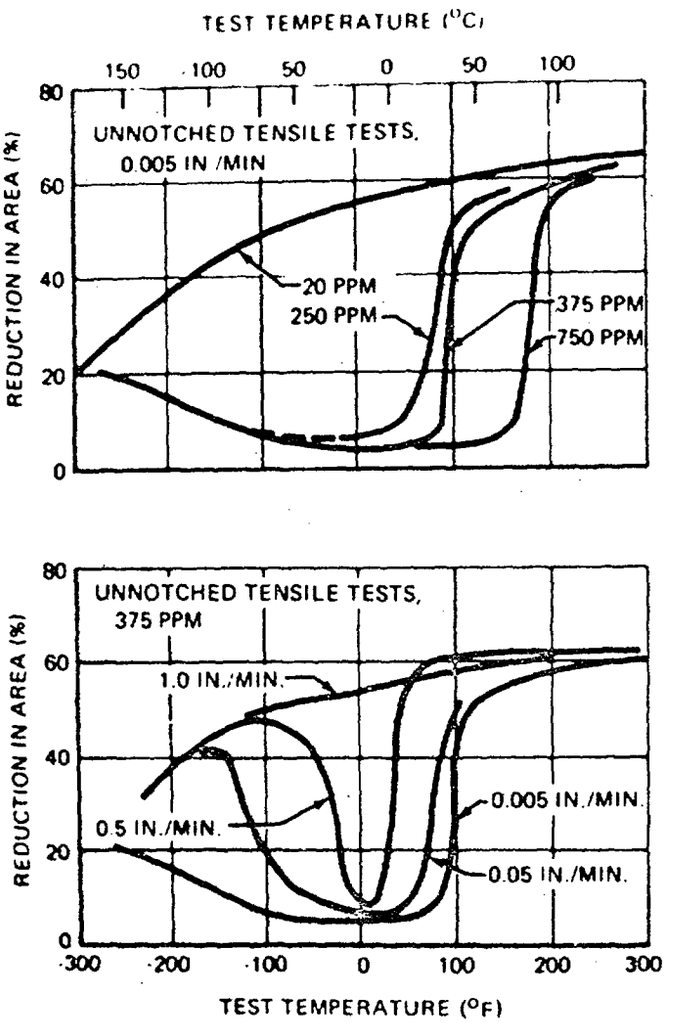

FIGURE 14: Effect of Hydrogen Content, Cross-Head Speed and Temperature on the Tensile Ductility of a Typical ($\alpha+\beta$) Titanium Alloy[91]

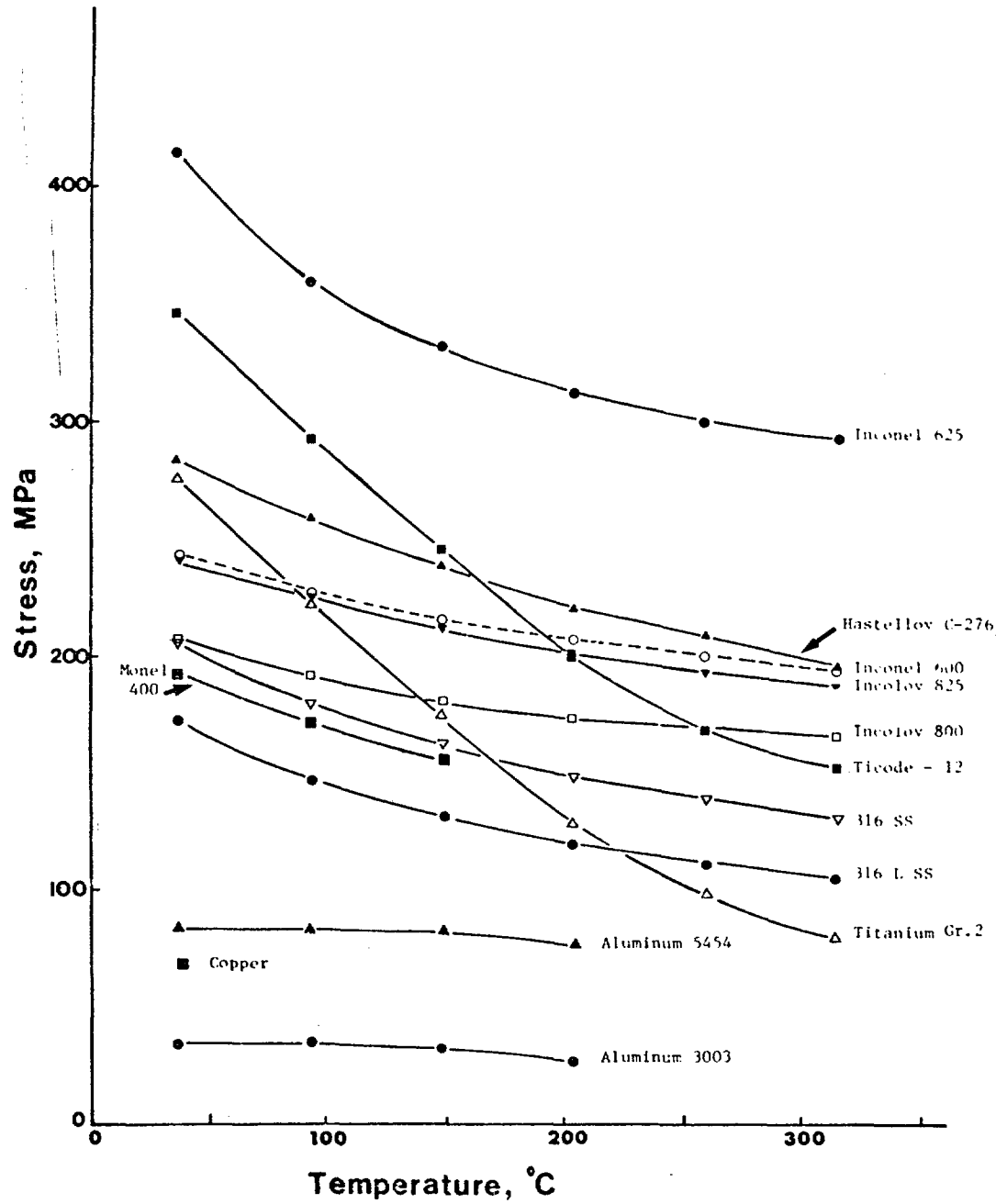

FIGURE 15: Yield Stress-Temperature Data for Various Alloys Taken from the A.S.M.E. Pressure Vessel Code. All data are taken from Section VIII, Division 2, with the exception of Inconel 625 which is taken from Section III. The curve for TiCode-12, which is not a code material, assumes the same temperature dependence as Titanium grade 2.

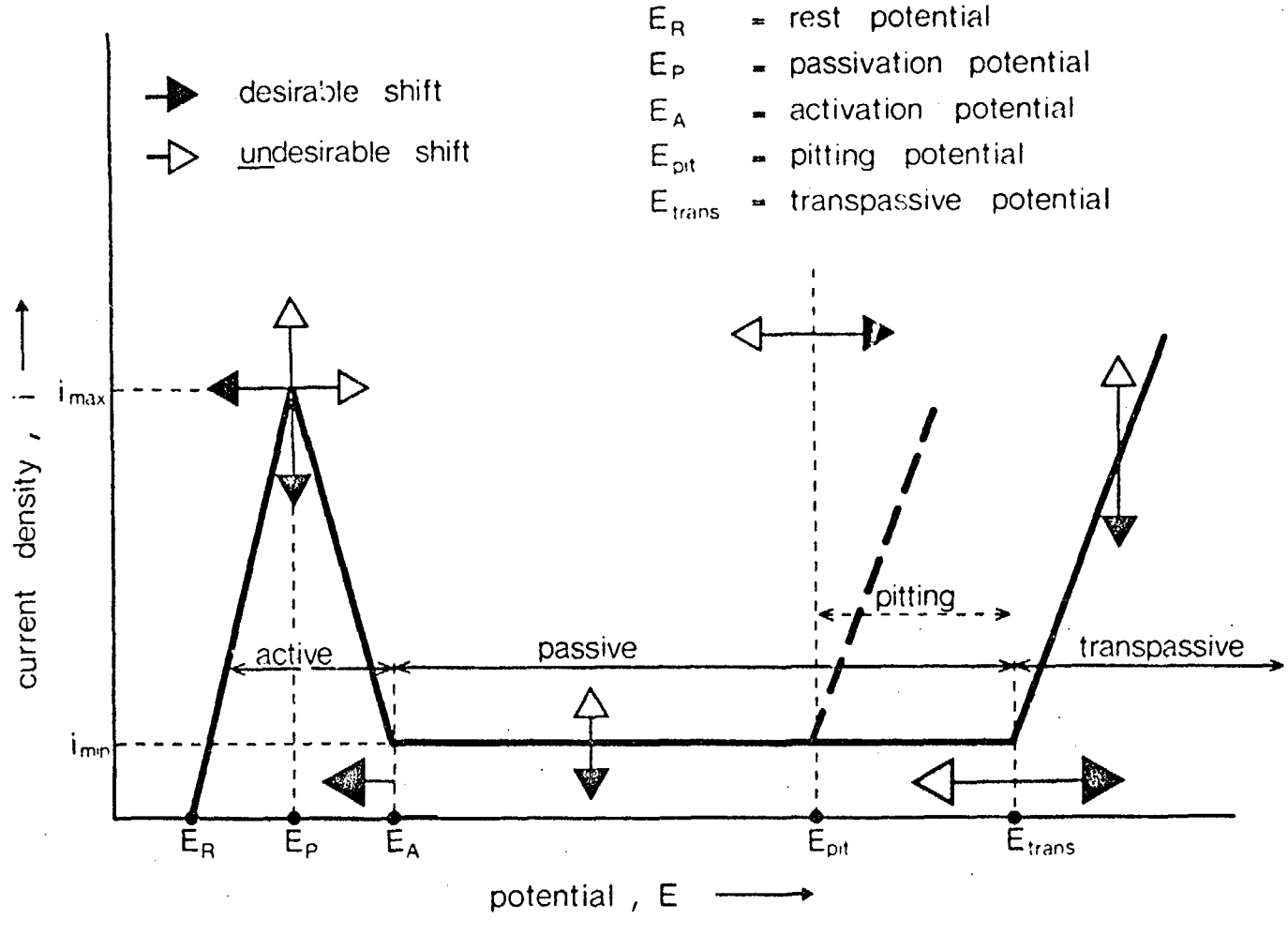

Figure 16: Schematic Illustration of Anodic Current Density Versus Electrode Potential Curve for Stainless Steels

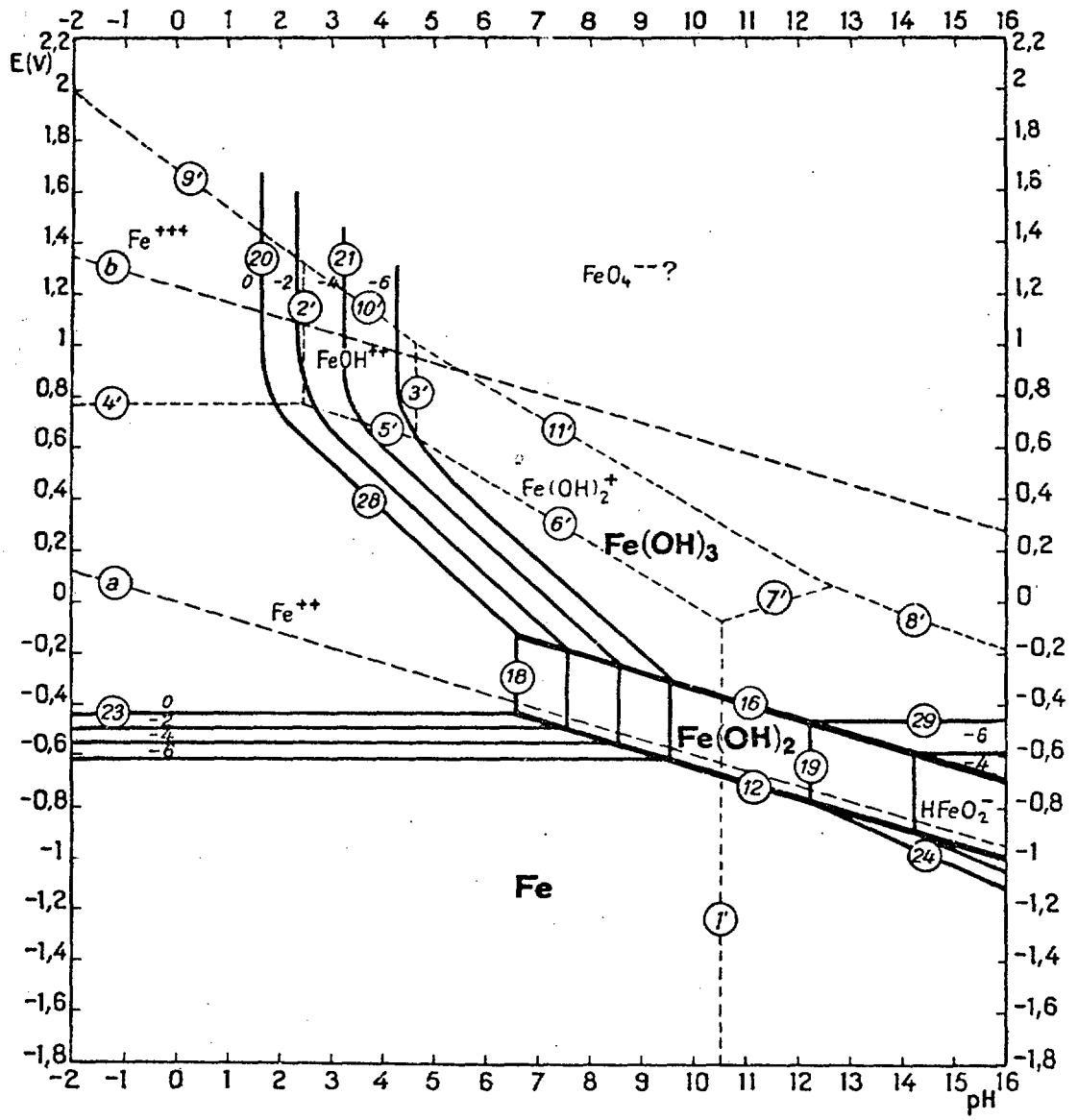

FIGURE 17: Potential-pH Equilibrium Diagram for the System Iron-Water, at 25°C(127)

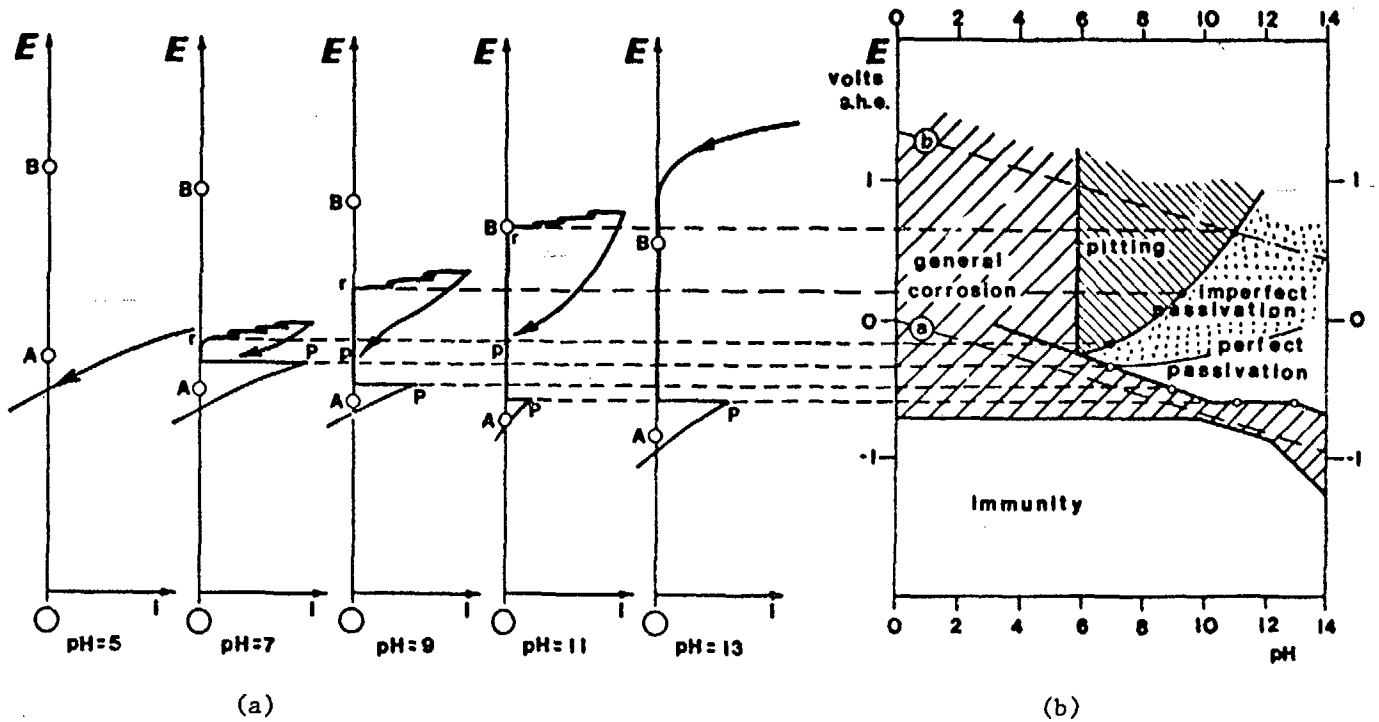

FIGURE 18: (a) Potentiokinetic Polarization Curves Using Electrochemical Hysteresis Method for Armco Iron in 10^{-2} Molar Chloride Solutions of Various pHs (r is the pitting potential, p the protection potential and P the passivation potential)

(b) Experimental Potential/pH Diagram Constructed from Electrochemical Hysteresis Data in (a)[129]

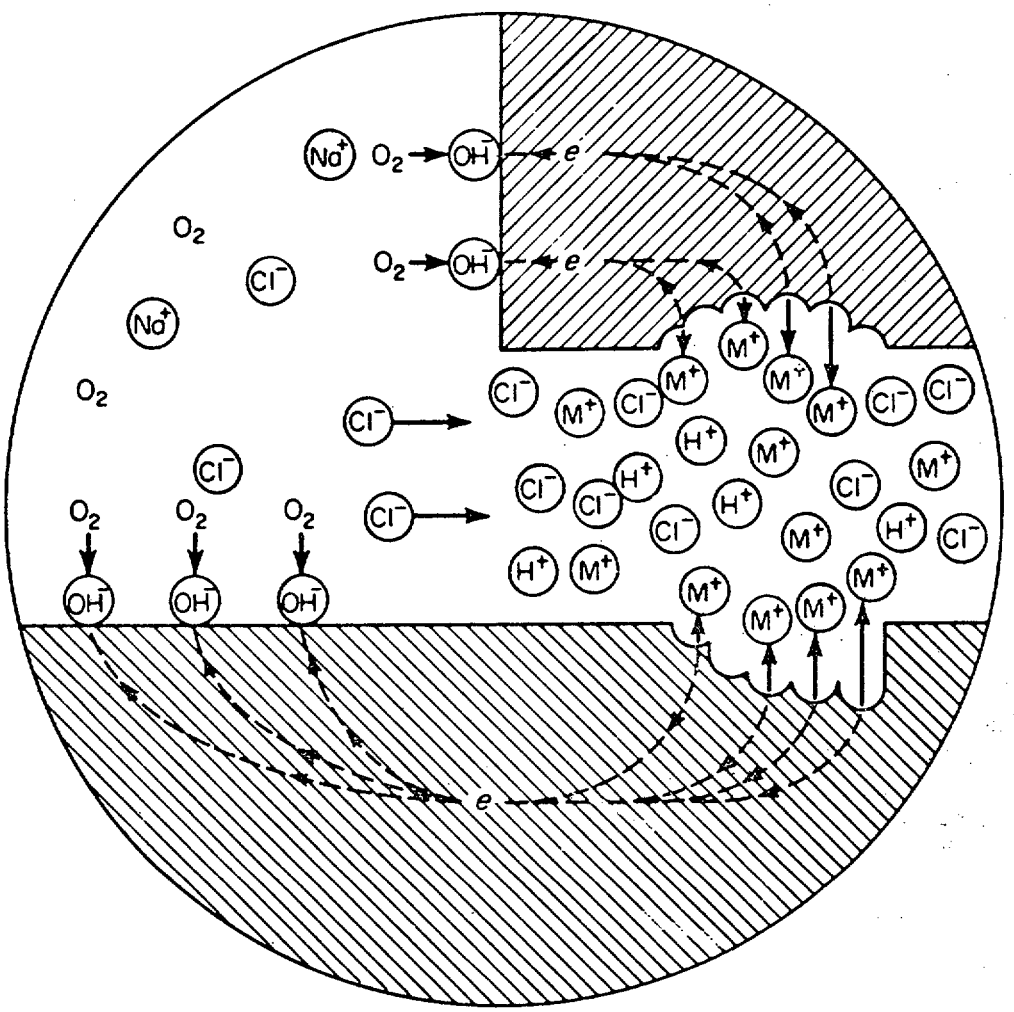

FIGURE 19: Schematic Illustration of Crevice Corrosion Mechanism Proposed by Fontana and Greene (121)

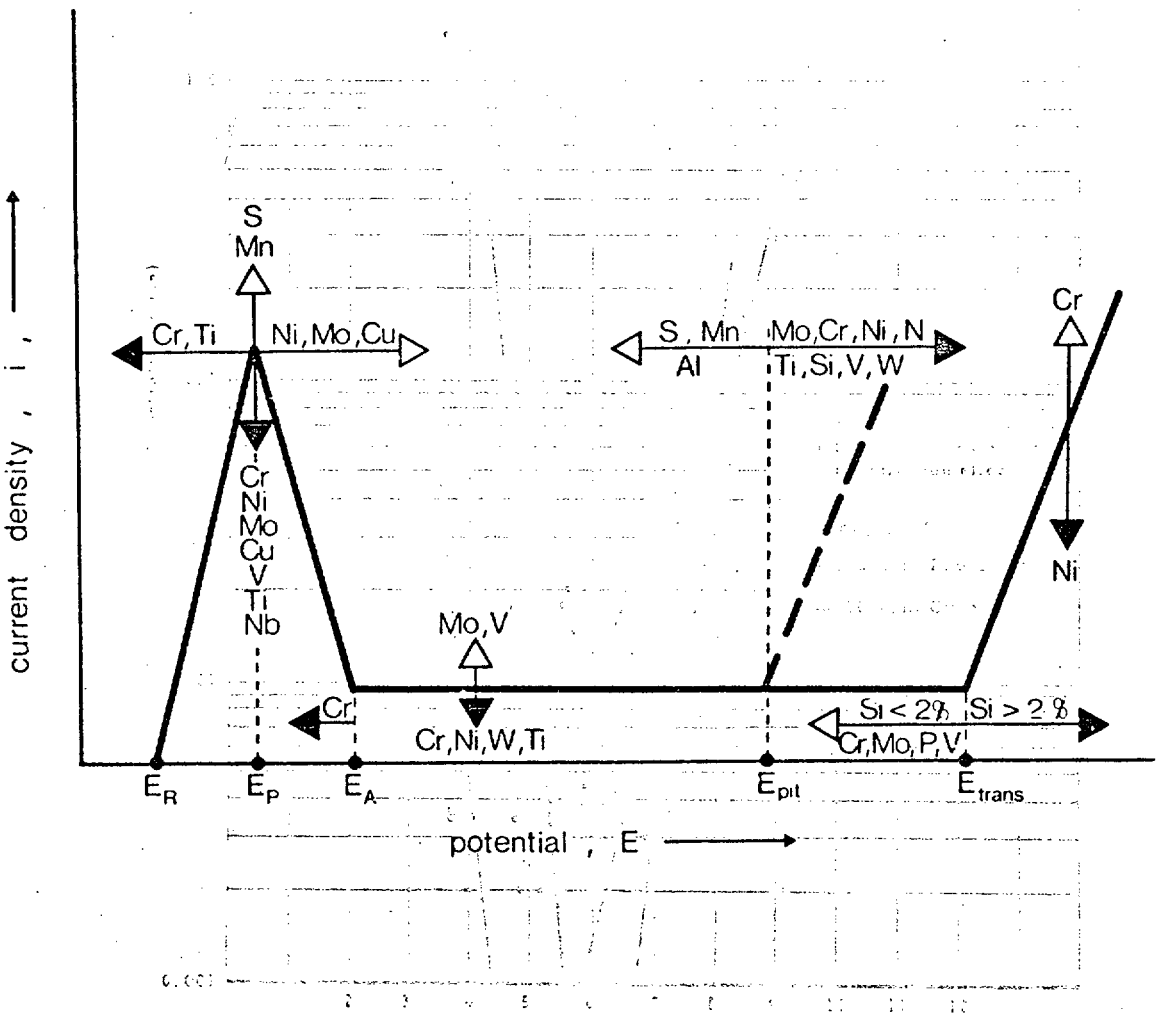

FIGURE 20: Schematic Illustration of the Effects of Alloying Elements on the Current Density Versus Electrode Potential Curve for Stainless Steels. The points referred to in the potential axis are defined in Figure 16.

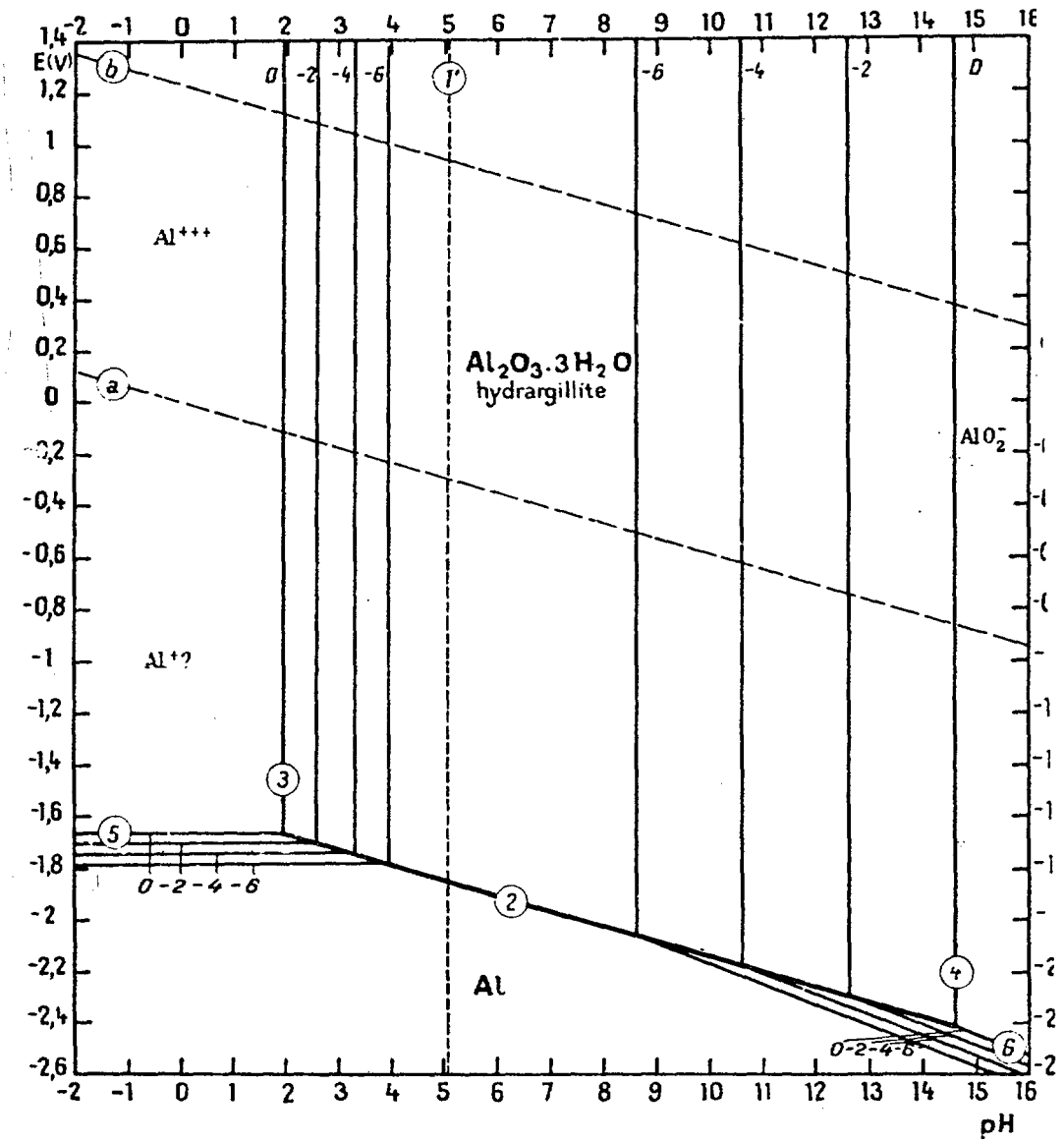

FIGURE 21: Potential-pH Diagram for the System Aluminum-Water, at 25°C (127

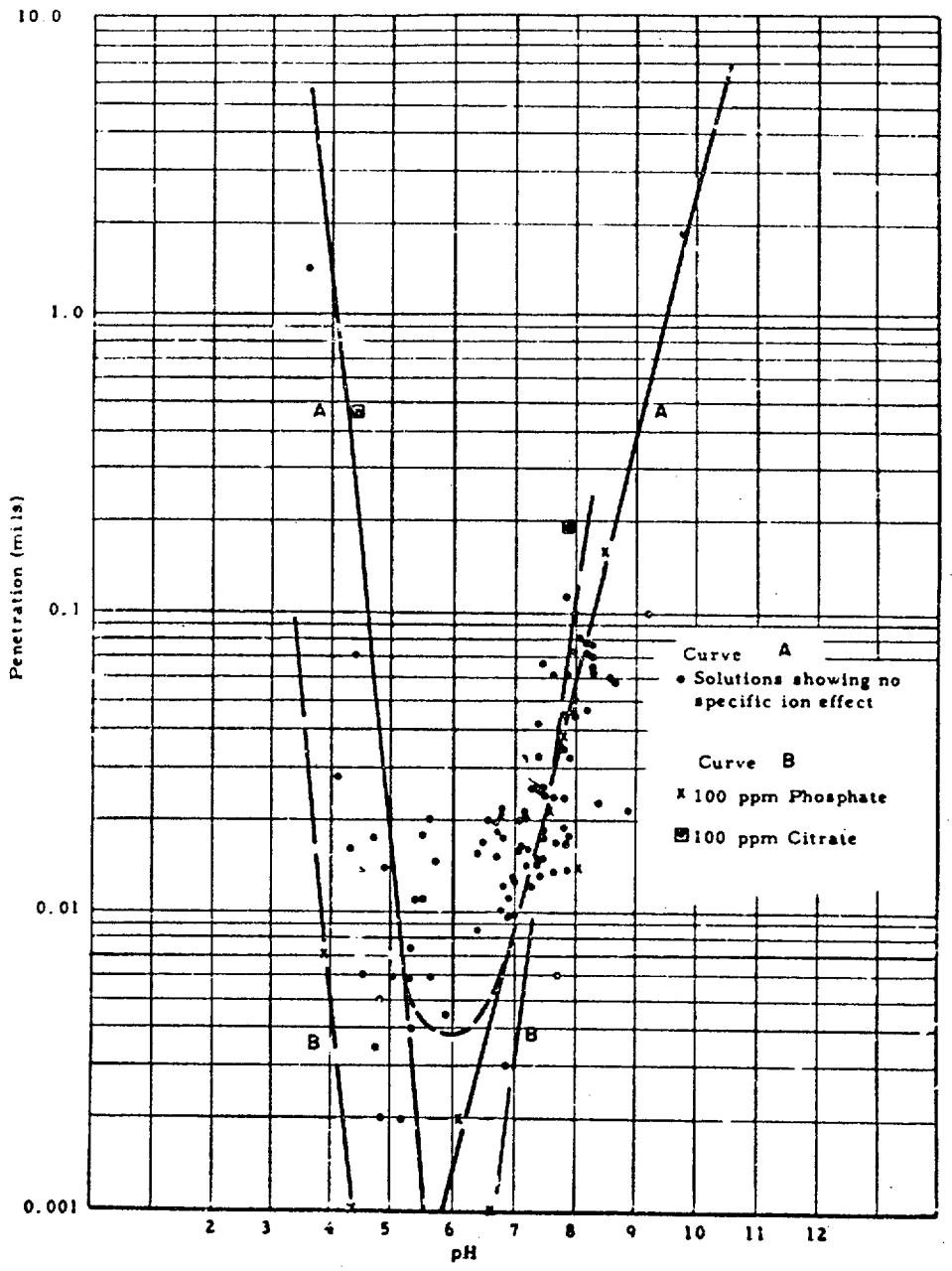

FIGURE 22: Corrosion of 1245 Aluminum as a Function of pH (14 days, 92°C)[146]

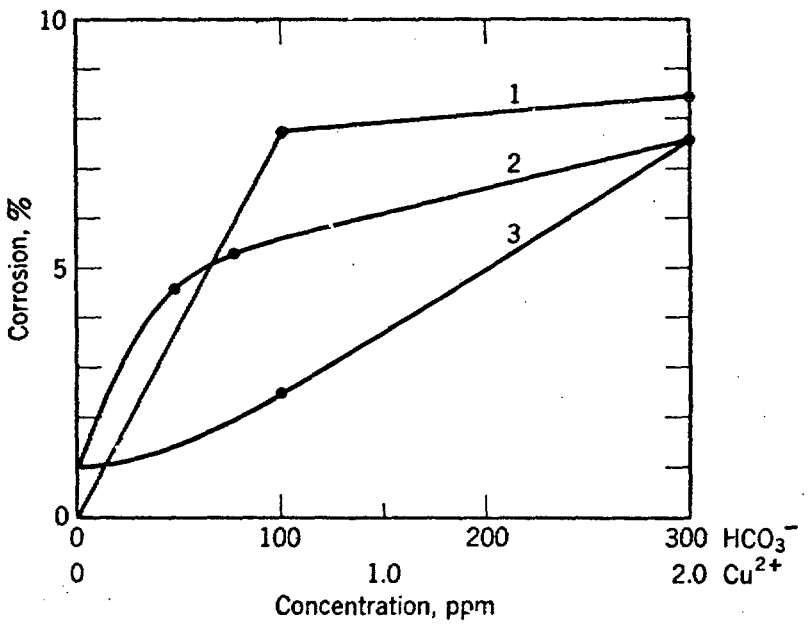

ppm

	Cl^-	HCO_3^-	Cu^{2+}
1.	*v*	300	2
2.	300	300	*v*
3.	300	*v*	2

v = variable

FIGURE 23: Aluminum Corrosion in Various Copper-Chloride-Bicarbonate Combinations at 26°C (144)

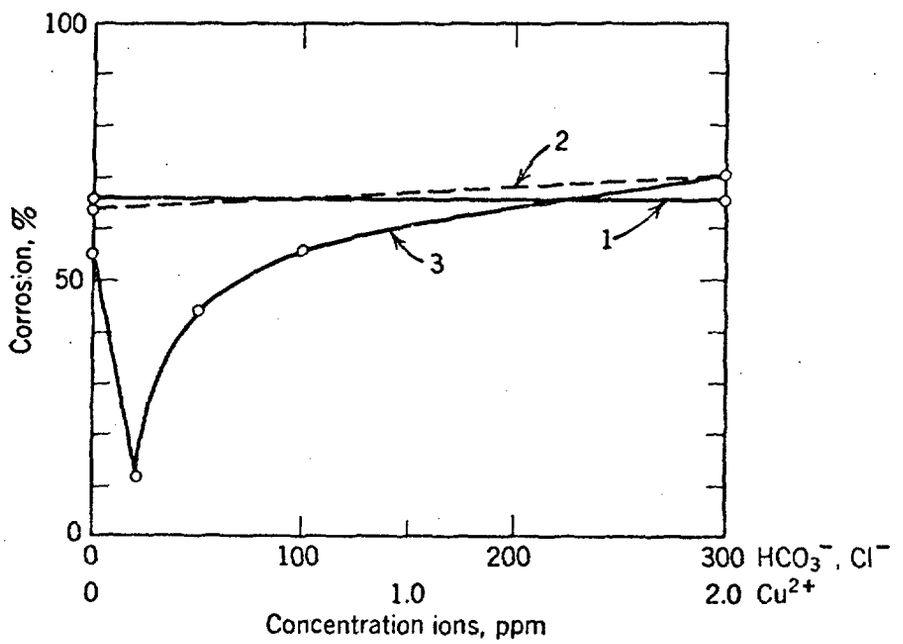

	ppm		
	Cl^-	HCO_3^-	Cu^{2+}
(1)	*v*	300	2
(2)	300	300	*v*
(3)	300	*v*	2

v = variable

FIGURE 24: Aluminum Corrosion in Various Copper-Chloride-Bicarbonate Combinations at 71°C (144)

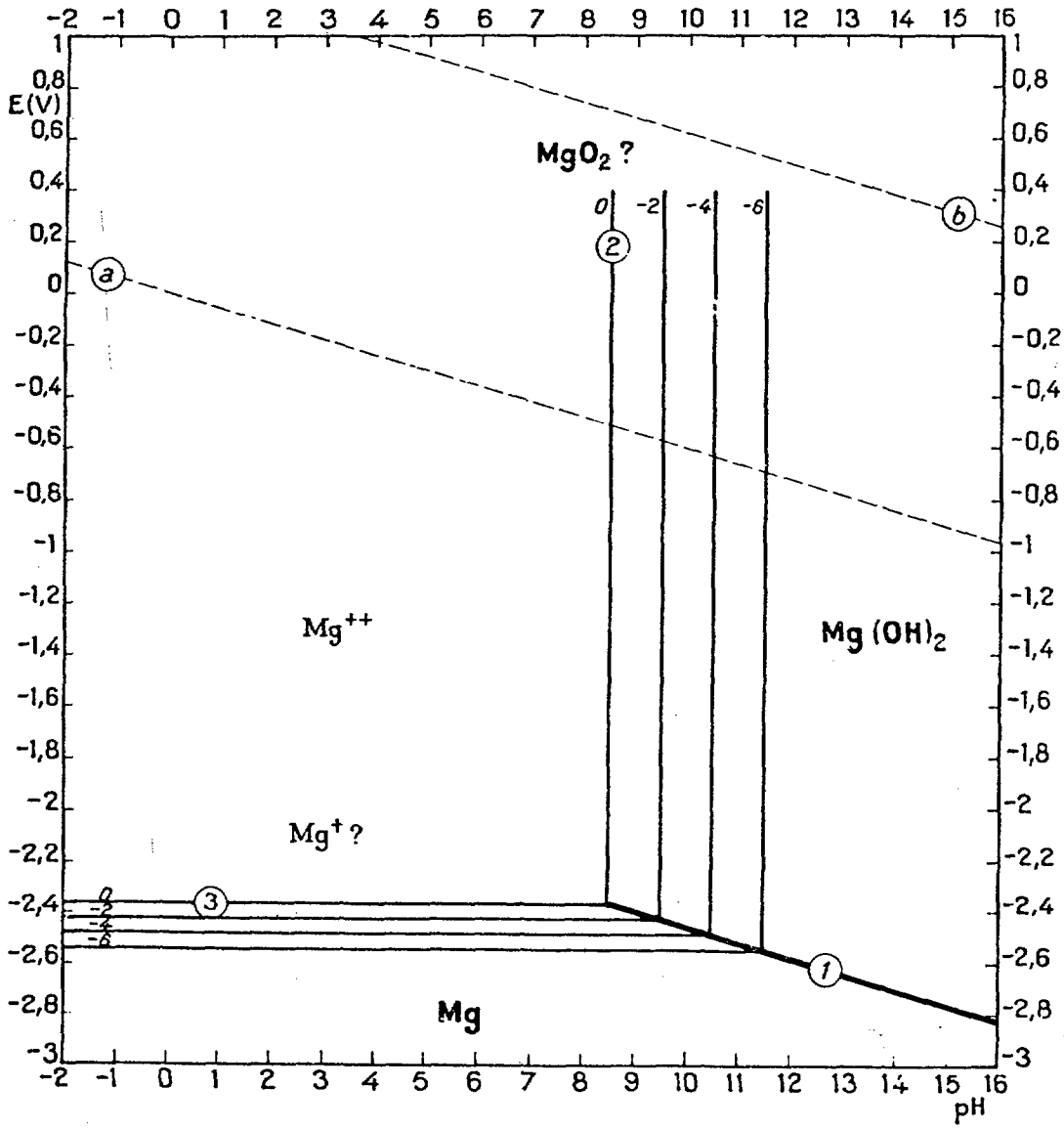

FIGURE 25: Potential-pH Equilibrium Diagram for the System Magnesium-Water at 25°C (127)

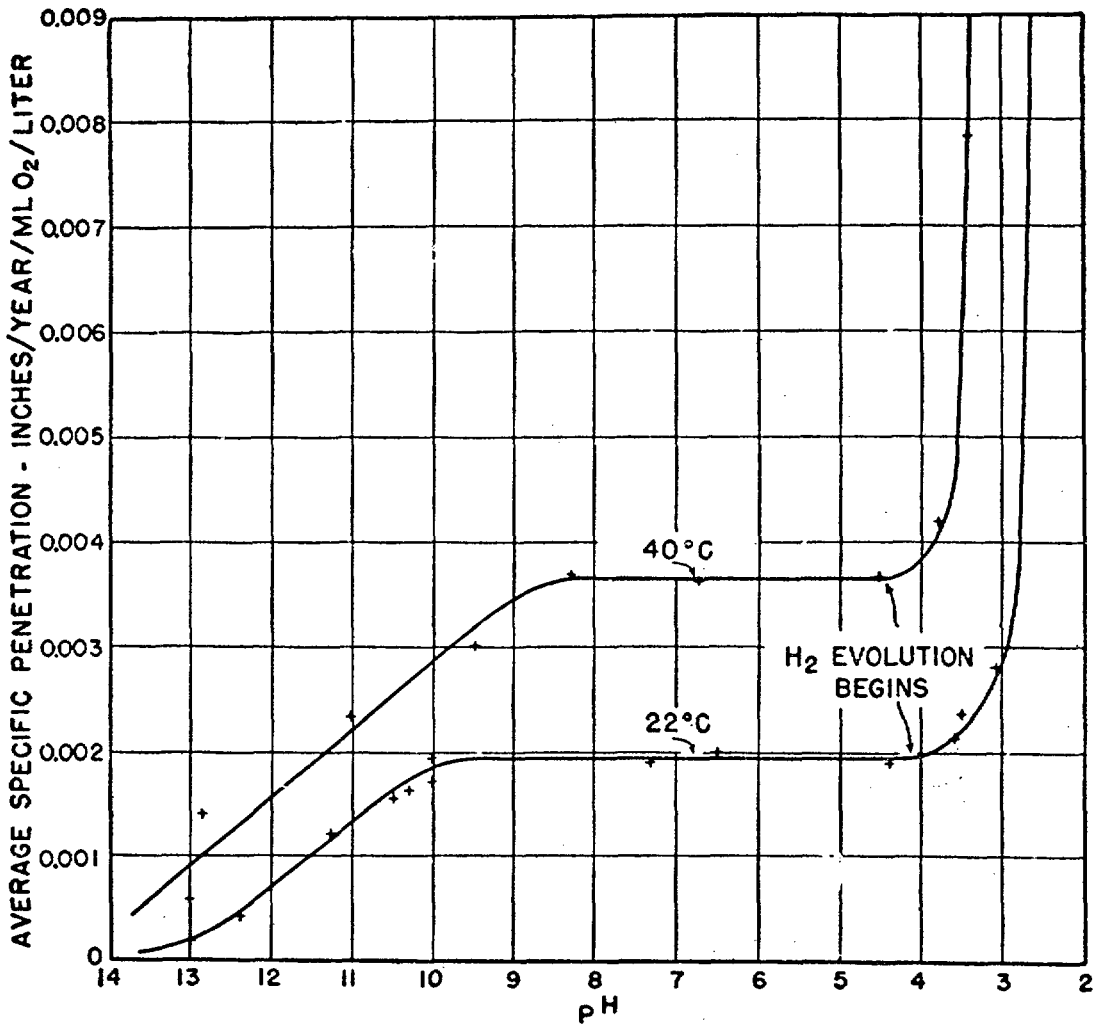

FIGURE 26: Effect of pH on the Corrosion of Mild Steel[151]

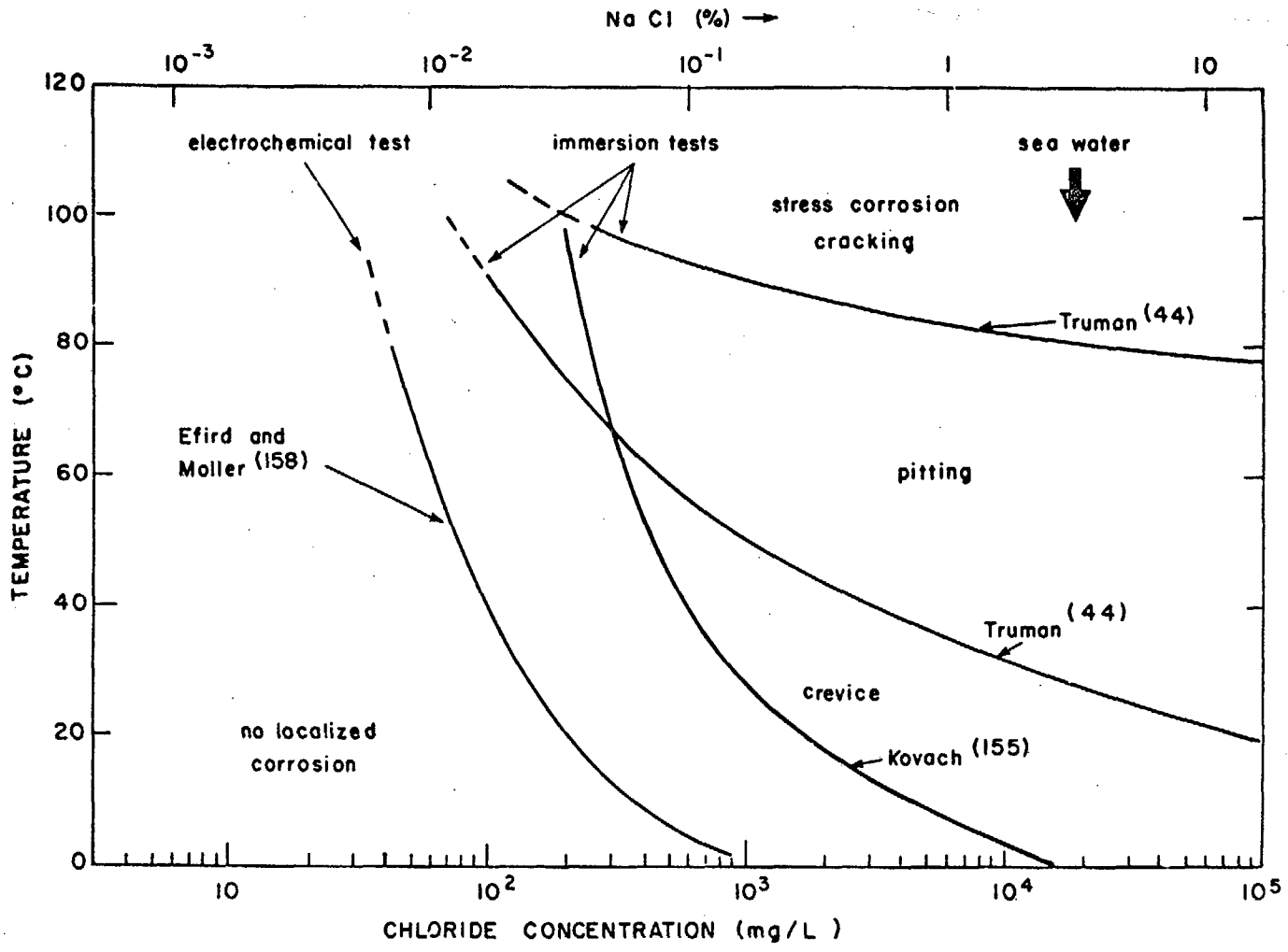

FIGURE 27: Localized Corrosion of Type 304 Stainless Steel in Water as a Function of Temperature and Chloride Concentration

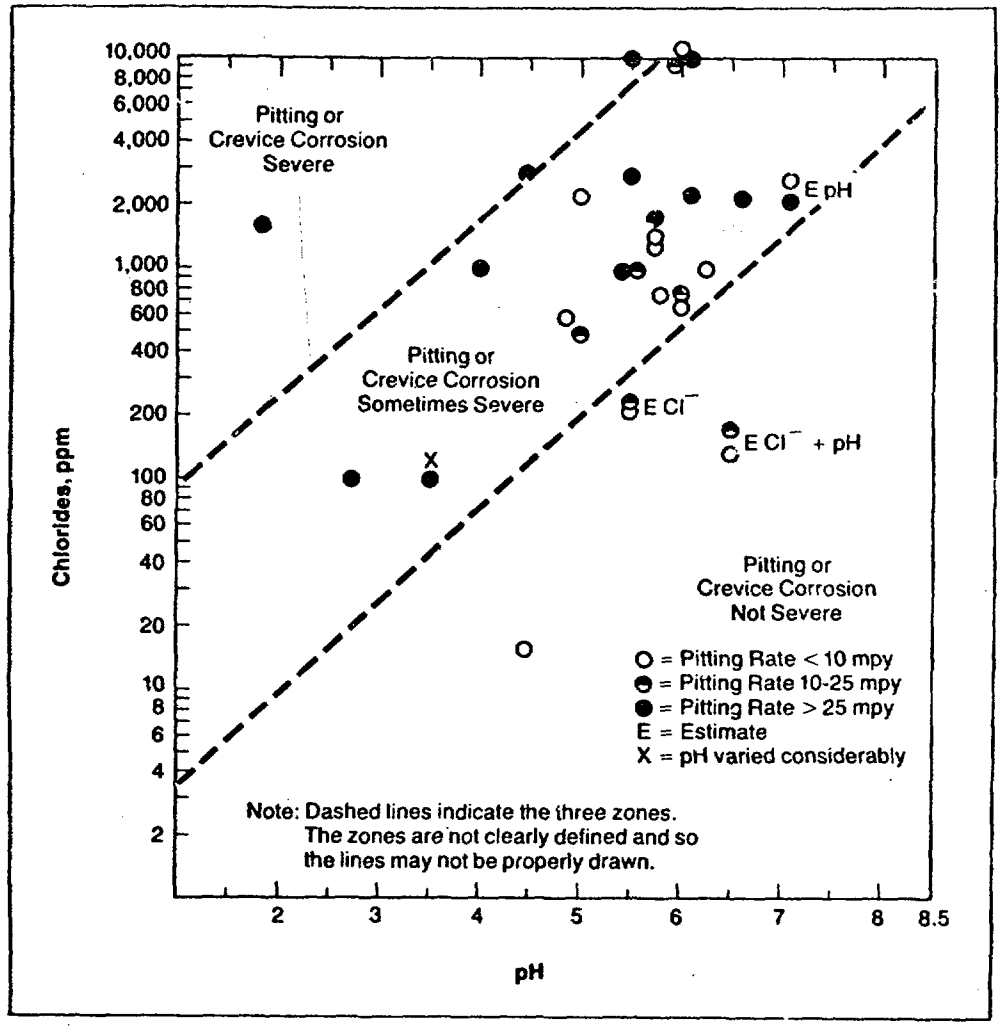

FIGURE 28: Corrosion of Type 316L Stainless Steel in SO_2 Scrubbing Environments (161)

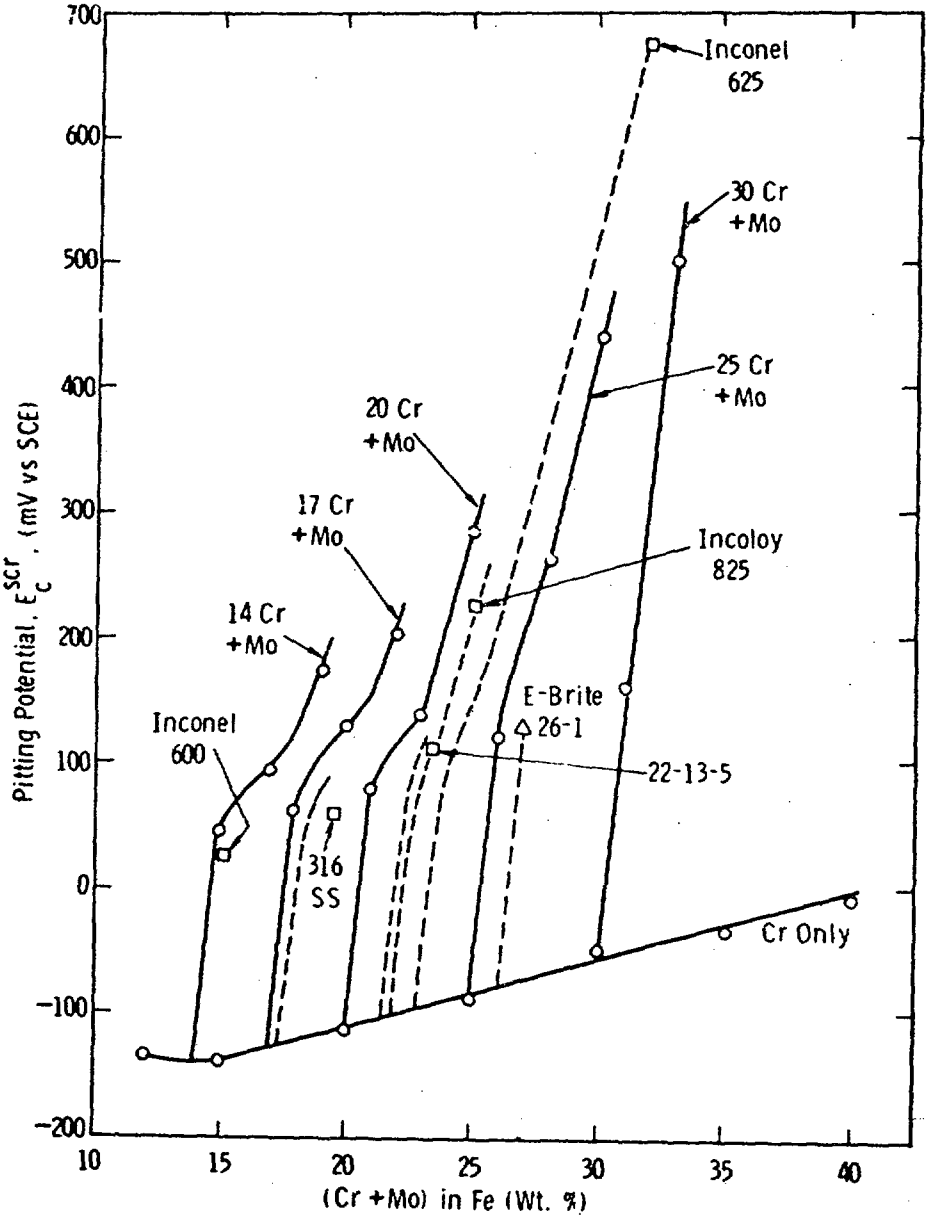

FIGURE 29: Comparison of the Critical Pitting Potentials of Fe-Cr-Mo Alloys with Several Commercial Alloys in Deaerated Synthetic Sea Water at 90°C, pH = 7.2(162)

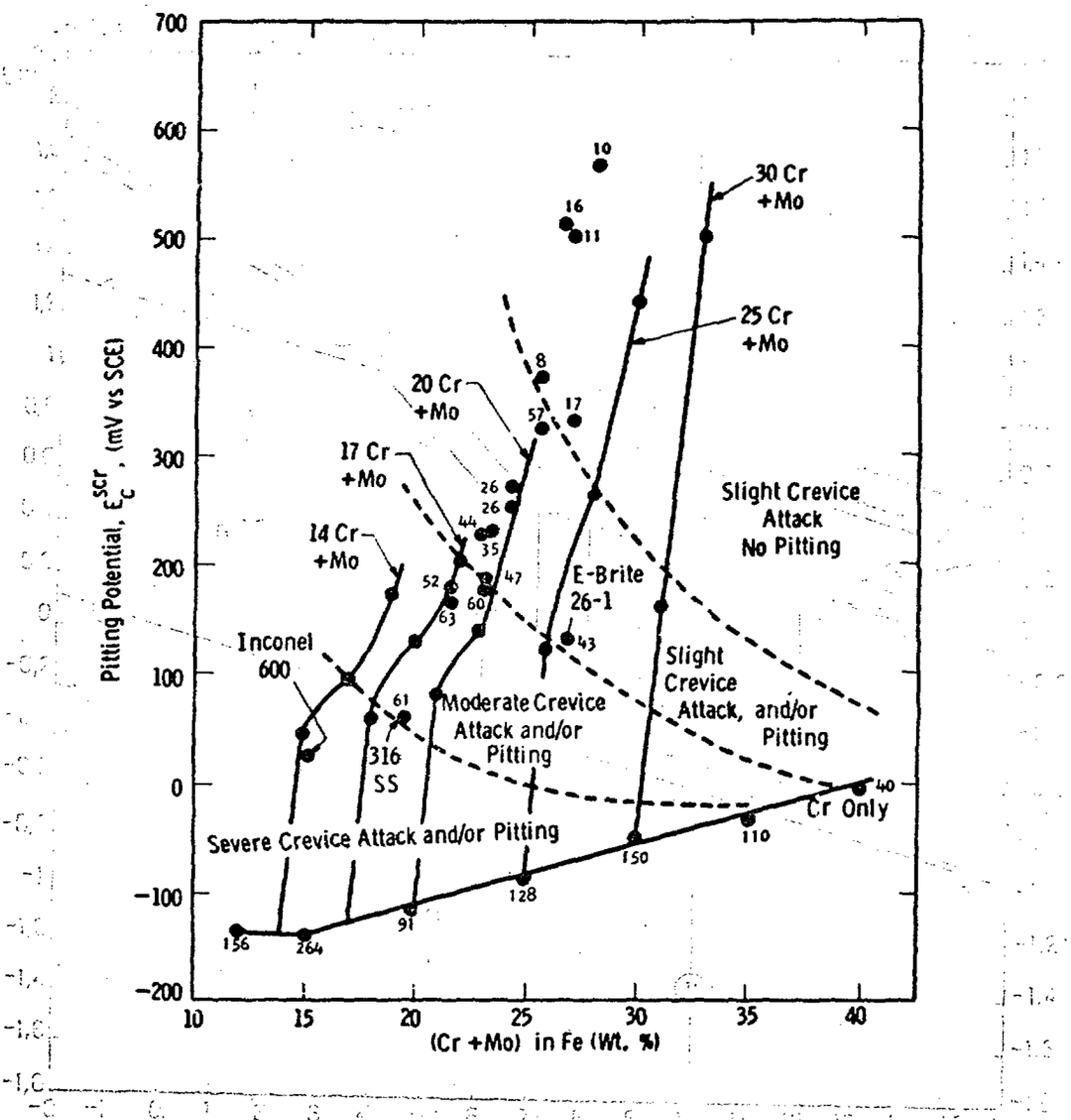

FIGURE 30: Relationship Between the Critical Pitting Potentials (E_c^{scr} measured in deaerated synthetic seawater at 90°C, pH = 7.2) of Fe-Cr-Mo Based Alloys and Their Resistance to Crevice Attack after a 14 Day Exposure to Synthetic Seawater at 121°C and ∿60 µg/L Oxygen. The numbers associated with individual points indicate the weight losses expressed in g x 10^{-4} after the 121°C exposure for samples with initial weights of ∿1 g(162)

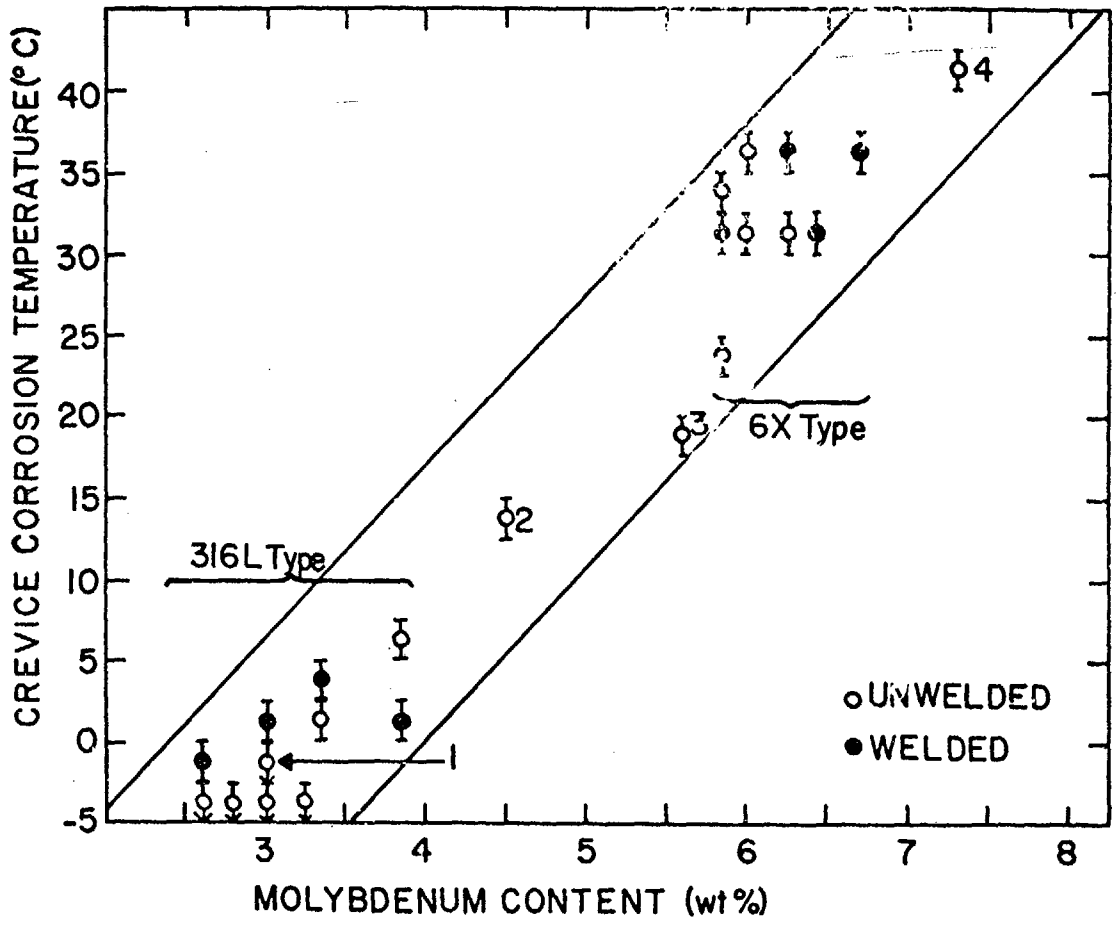

FIGURE 31: Crevice Corrosion Temperatures Versus Molybdenum Content for Experimental and Commercial Stainless Steels, Determined with Rubber Crevices in 10% FeCl$_3$ (164)

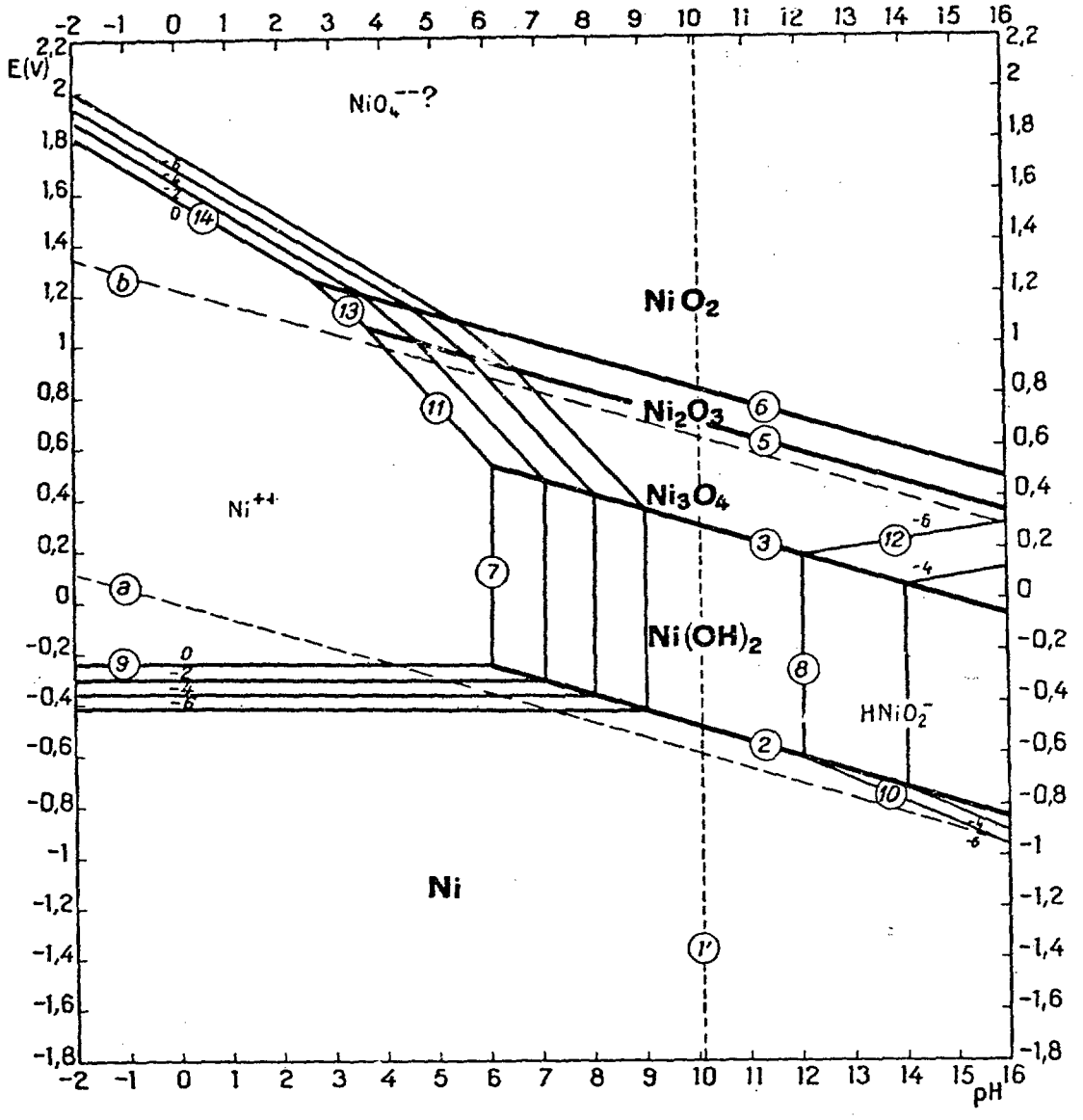

FIGURE 32: Potential-pH Equilibrium Diagram for the System Nickel-Water, at 25°C (127)

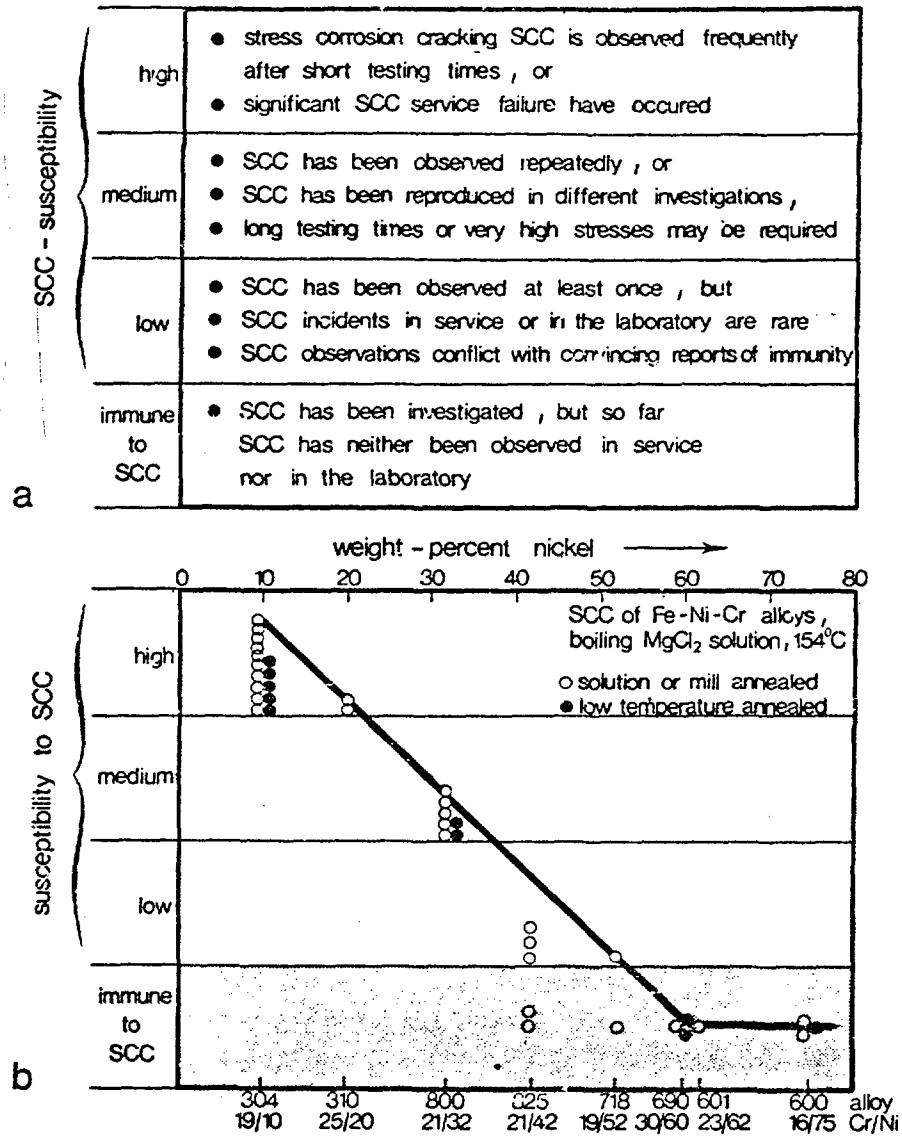

FIGURE 33: Influence of Nickel Content on SCC Susceptibility of Commercial Fe-Ni-Cr Alloys in Boiling $MgCl_2$ Solution (171)

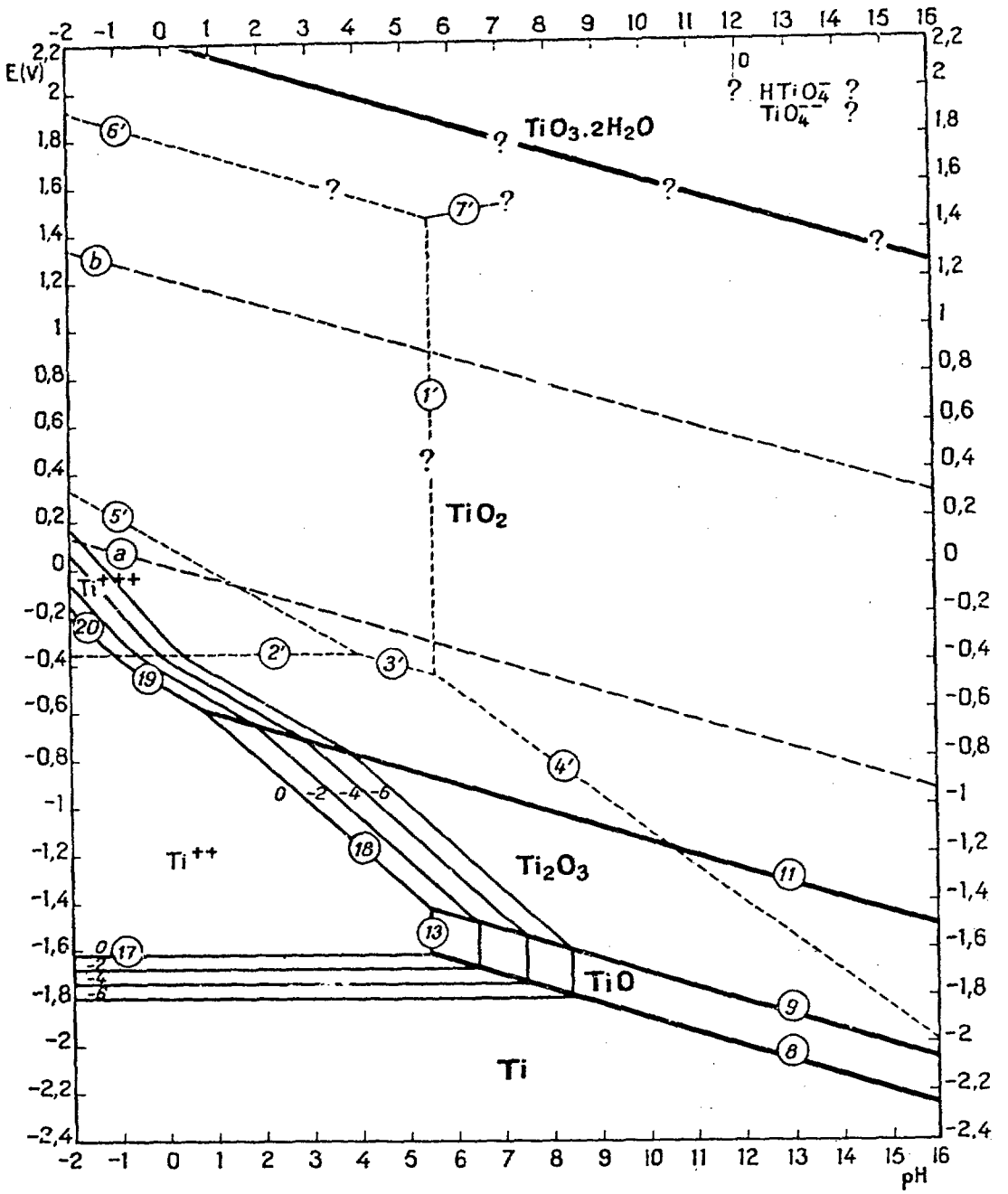

FIGURE 34: Potential-pH Equilibrium Diagram for the System Titanium-Water at 25°C (127)

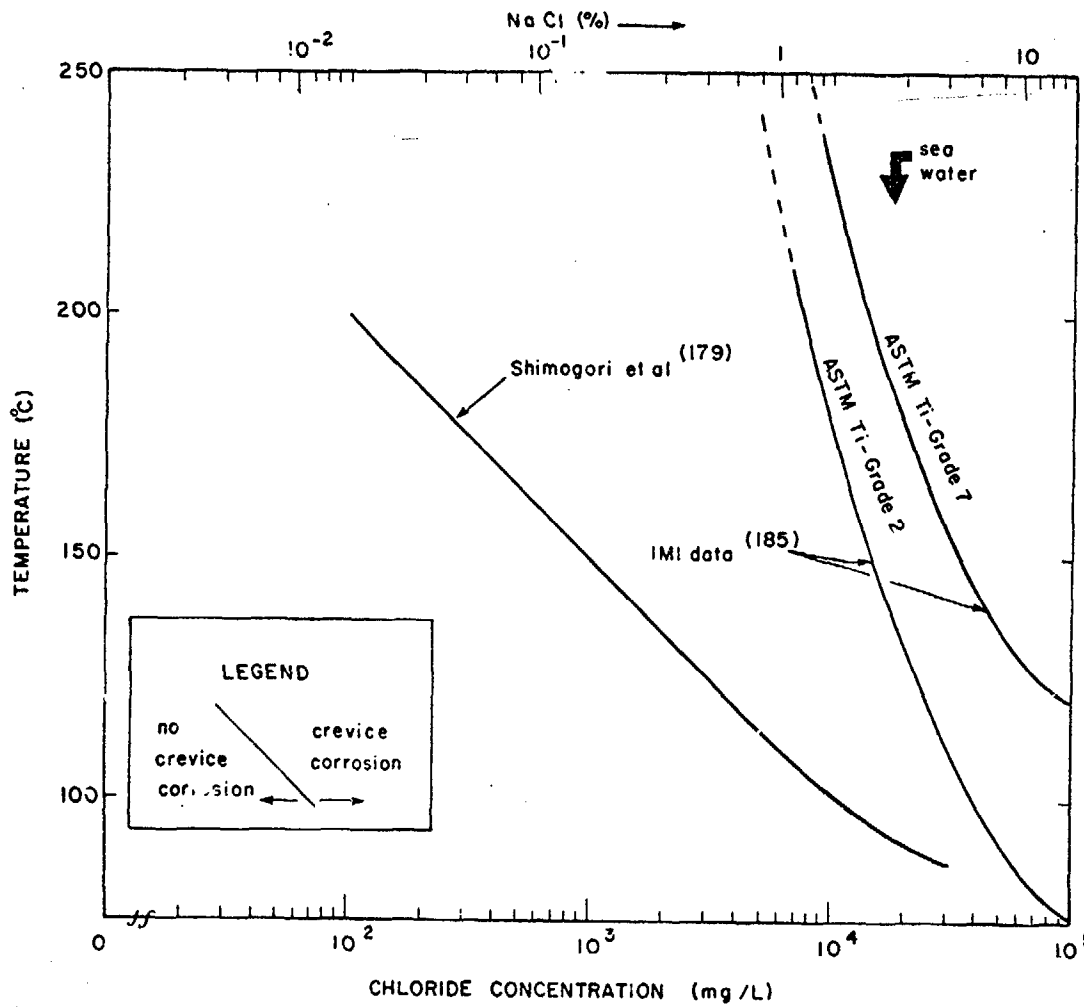

FIGURE 35: Crevice Corrosion of Titanium and Its Alloys in Aqueous Chloride Solutions

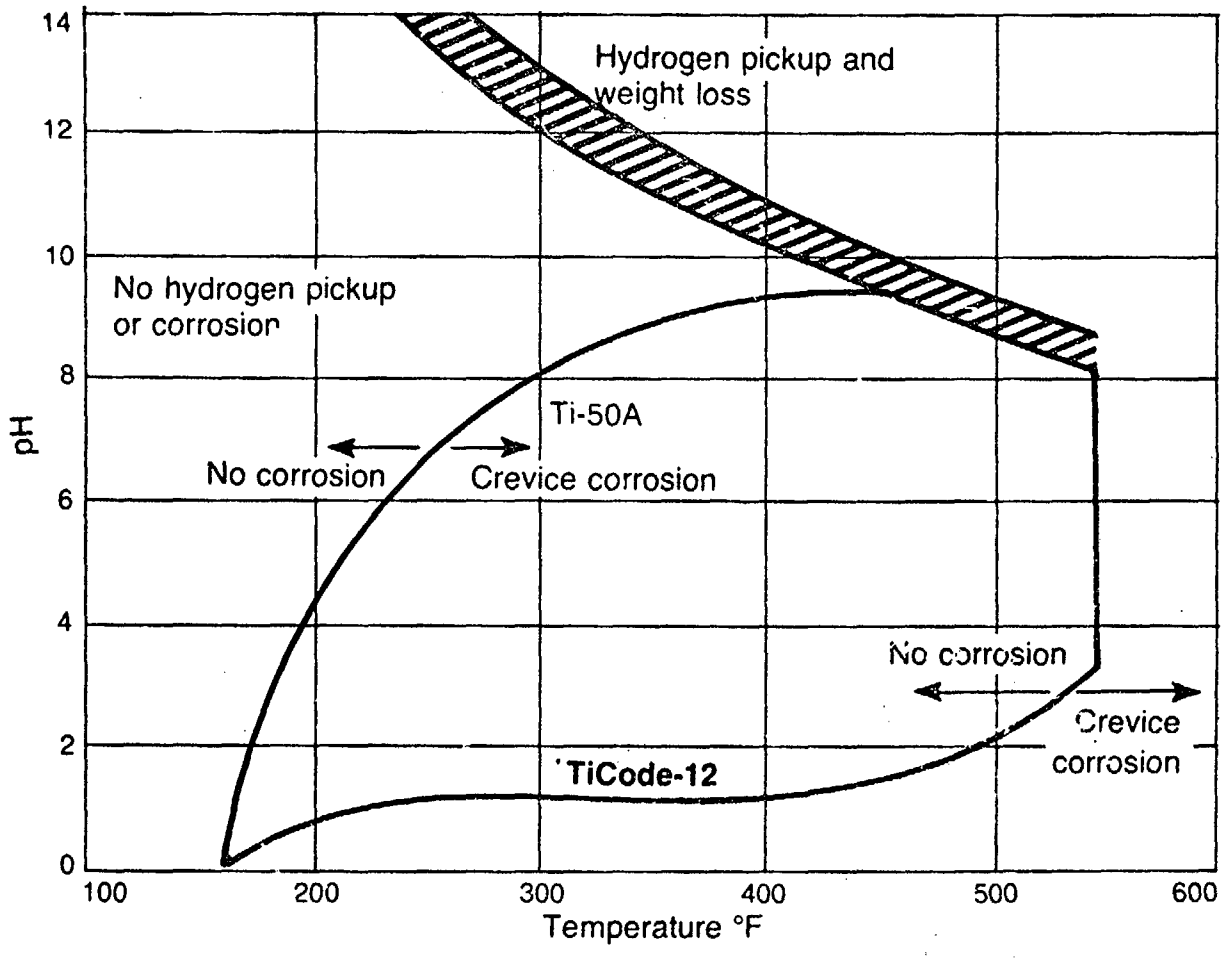

FIGURE 36: Effect of Temperature and pH on Crevice Corrosion of Unalloyed Titanium (Grade 2) and TiCode-12 in Saturated NaCl Brine(72)

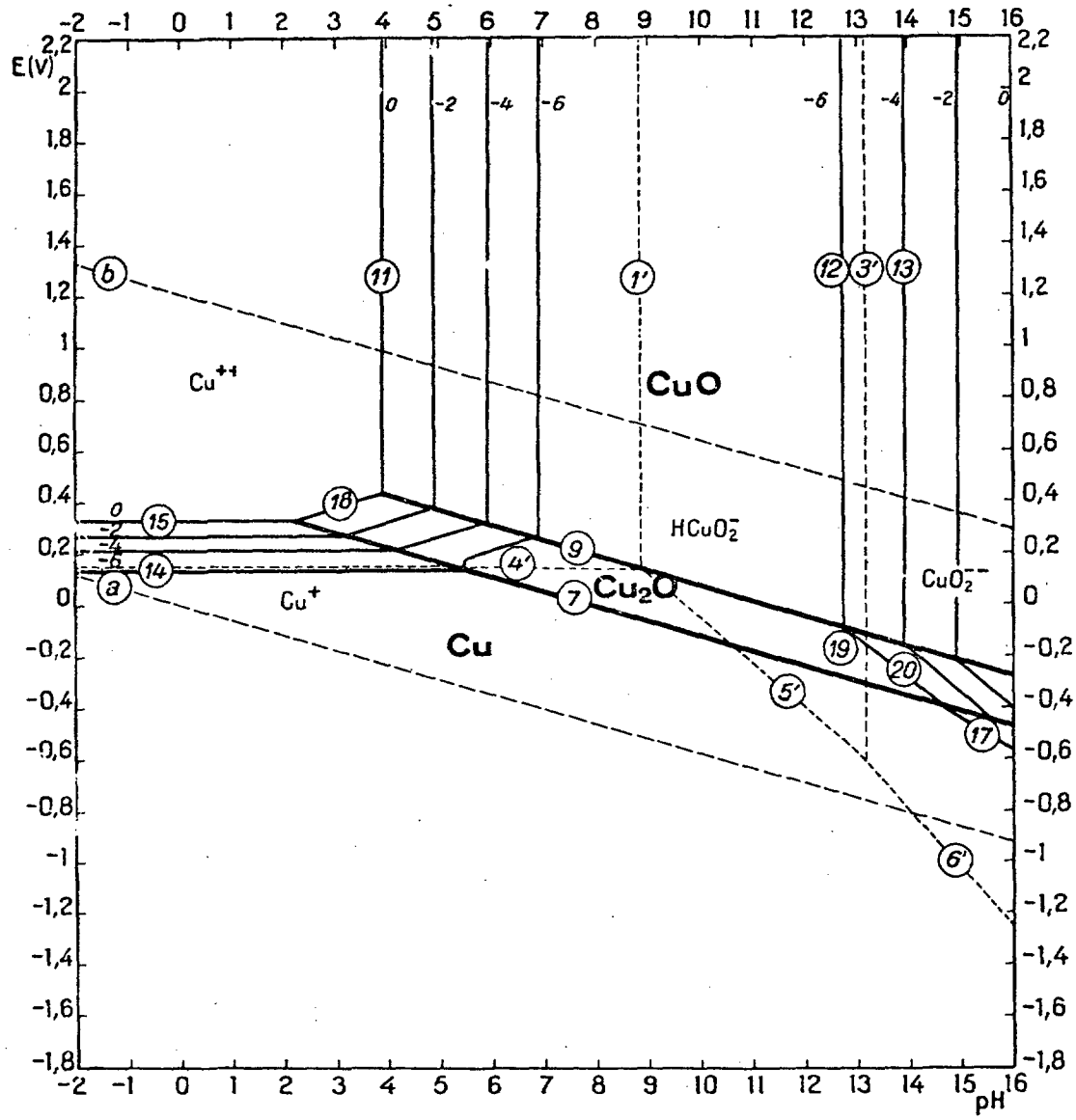

FIGURE 37: Potential-pH Equilibrium Diagram for the System Copper-Water, at 25°C (127)

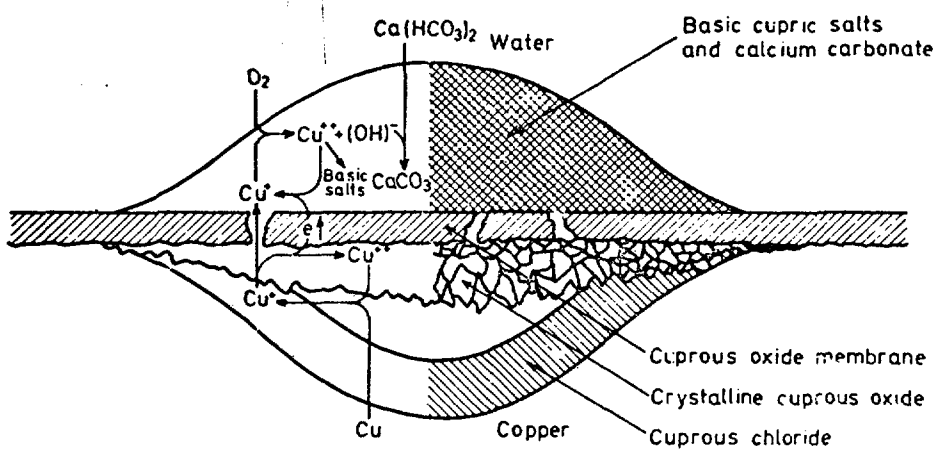

FIGURE 38: Pit Formed on a Copper Surface (protected by a film of Cu_2O) in a Hard Water[190]

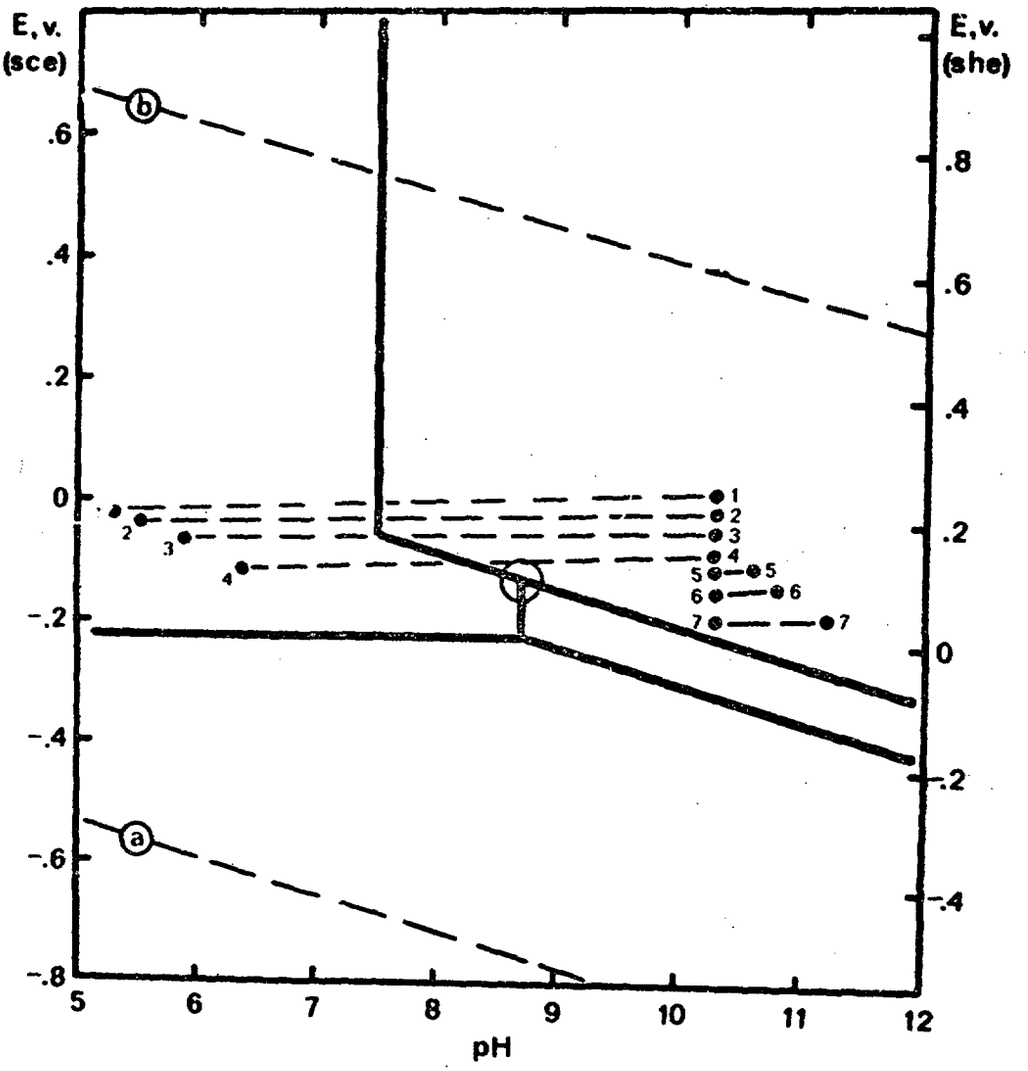

FIGURE 39: The Influence of External Potential on the Potential and pH Characteristics of a Crevice on 90-10 Cu-Ni. The numbers indicate simultaneous data for the crevice and the external surface. The intersection of the general corrosion region and the primary passivation line is circled for reference(192)

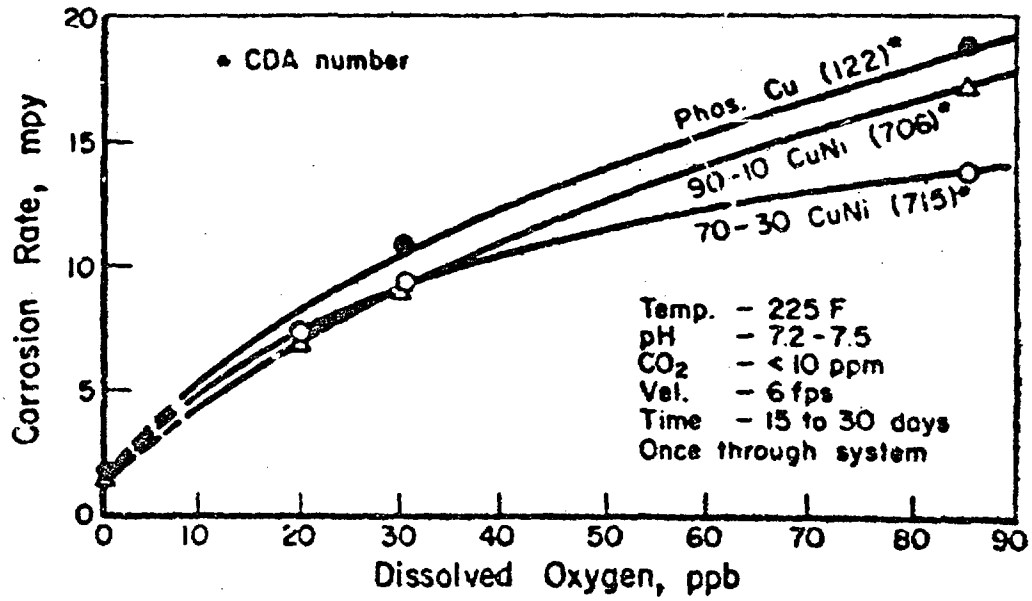

FIGURE 40: Effect of Dissolved Oxygen in Seawater on the Corrosion Rate of Copper Alloys (193)

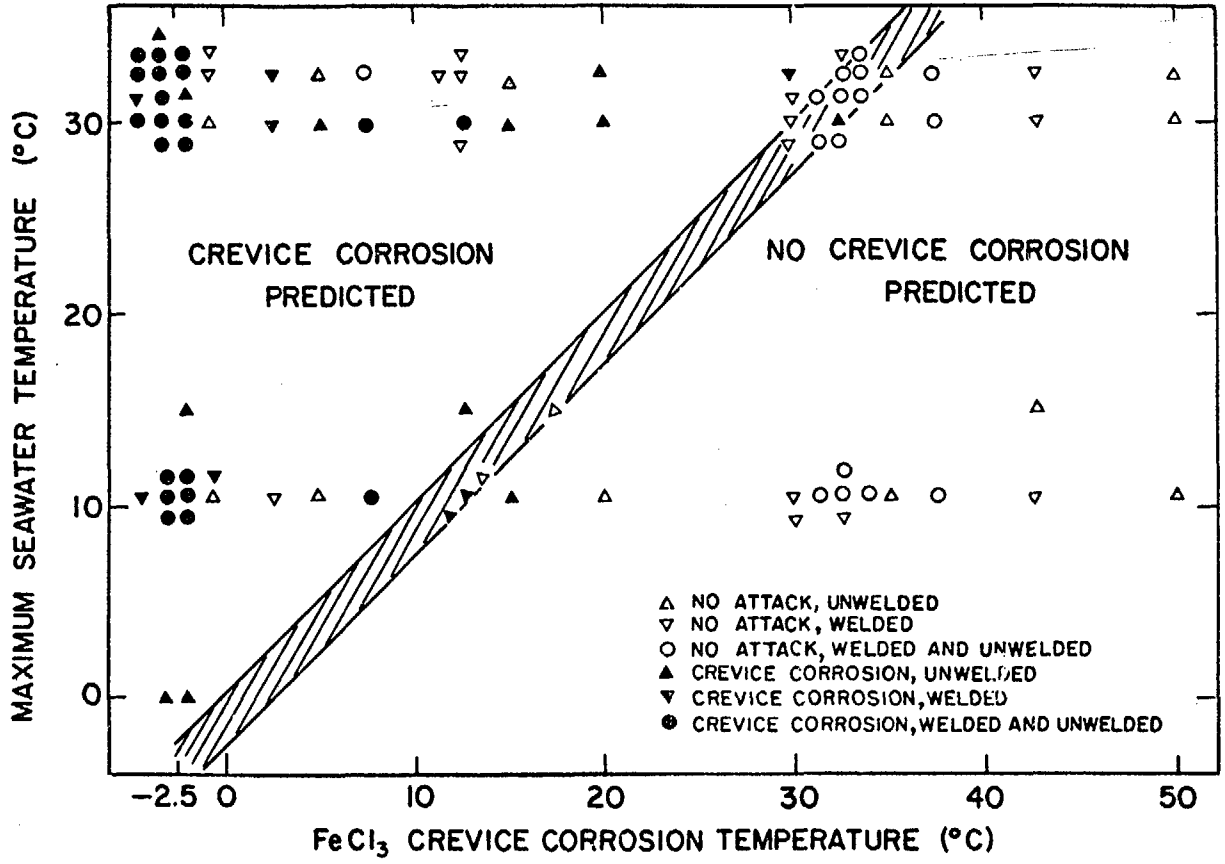

FIGURE 41: Results of Seawater Exposures of Austenitic Stainless Steel Showing Maximum Seawater Temperature and $FeCl_3$ Crevice Corrosion Temperature (CCT) for Each Coupon. Predictions of seawater performance from $FeCl_3$ CCT's are indicated: points to the right of the hatched line should be crevice corrosion free (seawater too cold) and points to the left should show crevice corrosion (seawater temperature ...

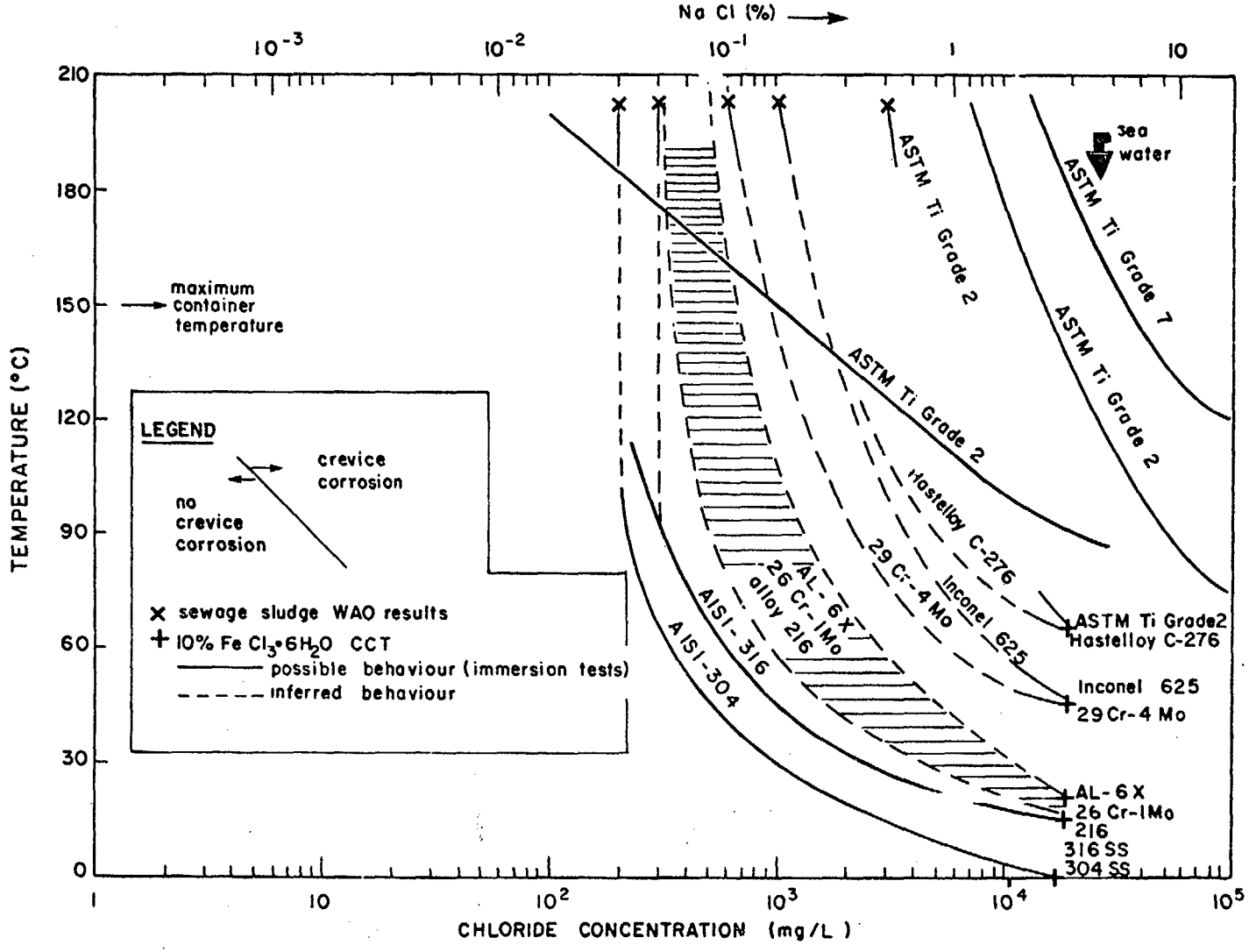

FIGURE 42: Crevice Corrosion of Various Alloys in Aqueous Chloride Solutions